Radio resource management for energy efficient cellular networks with intelligent reflecting surfaces

Mona Hassan Kassem

COLLEGE MATHSTIC
DOCTORAL BRETAGNE
BRETAGNE OCEANE

Université de Bretagne Occidentale

THÈSE DE DOCTORAT DE

L'UNIVERSITÉ DE BRETAGNE OCCIDENTALE

ÉCOLE DOCTORALE N° 644
Mathématiques et Sciences et Technologies de l'Information et de la Communication en Bretagne Océane
Spécialité : *Télécommunications*

Par
Mona HASSAN KASSEM

Radio Resource Management for Energy Efficient Cellular Networks with Intelligent Reflecting Surfaces

Thèse présentée et soutenue à Brest, le 12 Décembre 2025
Unité de recherche : Lab-STICC (Laboratoire des Sciences et Techniques de l'Information de la Communication et de Connaissance), CNRS, UMR 6285

Rapporteurs avant soutenance :

Abdelhafid ABOUAISSA	Professeur des université, Université de Haute Alsace, IUT de Colmar, France
Sofiane HAMRIOUI	Enseignant-chercheur HDR, ESAIP Ecole d'ingénieurs, Anger, France

Composition du Jury :

Président :	Karine AMIS	Professeur IMT Atlantique, Technopole Brest-Iroise, Brest, France
Examinateurs :	Raja CHIKY	Enseignant-chercheur HDR, Ingénieurs, XLIM, Limoges, France
	Ali MANSOUR	Professeur ENSTA IP Paris, Campus de Brest, France
Dir. de thèse :	Koffi-Clément YAO	Maître de conférences HDR, Université de Bretagne Occidentale, Brest

Invité(s) :

Hussein AL HAJ HASSAN	Ingénieur, PhD, chef d'équipe à Vedecom France, Versailles, France (Encadrant)
Abbass NASSER	Professeur Associé HDR, Holy-Spirit University of Kaslik, USEK, Liban (Co-encadrant)

Acknowledgement

I would like to express my deepest gratitude to all who supported me throughout this journey. Above all, I give thanks to God for guidance, patience, and perseverance.

— Prof. Koffi-Clement YAO, my primary supervisor, for his continuous guidance, expertise, and the autonomy he granted me as an independent researcher.

— Dr. Hussein AL HAJ HASSAN, for his substantial contributions, insightful discussions, and constant encouragement.

— Dr. Abbass NASSER, for his thought-provoking opinions and constructive criticism.

— My rapporteur, Prof. Abdelhafid ABOUAISSA and Dr. Sofiane HAMRIOUI, for their invaluable time, insightful feedback, and careful reading of this thesis.

— The examiners, Prof. Karine AMIS, Dr. Raja CHIKY, and Prof. Ali MANSOUR, for honoring me by accepting to evaluate my work.

— Postdoctoral researchers Hesham SADAT, Kahina BENSAF, and PhD student Nour RIZK, for their fruitful discussions and valuable insights.

— My parents, for their unconditional love, unwavering support, and high expectations.

— My husband, Ali, and my daughter Malak, whose love, encouragement, and patience have been constant motivators throughout this journey.

Mona HASSAN KASSEM

Table of Contents

List of Figures

List of Tables

Abbreviations

AAR	**A**verage **A**chievable **R**ate
AF	**A**mplify and **F**orward
AmBC	**Am**bient **B**ackscatter **C**ommunication
AO	**A**lternating **O**ptimization
AoA	**A**ngle **o**f **A**rrival
AoD	**A**ngle **o**f **D**eparture
AP	**A**ccess **P**oint
AWGN	**A**dditive **W**hite **G**aussian **N**oise
B5G	**B**eyond **5** **G**eneration
BCD	**B**lock **C**oordinate **D**escent
BER	**B**it **E**rror **R**ate
BPSK	**B**inary **P**hase and **S**hift **K**eying
BS	**B**ase **S**tation
CE	**C**hannel **E**stimation
CIR	**C**hannel **I**mpulse **R**esponse
CR	**C**ognitive **R**adio
CRNs	**C**ognitive **R**adio **N**etworks
CS	**C**ompressive **S**ensing
CSCG	**C**ircularly **S**ymmetric **C**omplex **G**aussian
CSI	**C**hannel **S**tate **I**nformation
CSS	**C**ooperative **S**pectrum **S**ensing
DE	**D**eterministic **E**quivalent
DF	**D**ecode and **F**orward
DL	**D**eep **L**earning
DRL	**D**eep **R**einforcement **L**earning
EE	**E**nergy **E**fficiency
EM	**E**lectro **M**agnetic
FD	**F**ull **D**uplex
FPGA	**F**ield **P**rogrammable **G**ate **A**rray

Gbps	**G**iga **b**it **p**er **s**econd
HIS	**H**igh **I**mpedance **S**urfaces
HWI	**H**ard**W**are **I**mpairments
HetNet	**Het**erogeneous **Net**work
HD	**H**alf **D**uplex
IID	**I**ndependent and **I**dentically **D**istributed
IoT	**I**nternet **o**f **T**hings
IRS	**I**ntelligent **R**eflecting **S**urfaces
IWW	**I**ntelligent **W**ireless **W**all
LS	**L**east **S**quares
LIS	**L**arge **I**ntelligent **S**urfaces
LoS	**L**ine **o**f **S**ight
MAC	**M**ultiple **A**ccess **C**hannel
MBS	**M**acro **B**ase **S**tation
MC	**M**utual **C**oupling
MEC	**M**obile **E**dge **C**omputing
m	**m**eters
MEMS	**M**icro **E**lectro **M**echanical **S**ystems
ML	**M**achine **L**earning
MIMO	**M**ultiple **I**nput **M**ultiple **O**utput
m-MIMO	**m**assive **MIMO**
MISO	**M**ultiple **I**nput **S**ingle **O**utput
MRC	**M**aximum **R**atio **C**ombining
MRT	**M**aximum **R**atio **T**ransmission
MU	**M**ulti **U**ser
MU-MISO	**M**ulti **U**ser **M**ultiple **I**nput **S**ingle **O**utput
MMSE	**M**inimum **M**ean **S**quare **E**rror
MSE	**M**ean **S**quare **E**rror
mm-wave	**m**illi**m**eter **wave**
NLoS	**N**on **L**ine **o**f **S**ight
NOMA	**N**on **O**rthogonal **M**ultiple **A**ccess
NLIP	**N**on **L**inear **I**nteger **P**roblem
OFDMA	**O**rthogonal **F**requency **D**ivision **M**ultiplexing
PB	**P**ower **B**eacon

PGM	**P**rojected **G**radient **M**ethod
PIS	**P**assive **I**ntelligent **S**urfaces
PIN	**P**ositive **I**ntrinsic **N**egative
PR	**P**rimary **R**eceiver
PU	**P**rimary **U**sers
QCQP	**Q**uadratically **C**onstrained **Q**uadratic **P**rogram
QAM	**Q**uadrature **A**mplitude **M**odulation
QoS	**Q**uality **o**f **S**ervice
RANs	**R**adio **A**ccess **N**etworks
RBM	**R**eflecting **B**eamforming **M**atrices
RF	**R**adio **F**requency
RM	**R**iemannian **M**anifold
RL	**R**einforcement **L**earning
RLC	**R**esistor **L**nductor **C**apacitor
Rx	**R**eceiver
SeUCE	**S**equential **U**ser **C**hannel **E**stimation
SiUCE	**S**imultaneous **U**ser **C**hannel **E**stimation
SDR	**S**emi **D**efinite **R**elaxations
SDP	**S**emi **D**efinite **P**rogram
SBS	**S**mall **B**ase **S**tation
SCA	**S**uccessive **C**omplex **A**pproximation
SE	**S**pectral **E**fficiency
SEP	**S**ymbol **E**rror **P**robability
SIC	**S**uccessive **I**nterference **C**ancellation
SIMO	**S**ingle **I**nput **M**ultiple **O**utput
SISO	**S**ingle **I**nput **S**ingle **O**utput
SM	**S**leep **M**ode
SNR	**S**ignal **t**o **N**oise **R**atio
SINR	**S**ignal **t**o **N**oise plus **I**nterference **R**atio
SS	**S**pectrum **S**ensing
STM	**S**trongest **T**ap **M**aximization
SU-MISO	**S**ingle **U**ser **M**ultiple **I**nput **S**ingle **O**utput
SU	**S**econdary **U**ser
Tx	**T**ransmitter

THz	**T**erra **H**ertz
UEs	**U**ser **E**quipments
ULA	**U**niform **L**inear **A**rray
UAV	**U**nmanned **A**erial **V**ehicle
V-BLAST	**V**ertical **B**ell **L**abs **A**yered **S**pace **T**ime
WPT	**W**ireless **P**ower **T**ransfer
WSR	**W**ireless **S**um **R**ate
ZF	**Z**ero **F**orcing
5G	Fifth **G**eneration
B5G	**B**eyond **5G**
6G	Sixth **G**eneration

List of Symbols

$\mathcal{A} = \{a_1, a_2, a_3, a_4\}$	Action space (Active, LSM, MSM, DSM)
$a_{i,j}$	LoS component of the channel
$\boldsymbol{\alpha}$	Amplitude of the reflection coefficient
$\alpha_{i,j}$	Path loss exponent of the channel
$\boldsymbol{a}_i^*$	Best selected SBS for user i
B_k	Bandwidth allocated to user k without IRS
B_T	Total bandwidth at the BS
$\mathcal{B}_k^I$	Bandwidth allocated to user k assisted by IRS
$b_{i,j}$	NLoS component of the NLoS component of the channel
β	Fraction of bandwidth
$D(a_t)$	Service degradation when SBS is in SMs
$D(a_t)$	Service degradation in mode a_t
$d_{\max}$	Maximum association distance
d_r	Distance between the IRS and the user
d_s	Distance between the BS and the user
d_{sr}	Distance between the BS and the IRS
dec_f	Decaying factor in Q-learning
dis_f	Discount factor in Q-learning
E_{max}	Total number of epochs during simulation
$\mathbf{f}$	Transmit beamforming vector
f_c	Carrier frequency
G_d	Antenna gain at the receiver
G_s	Antenna gain at the transmitter
h_r	Channel impulse response between IRS and user k
h_s	Channel impulse between the BS and the user
h_{sr}	Channel impulse response between BS and IRS
$\bar{h}_{i,j}$	LoS component of the channel
$\tilde{h}_{i,j}$	NLoS component of the channel
$[h_{sr}]_n$	n^{th} component of h_{sr}
I_{max}	Total simulation time
K	Total number of users
$K_{i,j}$	Rician K factor
$\mathcal{L}_i(t)$	Discretized load level at SBS i at time t
L_r	Learning rate in RL
M	Number of antennas at the BS
N	Total number of elements in the IRS

N_0	Variance of AWGN
N^{tot}	Total number of elements in the IRS (same as N)
$N_{users}(t)$	Number of users in each cell at time t
$N_{\text{users}}(t)$	Number of users at time t (Poisson distributed)
N_a^{min}	Size of a block in the IRS module
n_b	Number of IRS resources or blocks
n_k	AWGN (at the receiver k, at time t)
n_p	Number of possible user's positions within the cell
n_p^{ser}	Number of served users by the BS at certain position within the cell
$P(a_t)$	Power consumption in mode a_t
P_{active}	Power consumption of SBS in active mode
P_{ass}	Percentage of assistance
P_{cov}	Percentage of coverage of the BS
$P_{LSM}, P_{MSM}, P_{DSM}$	Power consumption of SBS in: LSM, MSM, DSM
p, p_k	Transmit power from the BS (general, by user k)
$P_{R_k}, P_{R_k}^I$	Received power by user k (without IRS, with IRS)
$\boldsymbol{q}_t$	System state at time t
$Q(q_t, a_t)$	Q-value for state q and action a
$Q(\boldsymbol{q}_t, a_t)$	Q-value for state-action pair $(\boldsymbol{q}_t, a_t)$
$rand(\mathcal{A})$	Random action uniformly selected from action set $\mathcal{A}$
$R_k, R_k(t)$	Bit rate for user k (general, at time t)
$R_k^I, R_k^I(t)$	Bit rate for user k with IRS (general, at time t)
$r(q_t, a_t)$	Reward obtained by taking action a in state q
r_t	Immediate reward at time t
s	Unit signal information
S	Transmit beamforming vector
S_c	Side length of the square shape of a cell
s_c	Side length of the small squares inside the cell
S_{B_k}	Bandwidth saving for user k
s_t	State of the system at time t
$\mathcal{S}$	Set of environment states in RL
$SNR_k, SNR_k(t)$	Signal to Noise Ratio at user k (general, at time t)
$SNR_k^I, SNR_k^I(t)$	Signal to Noise Ratio at user k with IRS (general, at time t)
$\mathcal{U}$	Set of users originally served by the SBS
$\mathbf{u}_i$	Position of user i
$\mathcal{U}_i$	Subsets of unserved users assisted via IRS towards SBSi
$\mathcal{U}_{\text{uns}}$	Set of unserved users after primary association
x	Gaussian input signal
x_i	Number of blocks assisted to user i
$\mathbf{x}_{s_j}$	Position of SBS j
$y, y_k, y_k(t)$	Received signal (general, by user k, at time t)

$\Delta_{\text{IRS}}(t)$	IRS performance gain at time t
ϵ	Exploration factor
ϵ	Probability threshold for ϵ-greedy action selection
$\lambda(t)$	Mean user arrival rate of the Poisson process at time t
Θ	IRS reflection coefficient
θ_i	Phase shift of the reflection coefficient
$\boldsymbol{\theta_{(AoD)}}$	Angle of Departure
σ_k^2	Noise power at user k
$\Psi(t)$	Energy-QoS tradeoff
$\|\|.\|\|$	Eucledien norm of a vector
$(.)^T$	Vector transpose operator
$(.^*)$	Conjugate operator
$E(.)$	Mathematical expectation
$\mathbb{I}(\cdot)$	Indicator function (1 if condition is true, 0 otherwise)

Chapter 1

Introduction

This chapter provides an overview of the background and research motivation that form the basis of this thesis. It then outlines the research scope, objectives, and finally provides an overview of the thesis structure.

1.1 Background

While the evolutionary progress of the fifth Generation (5G) has gained considerable momentum, the revolutionary scenario envisioned of 5G, characterized by a system predominantly operating at millimeter wave (mm-wave) frequencies and supporting a wide range of Internet of Things (IoTs) applications, has yet to be materialized [1]-[2]. Although the 5G wireless network is still deployed around the world, both academia and industry are excited about the future Beyond 5G (B5G) which requests to satisfy more demanding requirements than 5G, such as Energy Efficiency (EE), high reliability, Spectral Efficiency (SE), ultra high data rates, e.g. Gigabit per second (Gbps), global coverage and connectivity, and low latency [2]-[3]. The vision and expectation for the key performance requirements of the sixth Generation (6G) compared to 5G [4] is shown in Figure 1.1. Although the peak data rate for 5G was intended to be 20 Gbps, the goal for 6G is to provide a maximum data rate of 1000 Gbps and a user experience data rate of 1 Gbps. The performance of the entire network must be improved in order to deliver advanced multimedia services to a large number of users, for example, by aiming to achieve a SE that is twice as high as 5G. Therefore, it is critical to develop sustainably inventive and new technologies to enable future wireless network capacity increase at a moderate and manageable budget, complexity, and power consumption with the widespread adoption of user devices that will form the future of IoTs.

On the other hand, time varying wireless channels are a major challenge in building ultra reliable wireless communications because of user mobility. Traditional ways to address

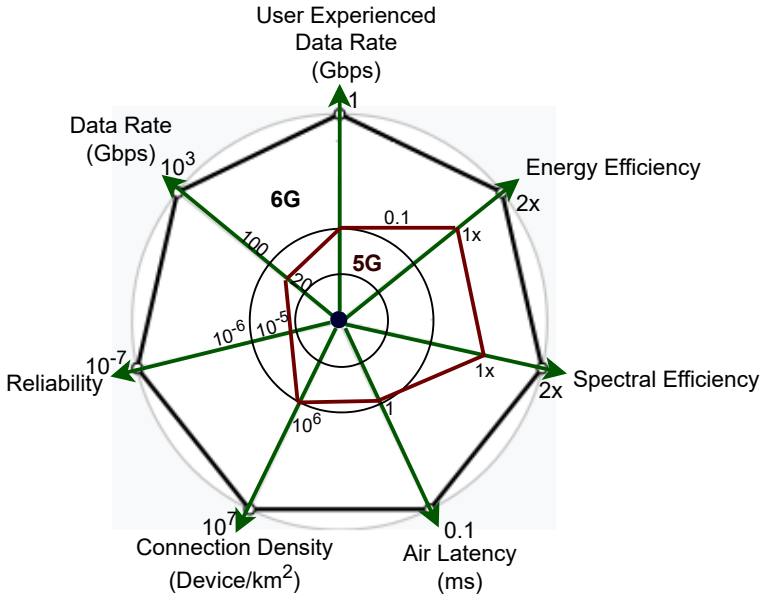

Figure 1.1 – Comparison between 5G and 6G.

this problem are to use different modulation, coding, and diversity plans to compensate for channel fading, or to adjust to it using modified power, beamforming methods, and rate management [5]. However, these traditional approaches require additional costs and they have a restricted amount of influence on the essentially random nature of wireless channels, making the basic obstacle to establishing high capacity and reliability wireless communications insurmountable.

Moreover, signal transmission is subject to scattering, reflection, and diffraction before reaching the destination, resulting in an excess of arbitrarily degraded and deferred extra versions of the source waves along various paths due to the unpredictability of the radio environment. This channel fading change becomes a fundamental restricting element in the optimization of the performance of EE and SE wireless networks. In addition, increasingly more active nodes, such as Access Points (APs), relays, and distributed antennas to shorten the communication distance to achieve enhanced network coverage and capacity. However, this incurs higher energy consumption and deployment/backhaul/maintenance cost, as well as the more severe and complicated network interference issue.

To utilize the large and available bandwidth, communication systems are migrating to higher frequency bands such as TeraHertz (THz). This shift inevitably requires deploying more active nodes and mounting them with more antennas to compensate for the higher propagation loss over distance.

In view of all the above issues and limitations, it is imperative to develop a new and innovative technology to achieve a sustainable capacity growth of future wireless networks with low and affordable cost, complexity, and energy consumption. It should be also noted that the existing modern physical layer solutions are deficient and overall progress is still modest, necessitating radical and new physical layer solutions. The attention is attracting in new communication patterns that take advantage of the extreme randomness of the propagation environment to simplify the transceiver components and the Quality of the Service (QoS).

1.2 Motivation

Recently, literature has shown that a novel technology called Intelligent Reflecting Surfaces (IRSs) is a viable option for enhancing system performance (e.g., data rate, energy efficiency, etc.) in cellular networks.

Generally speaking, IRS is a planar surface containing a large number of passive reflecting elements, each of which can induce a controllable amplitude and/or phase change to the incident signal independently. In particular, an IRS is intended to be deployed in situations where the signal quality between a source and its destination is poor or simply to aid the transmission. Therefore, by deploying IRSs in wireless networks and smartly coordinating their reflections, the signal propagation/wireless channels between transmitters and receivers can be flexibly reconfigured to achieve desired realizations and/or distributions. Thus, IRS provides a new means to fundamentally tackle wireless channel fading impairment and interference issues, and potentially achieves a significant improvement in wireless communication capacity and reliability.

Beyond its conceptual appeal, IRS also possesses various practical advantages for implementation. Its reflecting elements (e.g., low-cost printed dipoles) only passively reflect impinging signals without requiring any transmit Radio Frequency (RF) chains, thus can be implemented and operated with orders of magnitude lower hardware and energy costs compared to traditional active solutions. Furthermore, IRS operates in Full Duplex (FD)

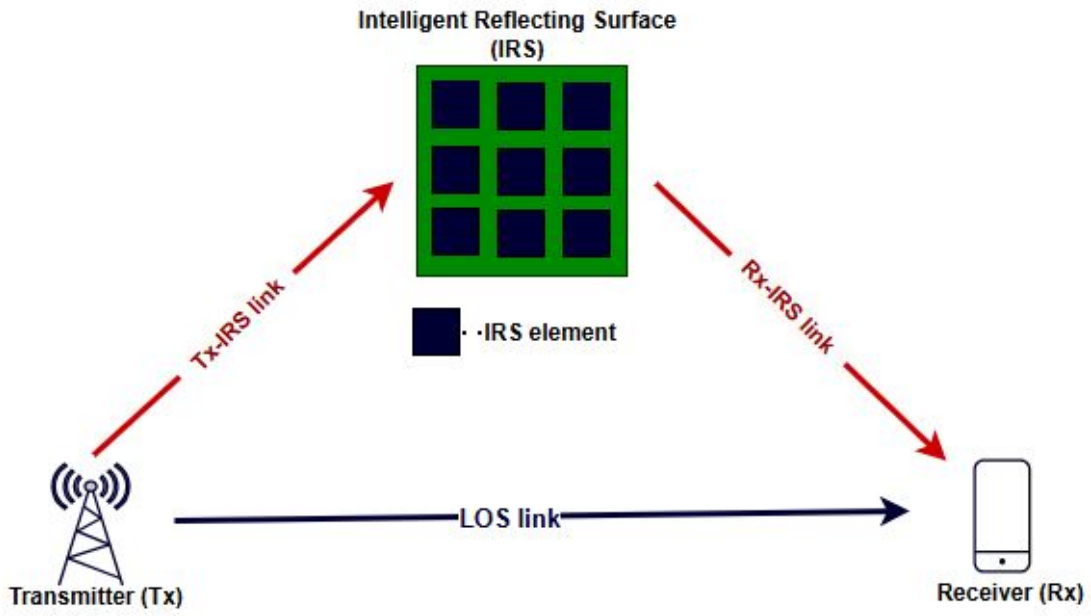

Figure 1.2 – A typical IRS-assisted wireless communication system.

mode naturally and is free from self-interference and antenna noise amplification. Additionally, IRS has a low profile, conformal geometry, and light weight, making it easy to mount on or remove from environmental objects for deployment or replacement. Finally, IRS serves as an auxiliary device that can be implemented transparently into existing wireless networks (e.g., cellular networks or WiFi), providing great flexibility and compatibility.

Consider a typical IRS-assisted wireless communication system as depicted in Figure 1.2. The IRS is used to enhance communication performance between a transmitter (Tx) and a receiver (Rx). The Rx receives the Line of Sight (LoS) signal through the direct link as well as constructive reflected signals from the IRS through the Tx-IRS-Rx link simultaneously. Consequently, the communication performance between Tx and Rx can be significantly improved.

A closer examination of the proposed IRS reveals that it can be considered as formed of blocks of resources that can be shared by several users, as illustrated in Figure 1.3.

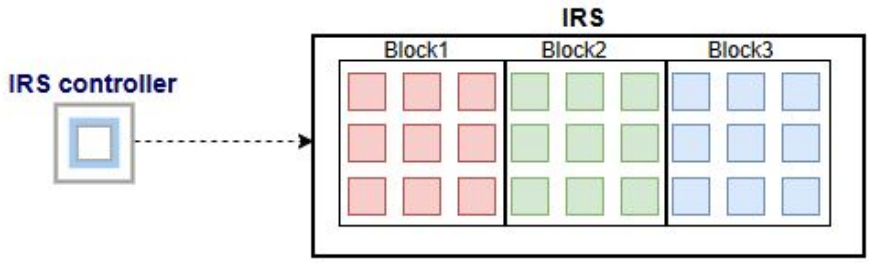

Figure 1.3 – IRS as blocks of resources.

1.3 Research Scope and Overview

The next generations of mobile communication systems B5G and 6G are expected to provide a great platform for a wide range of IRS aided communication applications. In this regard, IRS assisted communication can be seen as a key enabler of such systems [6]. Despite IRS based communication techniques being an actively researched topic over the past decade, there are still many open problems. With a focus on IRS theory, this thesis contributes to the wireless field by providing applied and fundamental research results that address open areas of IRS assisted technology with more focus on the position of the IRS versus the BS, different channel models, and the application of Reinforcement Learning (RL) for dynamic resource management. The thesis investigates IRS based communications under different channel conditions, modeled by conventional Rayleigh and Rician fading distributions for outdoor environments. Also, it explores the achievable data rate and the upper limit of the ergodic capacity, it provides a deep understanding of the factors that together affect the performance, and shows how this understanding can be exploited to better design B5G and 6G communication systems. The main contribution of this thesis provides is to understand how IRS resources can be managed to decrease the energy consumption of a wireless network and to improve better achievable data rate performance and achieve a better percentage of saving power in the far-field regime. By theoretically studying the performance, we aim to give insights on major factors to cover a certain area and to get better data rate for the users.

1.4 Research Objectives

The primary research objectives involve the following ones:

1. Investigate the bandwidth savings achievable for an IRS assisted single user com-

munication system, considering both LoS and Non Line of Sight (NLoS) channel conditions. Performance will be validated across variations in the number of users, IRS position, required bit rate, and cell radius.

2. Evaluate the performance of various IRS placements and propose two low-complexity heuristic algorithms for efficient management of IRS resources.
3. Explore the impact of different channel models (e.g., Rician vs. Rayleigh fading) on the upper bound of the ergodic capacity [1] performance, particularly noting the degradation when only Rayleigh fading is assumed.
4. Inspect user signal strengths in an IRS-assisted cellular network for various channel models, such as Rician and Rayleigh fading.
5. Optimize the number of antennas at the Base Station (BS) under a specified Signal to Noise Ratio (SNR) constraint. This is essential for reducing the complexity and cost of cellular network infrastructure during the planning phase.
6. Analyze system performance across different antenna configurations, including Single-Input Single-Output (SISO), Multiple-Input Single-Output (MISO), and Multi-User MISO (MU-MISO) systems.
7. Examine the power versus user drop trade-off problem in a cellular network architecture by deploying IRS technology with an intelligent cell switching mechanism.
8. Propose an intelligent distributed controller based on Reinforcement Learning (RL) to select the optimal Sleep Mode (SM) level for SBSs.
9. Maximize energy efficiency under real time traffic conditions while maintaining high Quality of Service (QoS) through seamless service continuity and IRS enabled coverage compensation.
10. Demonstrate that the integration of RL and IRS can achieve substantial energy savings without compromising the user experience or service quality.

1.4.1 Thesis Overview

The remainder of this thesis is organized as follows:

— **Chapter 2** provides the necessary background. It includes a review of IRS architecture and control mechanisms, performance analysis and optimization, channel

1. The ergodic capacity represents the average rate at which information can be transmitted over a channel, assuming that the channel conditions are varying randomly over time [7].

estimation, IRS deployment scenarios, future research directions, and finally, a summary of the chapter.

— **Chapter 3** investigates the percentage of bandwidth saved using IRS based schemes and analyzes the impact of different IRS placements. It also explores the performance of this technology in both LoS and NLoS channels and presents our two low-complexity heuristic algorithms.

— **Chapter 4** analyzes the performance of a Single User MISO (SU-MISO) system under a Rayleigh fading channel between the transmitter and the receiver, while assuming LoS connections between the Base Station (BS) and the IRS, and the IRS and the destination. The results validate the proposed approach and demonstrate that the introduction of the IRS enhances the overall network coverage and performance.

— **Chapter 5** addresses the problem of power saving optimization in B5G SBSs by implementing an IRS and multi-level SMs. We propose a distributed Q-learning algorithm to control the activity of a SBS, assisted by an IRS, to minimize both power consumption and the rate of user drops. The chapter also investigates the management of IRS resource blocks to assist unserved users.

— **Chapter 6** concludes the thesis with a summary of the findings, and outlines future directions and challenges for this research area.

Chapter 2

Literature Review

This chapter provides a comprehensive overview of Intelligent Reflecting Surfaces (IRSs), with emphasis on their hardware architecture, functionality, and evolving role in future wireless networks. The aim is to present fundamental concepts that support IRS operation while reviewing main advances in performance analysis, channel modeling, and optimization techniques. Furthermore, we highlight how Machine Learning (ML) methods can be integrated with IRS to improve adaptability and efficiency. Following the extensive review of IRS, we provide a dedicated analysis of general energy efficiency (EE) techniques in modern cellular networks, specifically focusing on intelligent resource management at the Base Station (BS) level. The goal is to establish the necessary background and identify existing research gaps for the novel contributions presented in this thesis.

The organization of this chapter is as follows: Section 2.1 introduces IRS hardware and functionality, including circuit, geometrical, and material tuning aspects. Section 2.2 discusses performance analysis and optimization approaches. Section 2.3 reviews different IRS channel estimation methods, while Section 2.4 covers IRS deployment strategies at both link and network levels. Section 2.5 examines the integration of machine learning with IRS. Section 2.6 then presents a review on techniques of decreasing the energy consumption of a network. Finally, Section 2.7 outlines promising research directions, and Section 2.8 provides a summary of the chapter.

2.1 IRS Hardware and Functionality

In this section, we present the fundamentals of IRS assisted wireless communication, encompassing the primary IRS architectures, hardware components, and control mechanisms, along with the signal and channel models discussed in existing literature.

2.1.1 IRS Architecture and Control Mechanism

Fresnel equations and Snell's law [1]control the intensities and the directions of the reflected and diffracted waves [8]. When the wave impacts with a meta surface, the situation changes. A shifting in the resonance frequency and consequently changes in the boundary conditions might emerge from the periodic arrangement of the scattering components. Consequently, extra phase shifts will be carried by the reflected and diffracted waves. The Electromagnetic (EM) characteristics of the meta surface will be fixed once it is produced with a certain physical structure, enabling it to be used for a given goal, such as an ideal absorber working at a specific frequency.

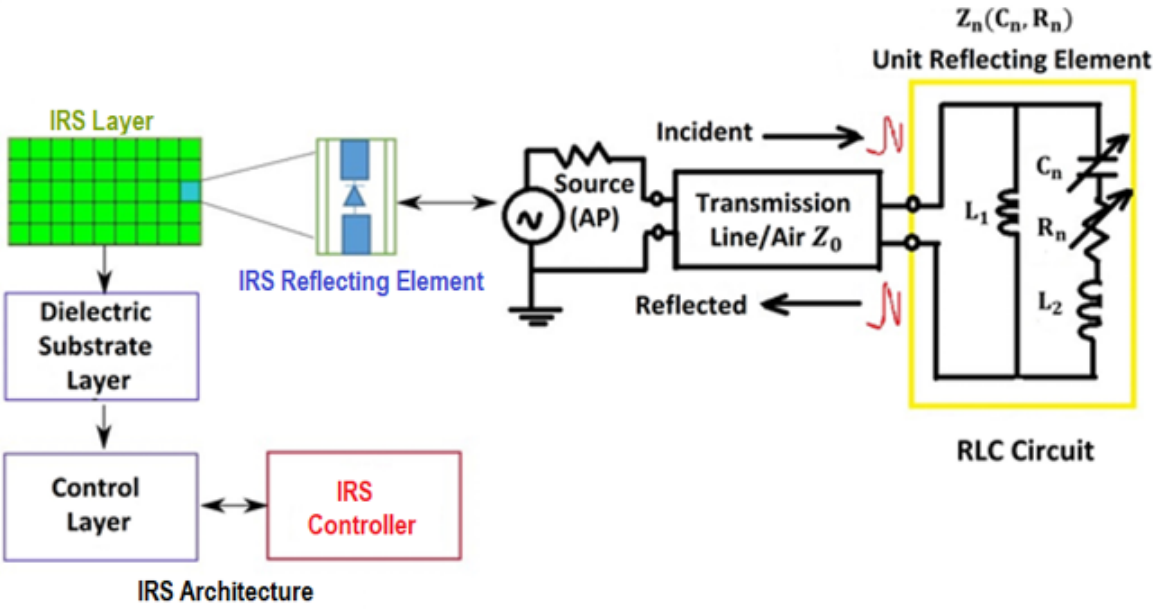

Figure 2.1 – Structure of the IRS including only its reflecting element and the equivalent RLC circuit model (without layer 2) [9].

The IRS is made up of a programmable meta surface that can completely regulate the phase changes that individual scattering components experience. An external stimulus can be applied to the scattering components, changing their physical characteristics and thus altering the meta surface's EM properties without reconstruction [10]. Figure 2.1 shows a typical IRS design [9], which includes three layers and a smart controller. A dielectric substrate, in the first layer (IRS layer), is build of with several tunable and

1. Fresnel equations and Snell's law describe the behavior of light waves at the boundary between two media with different refractive indices.

reconfigurable metallic patches put on it to directly regulate incoming waves. The second layer is typically made up of copper substance to avoid transmission power losses due to IRS reflection. In contrast, in the third layer, a control integrated board is in charge of both excitation and real-time control of the reflection amplitudes and phase shifts of the reflecting elements. In addition, a smart controller linked to each IRS also activates and decides the adaptation of the reflection, which may be done with a Field Programmable Gate Array [2](FPGA). Other network components such as user terminals and BSs can be connected to each other over wireless or wired backhaul and control lines due to the role of the IRS controller as a gateway. In practice, dedicated sensors can be deployed in the first layer, for example, mixed with IRS reflecting elements, to detect surrounding radio signals of interest and help the smart controller design reflection coefficients, to improve IRS's environmental learning capability [3].
There are three basic sorts for the varied tuning processes that have been verified in the literature, namely:

1. **Circuit tuning**: Includes modification or integration of individual impedance into the unit cell circuit model using changeable capacitors and switches inside and among unit cells.
2. **Geometric tuning**: Change the form of the unit cell physically, causing the association circuit model to change dramatically.
3. **Material tuning**: Modify the material properties of a substrate or small section of a unit cell to change the responsiveness and characteristics of the small component of the unit cell (substrate layer).

Circuit tuning

The EM behavior of actual passive transmission lines, antennas, and meta materials can be modeled as a collection of equivalent inductive, capacitive, and resistive circuits. This way of breaking down complex geometric shapes into a known circuit model is highly useful for estimating how the updated designs would perform. Meta material circuit tuning is described as methods for introducing, changing, and controlling specific components in the meta material's equivalent circuit. Due to their simplicity in their combination with

2. FPGA is a type of integrated circuit that can be reconfigured after manufacturing. It consists of a matrix of configurable logic blocks interconnected by a programmable routing network. FPGAs are used in various applications, including digital signal processing, artificial intelligence, and high performance computing.

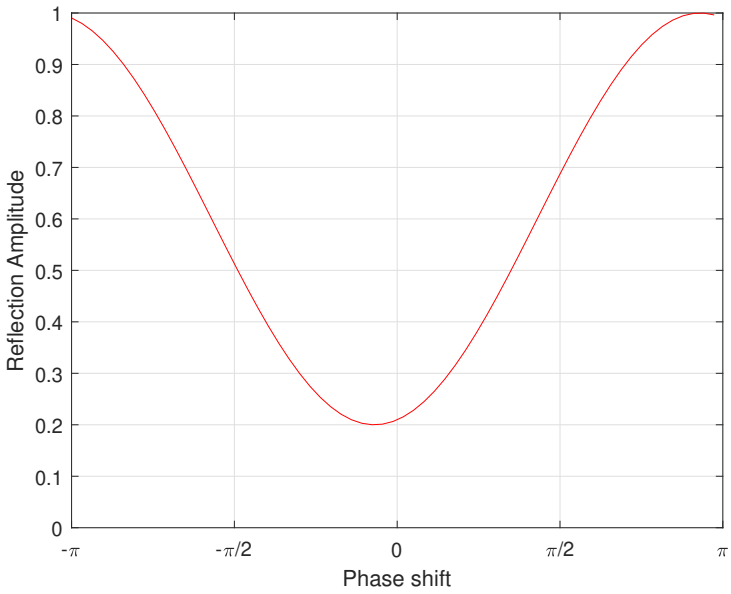

Figure 2.2 – Reflected amplitude vs. phase shift for IRS element.

a variety of meta materials, varactor diodes [3] are the most frequently used tuning method [11]. The combination of a varactor in a meta material design is frequently referred to as active meta material even though the device remains inactive for radio frequencies and is only active in its desire for a direct current bias [12].

In most situations, varactors have been supposed to be perfect or nearly ideal linear capacitors with good accuracy, although numerous researches have looked at the non linearity aspect of varactors at different power levels [13]. In terms of applicability and simplicity of integration, the use of Positive Intrinsic Negative [4] (PIN) diodes [14] in a meta material is similar to the use of varactors, although these actuators influence resistance rather than capacitance. In practice, independent amplitude and phase shift control of every IRS element is preferable for superior reflection design. However, this needs more design elements and complex architectural patterns than simply controlling phase or amplitude independently [15]. Whereas continuously adjusting the reflection coefficient is advantageous for improving communication performance, it is challenging to put into practice because better quality reflective components need not only more expensive but also more

3. Varactor diodes are semi conductor diodes whose capacitance varies with applied reverse voltage. They are used in various applications, including frequency tuning in RF circuits, voltage controlled oscillators, and parametric amplifiers.

4. PIN diodes are semi conductor diodes with a wide intrinsic region between the p-type and n-type regions. They have high switching speed, low forward voltage drop, and high reverse breakdown voltage.

complicated hardware architecture. Such as, at least $\log_2(8) = 3$ PIN diodes are required to allow 8 levels of phase changes per IRS unit. By suitably quantizing the intervals $[0, 1]$ and $[0, 2\pi]$, we can calculate the discrete amplitude and phase shift values, respectively. Although phase shift control (or phase beamforming) can achieve better passive beamforming performance than amplitude control (or amplitude beamforming), it is more expensive to implement for an IRS when the number of control bits and discrete levels for each reflective element are the same. The authors in [16] proposed a practical reflection model by simulating every reflective component as a resonant circuit with specific capacitance, inductance, and resistance values. Based on their prototype, it was discovered that the reflecting element's amplitude response and phase shift are not linearly related, and thus, not separately controllable. The reflection amplitude achieves a minimum value at zero phase shift, as shown in Figure 2.2, but increases uniformly as the phase shift approaches π or $-\pi$, asymptotically approaching one.

Geometrical tuning

Many meta materials rely on conductive components that may combine with overlapping EM signals to produce the required magnetic or electric resonance or other beneficial behavior. Since meta material characteristics are generally influenced by the form, direction, size, and proximity of conducting components, methods that change the geometric features of the conductive elements can be a powerful tool for adjusting or switching meta material response. By changing conducting components with respect to each other, meta materials may be geometrically adjusted. Micro Electro Mechanical Systems [5](MEMS) are often used in THz meta materials to accomplish the mechanical movement of conducting components. The coupling between conducting components varies as they are pushed nearer or farther away, resulting in variations in resonance frequency or resonance strength. Moving conducting elements can also change the shape of the element. The stretching of the substrate, furthermore to separate the elements on the substrate, resulting in significant variations in the resonance frequency of the elements, is a unique approach for moving conducting components in a meta material. Several tunable High

5. Micro Electro Mechanical Systems are tiny devices fabricated using micro-fabrication techniques that integrate electrical and mechanical components on a single chip, with feature sizes typically ranging from micrometers to millimeters. They are widely used in applications such as accelerometers, gyroscopes, and optical switches.

Impedance Surfaces[6](HIS) have been shown to change the phase of the reflected wave by mechanically sliding an upper plate of elements along the surface or vertically [11]. Geometrical tuning may result in essential variations in meta material features since the geometry of the conducting elements has such a large influence on the related resonant frequency[7]. Geometrical tuning, on the other hand, is difficult to execute since it requires a physical control mechanism.

Material tuning

While altering the structure of the resonant components provides a number of tuning possibilities, the properties of the meta material are ultimately determined by the constituent materials utilized to create the unit cell. Various constituent materials have been examined and used for tuning meta materials by changing the permittivity[8], permeability[9], and conductivity[10]of unit cell sections.

Among the three tuning approaches, circuit tuning has been the most widely adopted in practice due to its rapid response, minimal reflection loss, low power consumption, and low implementation cost [6]. Figure 2.1, extracted from [9], presents an example of a reflecting element and its corresponding Resistor Inductor Capacitor (RLC) circuit based on a PIN diode installed in the center of the element.

The preceding discussion establishes that the physical realization of an IRS is fundamentally an engineering problem involving a delicate balance between reflection gain, tunability speed, and hardware complexity. Whether achieved through circuit, geometric, or material tuning, the goal remains to precisely control the phase and amplitude of the reflected electromagnetic wave. This physical control, enabled by the architectural ele-

6. High Impedance Surfaces are artificial surfaces designed to have a high impedance to EM waves. They are used in various applications such as antenna design.

7. The geometry of conducting elements is a critical factor in determining the resonant frequency of electrical systems. By carefully considering the length, shape, and spacing of these elements, engineers can design systems that operate at specific frequencies and meet desired performance requirements, for example, a half wave dipole antenna has a resonant frequency corresponding to a wavelength that is twice its length.

8. Permittivity is a measure of a material's ability to store electric energy. It is a property of a material that determines the electric field strength in response to an applied electric field.

9. Permeability is a measure of a material's ability to conduct magnetic flux. It is a property of a material that determines the magnetic field strength in response to an applied magnetic field.

10. Conductivity is a measure of a material's ability to conduct electric current or heat. It is the inverse of resistivity, which is a measure of a material's ability to resist the flow of electric current or heat

ments and tuning mechanisms reviewed above, directly dictates the performance of the wireless system. However, to effectively design and optimize systems that leverage this physical control, an accurate analytical understanding of signal propagation is required. Therefore, the subsequent section shifts focus from the hardware to the mathematical models, beginning with a detailed examination of signal and channel models in IRS assisted communication environments.

2.1.2 Signal and channel model

The integration of IRSs into the wireless environment introduces a paradigm shift from passive, unpredictable radio channels to controllable, software defined propagation spaces. To accurately model and predict the performance of IRS aided communication systems, it is essential to move beyond traditional channel models. This section reviews the foundational analytical frameworks necessary to characterize wave propagation in IRS environments. We begin by examining the core challenge of channel fading and the necessary evolution from classical stochastic models, followed by a detailed analysis of pathloss models that capture the unique spatial and EM properties of reconfigurable surfaces.

Channel fading

To achieve the idea of smart environments, IRS can be covered on the front of buildings in the wireless environment, such as solid structures and buildings of houses, or carried on aerial vehicles, such as Unmanned Aerial Vehicles (UAV) [17]. Therefore, for modeling and performance analysis of IRS aided wireless communication, it is necessary to employ analytical models that account for the geographical placement of IRS elements, their EM characteristics, and the wave modifications introduced by adjacent IRS elements in the environment. A transmitted radio signal in a typical wireless communication environment is in contact with many objects along the route, resulting in duplicates of the transmitted wave that occur in reflection, diffraction, and dispersion. Multipath components are signal copies that arrive at the receiver with unexpectedly and randomly different amplitudes, phase shifts, and signal delays, causing considerable distortions in the received signal due to their relative constructive or destructive addition. This is termed fading in wireless communication systems and it is a key factor in existing and future wireless communication systems. The main objective of IRS is to introduce controllable wire-

less communication in which the extremely unpredictable radio channel is turned into a controllable space by carefully modifying EM signal propagation in a software controlled manner. A channel model that contains the key characteristics of any wireless technology is required for an accurate performance assessment. The most theoretical research on wireless systems technologies under scattering conditions has been and continues to be derived from the Independent and Identically Distributed (IID) Rayleigh fading channel model [18] - [19] - [20]. When using a rectangular IRS, the authors in [21] indicate that such a paradigm does not exist realistically and present an equivalent physically valid Rayleigh fading model that could be used as a reference for evaluating IRS assisted communications. The received signal y_k can be represented as [22]:

$$y_k = (h_{s,k} + h_{sr}^T \Theta h_{r,k})\sqrt{p}s + n_k \tag{2.1}$$

where the channel between BS and IRS with N elements is denoted by h_{sr}, while $[h_{sr}]_n$ represents the nth component. $h_{s,k}$ represents the channel between the BS and the user k. The channel between IRS and destination k is denoted by $h_{r,k}$. p and s are, respectively, the transmitted power and the unit power signal information. $n_k \sim \mathcal{N}_{\mathbb{C}}(0, \sigma_k^2)$ represents the receiver noise. The IRS's properties are fully represented by the diagonal matrix:

$$\Theta = \alpha diag(e^{j\theta_1}, \ldots, e^{j\theta_N}), \tag{2.2}$$

where $\alpha \in (0, 1]$ represents the amplitude reflection coefficient and $\theta_1 \ldots \theta_N$ are the phase shift variables.

Pathloss

In the perfect propagation scenario, with no user movement and no unanticipated environmental consequences, a single uncontrolled ground reflection might cause significant signal degradation. The authors in [23] assume that a changeable meta surface covers the entire ground. The IRS can be considered as a perfect phase shifter, designed to change the reflected signal phase so that the LoS and reflected radiations add up constructively, increasing the signal strength. It has been shown that the usage of intelligent programmable surfaces has the ability to alter the scaling rule that regulates the received signal power with distance. Although, the results concluded by [23] are promising, they are not practical and realistic because they were based on several assumptions, including the ability to tune the reflected phases without any analogue to digital conversion error

and for any incident and scattered angle, as well as the lack of reflection impairments and comprehensive awareness of the phase status at the IRS. Furthermore, for more actual system models, optimizing the phases is typically not a simple process, and it is not related to our scope in this research. By researching the physics and EM characteristics of IRSs, the authors in [24] developed a free space pathloss model for IRS assisted wireless communications for various situations which can be divided into two groups:

— IRS assisted beamforming
— IRS assisted broadcasting

The suggested models reveal the relations between the free space pathloss of IRS and the distances from the transmitter and receiver to the IRS. To explain the free space pathloss of IRS assisted beamforming and broadcasting, three perceptive models for free space path loss were derived:

— The far field beamforming equation
— The near field beamforming equation
— the near field broadcasting equation

The authors in [25] improved the pathloss models derived in [24] by formulating the joint radiation pattern of the antennas and the unit cells in addition to elucidating the relation between the size and the scattering gain of the unit cell. The authors in [26] calculate the far field pathloss using physical optics methods [11] and give the explanation why the surface contains multiple reconfigurable elements that individually behave as diffuse scatterers but may collectively beamform the signal in a desirable direction with a certain beamwidth. Therefore, an IRS can be considered as an array of sub-wavelength sized diffuse scatterers that aiming the phase of their reflected signals at the receiver, resulting in anomalous reflection. Figure 2.3 illustrates the pathloss as a function of the observation angle for various IRS sizes [26]. The main beamwidth narrows as the IRS surface area expands. When the dimension is sub-wavelength (sub-λ), the IRS virtually functions as a diffuse scatterer (less than $\lambda/2$). The authors verified that the power of the received signal is proportional to the square of the IRS area and to $1/(d_{sr}d_r)^2$, where d_{sr} is the distance between the transmitter and the IRS and d_r is the distance between the IRS and the receiver. This contradicts the hypothesis [23] that the power received is proportional to $1/(d_{sr} + d_r)^2$. To counterbalance for the enormous power loss caused by the twofold attenuation, a significant number of IRS reflecting components must be used to combine

11. Physical optics is a high-frequency approximation technique used in electromagnetics to compute scattering and diffraction from large surfaces by approximating induced currents on the surface.

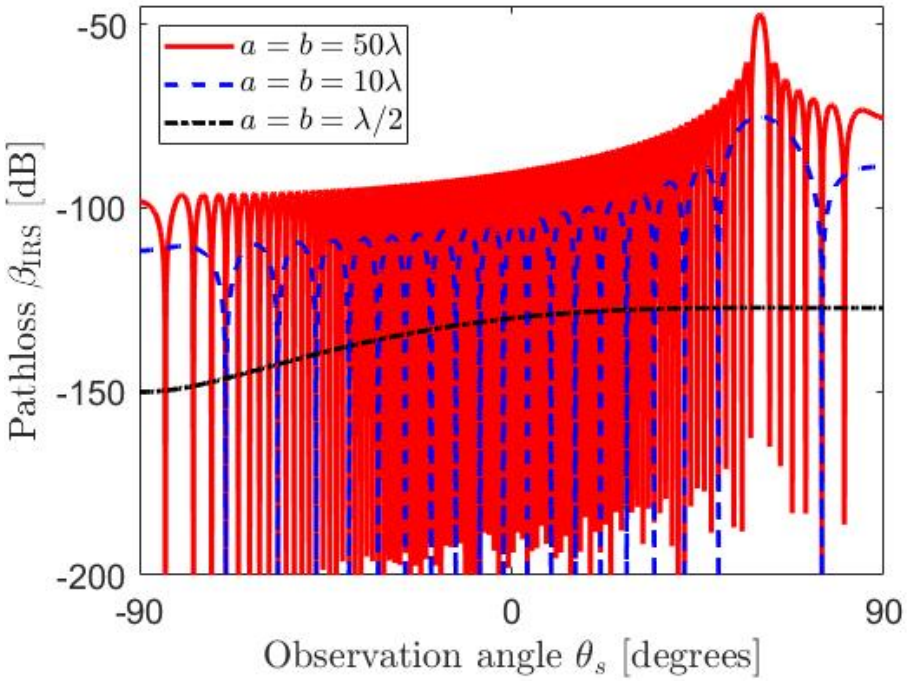

Figure 2.3 – Pathloss of the reflected path.

their reflection magnitude and phases to obtain higher passive beamforming gains. IRS comprises of several sub-wavelength components that scatter incident waves with distinct phase shifts in order to perform constructive beamforming in a certain direction. Utilizing the Huygens Fresnel principle [12] and the scalar theory of diffraction [13], the authors in [28] describe the pathloss in IRSs in both near and far fields. IRSs are represented as homogeneous layers of EM material with insignificant depth. The authors show the regimes in which the pathloss relies on the summation and multiplication of the distances between the IRS and the source, as well as the IRS and the receiver, using the stationary phase technique [14]. The analytical technique presented is proven to be sufficiently generic for use with a consistent reflecting surface, anomalously behaving reflectors, and lenses with

12. The Huygens Fresnel principle states that every point on a wavefront might be considered as a secondary source of spherical waves. The superposition of these secondary waves defines the shape of the wavefront at a later time [27].

13. The scalar theory of diffraction is a simplified model that approximates the propagation of EM waves in the far field. It assumes that the electric and magnetic fields are scalar quantities and neglects the vector nature of these fields. This approximation is valid when the wavelength of the radiation is much smaller than the dimensions of the diffracting object [27].

14. A mathematical approximation method for rapidly oscillating integrals, where the primary contribution comes from points where the function's phase derivative is zero (stationary phase points).

highly concentrating and reflecting features. The authors in [29] have given a viewpoint that unites IRS opposing behavior as a scatterer and as a mirror. It has been verified that the IRS may be seen as one, or two-dimensional object, relying on its size and distance, and its radiated power exhibits a dependency on the fourth, third, or second power of the distance, respectively. In addition, the Fresnel zone decomposition [15] is utilized to obtain a better understanding of how the various variables interact. More accurately, the importance of phase in determining the eventual pathloss exponent is discovered and demonstrated how free space propagation may be exceeded via smart dephasing. The results are calculated numerically, and the signal received in terms of distance has an unclear analytical meaning. [30] studies similar observations.

The analytical models developed in this section are essential for understanding the theoretical limitations and capabilities of IRS enabled links. Building upon this foundation, the focus now shifts from modeling the channel to evaluating and maximizing system effectiveness, which is the subject of the next section.

2.2 Performance Analysis and Optimization

This part is divided into two sections. In the first section, we present the performance analysis of the IRS utilizing different performance metrics like bit error probability and sum rate for evaluating the overall behavior of the wireless systems aided IRS and under various channels and environments. Additionally, the second part concentrates on the IRS reflection optimization techniques and algorithms.

2.2.1 Performance analysis

We will introduce the IRS advantages and performance comparisons with other wireless systems. Also, we present the behavior and the usage of the IRS as reflector, receiver and transmitter taking into consideration the performance metrics proposed in the literature for IRS supported wireless communication systems like bit error probability, coverage or outage probability, achievable data rate and ergodic capacity.
We present the advantages of IRS assisted wireless communications:

15. Fresnel zone decomposition is a method used to analyze the propagation of EM waves through a medium with varying refractive index. It divides the medium into a series of concentric zones, known as Fresnel zones, and calculates the contribution of each zone to the total field at a given point [27].

— **Densely Deployed and Sustainable Operation:** If IRSs are formed of smart meta surfaces, there are plenty of sub-wavelength unit cells in them [31]. Similar sub-wavelength heavy installations of small sub-wavelength dispersing devices are not typically utilized in radio communications, where Mutual Coupling (MC) among the reflecting elements is frequently avoided by design, by confirming that the scattering units are sufficiently far apart. This open the door for the development of novel wave and propagation scenarios that may have an effect on wireless networks' ultimate performance limits, also the introduction of new scenarios in design in which wireless systems are built to be MC fully cognizant. IRS is simply applied and removed from a variety of surfaces, including front of buildings, top ceilings, and interior walls. The IRS can be remotely powered and battery free, thanks to RFbased energy harvesting, which removes the need for active equipments that demand signal processing methods and power consumption.

— **New Signal Processing is not need for IRS assisted Communication:** The semi passive feature of IRSs paves the way for new possibilities for re-defining communication, permitting data to be transferred without the use of EM waves, instead of reprocessing existing EM signals. This may be extremely deployed in terms of minimizing EM pollution and lowering human EM exposure, which is often raised by using more network equipment and utilizing more spectra. This could be essential for the effective installations of wireless technology in areas that are vulnerable to EM fields (e.g., in hospitals).

— **Notably Focusing Capabilities:** This high focusing capability could be deployed for a variety of aims, including firstly, it enables interference free communication in densely populated areas, next, enabling accurate radio identifications of users and environment modeling, and thirdly, fill the batteries of limited power equipment by means of transfer the power wirelessly. The Intelligent Wireless Wall (IWW) is a real world example of this notable focusing characteristic. The IWW consists of an IRS that does beamforming and beam steering, furthermore ML algorithms that can accurately and automatically identify human activity [32].

— **Flexible Reconfiguration and Enhanced Capacity:** The IRS may be employed to configure the wireless channel to offer a larger link capacity while con-

suming less power for point to point communications. When the IRS is utilized, interference reduction becomes more effective, resulting in improved signal performance for end users at the cell's edge. Scattering components in multi user cellular networks can be shared and separated to optimise data transfer for many users. As a result, the IRS assisted wireless network may be able to improve QoS provisioning as well as sum rate performance or max-min fairness among users.

— **Exploring of New Wireless Application:** The IRS's advancement is likely to pave the way for new and exciting research directions. The IRS, for example, was recently presented as a unique technique for preventing wireless eavesdropping assaults by regulating the transfer at the source and the optimized reflections at the IRS at the same time. The achievable secrecy rate is significantly improved by deploying IRSs close to the legitimate or eavesdropping user and appropriately configuring the IRS passive beamforming to elevate or lower the achievable rate of the legitimate or eavesdropping user [33].

Even though the said property is in IRS aided secrecy communication, Channel State Information (CSI) is still needed between the transmitter and eavesdroppers also between the IRS and the eavesdropper. The challenge is obvious when the eavesdroppers intentionally continue to be covert, hidden or secret due to the fact that their CSI link cannot be estimated properly from their signal leakage, and therefore necessitates new channel estimation methods and robust IRS beamforming taking into account the imperfect CSI of the eavesdropper [34]. Furthermore, in large scale secrecy wireless communication networks with thousands of users, legitimate or eavesdroppers, also highly dense IRS deployments, IRS is a key to increase network security throughput and improve physical layer security for future 6G wireless modern systems where 1000x raises in data rates yield a target of 1 Terabit/sec are needed, according to Figure 1.1 . As a result, meeting these challenges of channel estimations and robust IRS beamforming in 6G massive networks deserve further investigations. Several other research fields that are evolving, including wireless power transfer, UAV communications [35], and Mobile Edge Computing (MEC), take advantage of IRS technology.

In order to appreciate the advantages of IRSs technology, it is necessary to compare with different types of relay networks and surfaces which are not coated with IRS. The SNR for IRS and Decode and Forward (DF) relay as per Figure 2.4 can be expressed as

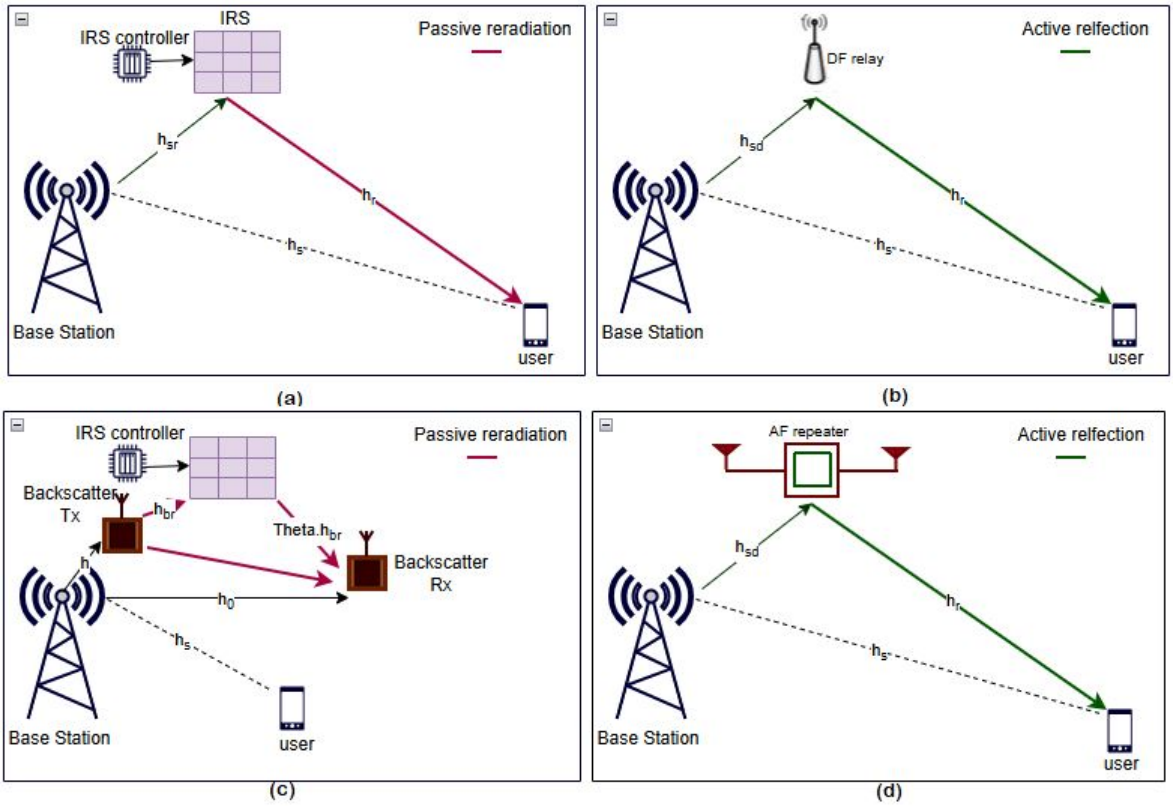

Figure 2.4 – Comparison of different wireless systems. (a) IRS assisted wireless communication, (b) DF relay assisted wireless communication, (c) Wireless backscatter communication, (d) AF repeater assisted wireless communication. h_{sr}, h_s and h_r represent the BS-IRS, BS-users, and IRS-users channels, respectively.

follows [31]:

$$SNR_{IRS} = \frac{p \mid h_s + h_{sr}^T \Theta h_r \mid^2}{\sigma^2}, \tag{2.3}$$

$$SNR_{DF} = \min\left(\frac{p_1 h_{sr}}{\sigma^2}, \frac{p_1 h_s + p_2 h_r}{\sigma^2}\right), \tag{2.4}$$

Where p is the transmit power in IRS model, and σ^2 is the noise power spectral density. In the DF model, p_1 and p_2 are the transmitted powers from the source and the relay, respectively. The channel from the source to the destination is denoted by h_s, while h_r represents the channel between the relay (or IRS) and the destination. h_{sr} is the channel between the source and the relay (or IRS). Therefore, the SE (ζ) can be calculated for

IRS/relay supported network as follows [36]:

$$\zeta_{IRS/DF} = \log_2\left(1 + SNR_{IRS/DF}\right) \tag{2.5}$$

A typical IRS assisted system model wireless communication is represented in Figure 2.4 (a). An IRS controller is employed to program the IRS reflecting elements. In addition, the IRS controller communicates with the BS via another wireless signal in order for the BS to control the IRS reflections by creating a phase shift matrix Θ that results from modifying huge low cost passive reflecting elements to configure the channel, and this represents the concept of passive signal reflections that is introduced in the research. Repeaters work in AF mode, while relays work in DF mode. Compared to AF repeaters, DF relays, as in Figure 2.4 (b), can offer superior noise immunity and reduction in inter-cell interference. On the other hand, the DF relay needs a complex transceiver and may increase the transmission latency [37] - [38]. In IRS assisted and AF/DF relay assisted communications, the receiver decodes the information symbols transmitted by the source. However, in wireless backscatter communications, it decodes the information symbols embedded in a strong interference signal.

Backscatter, as shown in Figure 2.4 (c), reflects an incoming RF signal as well as modifying and modulating it for secondary transmission, or backscatter. It is unnecessary to use and maintain separate RF sources because already available RF sources are used, resulting in cost and power savings. Impedance mismatching is the fundamental concept behind reflecting and altering RF signals [39]. It uses the impedance of an antenna to encode data into previously existing waves, but it has low data rate transmission speeds and lacks data security. Massive backscatter communication [40] is a new idea that utilizes a programmable meta surface to change the propagation environment of stray ambient waves. The meta surface's huge aperture and many degrees of freedom permit for exceptional signal control and, as a result, safe and high speed data transmission. The proposed backscatter wireless communication strategy in which the transmitter depends on a programmable meta surface to modulate the propagation environment instead of a single or a few impedance modulated dipole antennas opens the door for considerably larger control over the wave. More intriguingly, Ambient Backscatter Communication [16](AmBC) was designed to solve communication and power consumption concerns in indoor and limited

16. Ambient backscatter communication is a wireless communication technique that enables devices to harvest energy from ambient RF signals and use them to transmit data by reflecting modulated signals back to a receiver.

power IoT technologies. The authors in [41] introduce a novel approach to AmBC in the frequency domain using ambient Orthogonal Frequency Division Multiplexing (OFDM) subcarriers in combination with the IRS. The greater performance in terms of data rate and Bit Error Rate (BER) is demonstrated by analytical and numerical analyses. According to Figure 2.4 (d), the Amplify and Forward (AF) repeater simply amplifies and sends the received RF signal, including noise, to users placed in a coverage gap by introducing amplifying channel coefficients. Repeaters are commonly used in places where signal coverage is a problem and to enlarge the cell coverage, however, it has a drawback of amplifying the noise as well, which by return will degrade the received SNR.

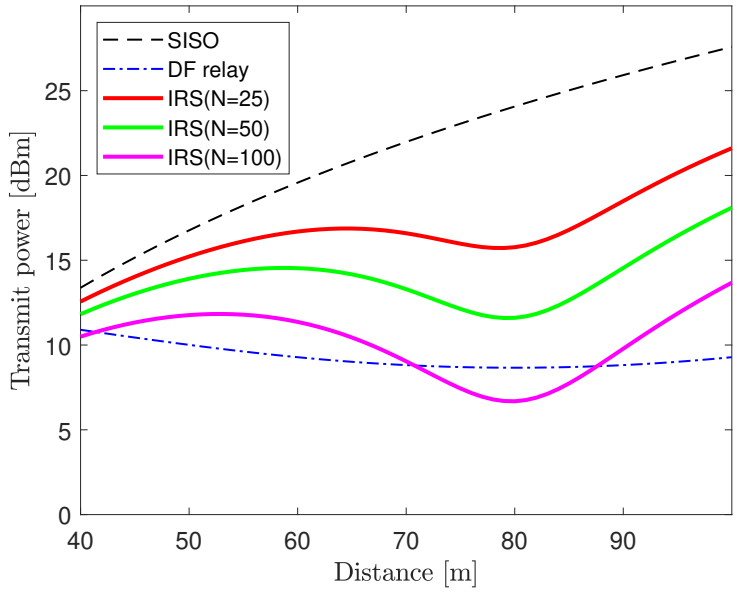

Figure 2.5 – Transmit power to achieve the rate 6 bit/s/Hz.

The transmitted power needed to achieve a certain rate has been studied in [31] - [42] and a comparison between the DF relay and the IRS was studied. Figure 2.5 shows that the power transmitted needed in the IRS case reduces as the number of elements grows, and the distance to the DF relaying scenario is least when the receiver is either near to the transmitter or the IRS. When the distance is 80 meters (m), the IRS must have around or less than 100 elements to outperform DF relaying, demonstrating the importance of IRS technology in future wireless generations.

2.2.2 Measurable Metric Performance of IRSs

The authors in [43] have proposed new models for Multiple Input Multiple Output (MIMO) systems, with the aid of IRSs. The schemes of Vertical Bell Labs lAyered Space Time (V-BLAST) and Alamouti have been presented. Both schemes have shown enhanced BER performance gains and SE and do not need significant changes to existing MIMO models, particularly in their receiver design, making them viable and workable options for future wireless communications. Nevertheless, the authors ignored a workable phase shift setup, which takes into consideration phase dependent amplitude differences, in the model of the suggested schemes. In [44], the authors determined the precise probability that a randomly located IRS might reflect for a certain transceiver using generalized reflection rules. The analytical findings show that the length of a randomly positioned reflector has no impact on the possibility of reflection. However, this approach implies that all IRSs have the same length, which does not reflect the real world network situation. Furthermore, the authors focus only on the likelihood of reflection, with no assessment of how the large scale IRS can increase transmission performance. The researchers in [45] - [46] explored the outage probability of IRS assisted wireless systems. The first authors suggested that the IRS could be used to increase the LoS likelihood for indoor mm-wave setups. The authors develop the outage probability and then optimize the IRS's deployment position to moreover reduce the outage probability while the second authors mentioned that for NLoS components, the outage performance is initially assessed and optimized in the slow fading scenario. The optimal outage probability decreases with the size of the IRS when LoS components are bigger than NLoS components. The authors next describe the asymptotically ideal outage probability in the high SNR zone, indicating that it decreases as the LoS component powers grow. In contrast to the authors in [45], who look at point to point mm-wave communications, the authors in [47] suppose a generalized mm-wave downlink cellular network with random barriers and reflectors. The findings indicate that only the placement of high density reflectors can result in a considerable raise in mm-wave coverage while reflected signals must travel greater distances than direct signals in low density networks, and coverage probability does not differ from that of blockages. A limitation on this work is that the authors did not takes into consideration the optimized deployment for the reflectors results, the performance coverage of the network was not promising. In [46], the performance of outage probability in IRS assisted vehicular communication networks is examined. Using the central limit theorem and series expansion, the authors derived the expression for outage probability. The IRS

can significantly reduce the probability of outages for vehicles in its area, according to numerical results. Yet, the authors in [48] studied the outage probability of IRS aided full duplex two way communication systems which characterizes the performance of overcoming transmitted data loss induced by extended deep fades. The authors computed the probability distribution of the cascaded end to end equivalent channel deploying an IRS beamformer of his preference. According to the authors [48] -[46], the number of reflecting components has a considerable influence on system reliability. A shortcoming of their work is that the analysis was revealed under the assumption of continuous phase shifts and amplitude.

For calculating the BER of the Large Intelligent Surfaces [17] (LIS) assisted systems, the authors in [49] proposed an approximation and upper bound equation. Under the influence of Nakagami-m fading channels [18], the author investigated at M-Quadrature Amplitude Modulation (QAM) modulations and Binary Phase Shift Keying (BPSK). For number of elements $N < 4$, the authors derived the exact distribution of the channel coefficient and utilized a Gaussian approximation for the in-phase and quadrature components since the exact calculation becomes too complicated for large values of N. Nevertheless, the exact derivation for the BER was only for two and three elements and the scenario is more advanced when the number of elements is huge. Unlike the authors in [49], the researchers in [50] developed a broad mathematical model for calculating the Symbol Error Probability (SEP) by determining the number of elements used in the simulations was in terms of hundred and the distribution of the received SNR. Otherwise, the exact BER analysis of a two-user Non Orthogonal Multiple Access (NOMA) system using square QAM is discussed in [51]. In contrast from previous work, there are no restrictions on the modulation order of QAM symbols for any user. In Raleigh fading channels, closed form formulas for the BER of the Successive Interference Cancellation (SIC) receiver have been formulated. The BER performance of an IRS aided NOMA downlink system is derived in closed form in [52]. In [53], the researchers examine an IRS assisted wireless system with and without a direct link between the BS and the user, using a finite number of IRS elements. The authors provide a BER and Average Achievable Rate (AAR) study of IRS based systems, considering maximum received power. The authors develop a closed form

17. Large Intelligent Surfaces are emerging wireless communication technologies that utilize large-scale arrays of antenna elements to control the propagation of EM waves. It can enhance wireless communication systems by improving coverage, capacity, and energy efficiency.

18. Nakagami-m fading channels are statistical models used to characterize the fading of wireless signals. They are often used to model a variety of fading scenarios, including Rayleigh fading, Rician fading, and log-normal fading.

BER approximation that allows forecasting asymptotic performance variation as SNRs and IRS elements raise. Simulation results present more accurate BERs than previous studies [50]. However, in [54], the performance of IRS assisted wireless communications over Rician fading channels is discussed. For several performance metrics, such as outage probability, channel capacity, and average SEP, the authors construct new accurate closed form approximations. To give a better explanation of the system behavior, asymptotic equations for the outage probability at high SNR levels, as well as closed form formulations for the system diversity order and coding gain are provided. The performance analysis in the past works ignored practical implementations like imperfect CSI. In [55], the asymptotic optimality of the achievable rate is investigated in a downlink IRS system, which takes place in a real world IRS environment with all its limitations. The suggested passive beamformer attain asymptotic optimal performance by manipulating the incident wave characteristics, under practical reflection coefficients. To enhance the feasible system sum rate, a modulating mechanism is provided that may be applied in an IRS without interacting with current users, and its average SER is asymptotically determined. The simulation results reveal that the proposed methods agree closely with their upper bounds in the presence of multiple IRS references. An obvious concern about this work is that an IRS cannot coherently align with all users connected to BS via IRS. The authors in [56] define IRS's ideal phase shifts based on limited feedback from the mobile user to describe the possible data rate from the BS to the user, in an IRS aided mm-wave MIMO system. Additionally, to enhance data throughput, simulation findings demonstrate that by deployed the IRS with perfect CSI, the positioning and orientation error bounds can both be decreased while the authors in [57] show the way that IRS can be employed and optimized to boost the rank of the channel matrix, resulting in significant capacity improvements. Since the previous works make employ of a perfect IRS with unlimited phase resolution, the capacity related study that arises has an undefined mismatch with practical systems. When a practical IRS is implemented with constrained phase shifts, the authors [58] produce an approximation of the feasible data rate and discuss performance deterioration. In [59], the authors employ a basic receiver architecture to explore the deterioration of attainable rate and discuss the correlation design of equipment deficiencies as a function of the distance between reflective elements. The authors in [60] defined the spatial throughput of a single cell multi user system supported by numerous IRSs that are randomly placed in the cell, conversely to earlier works that concentrate on link level performance optimization for IRS assisted wireless applications. When the number of

IRSs exceeds a specific value, the simulations reveal the analysis is correct, and the IRS assisted system outperforms the FD relay aided counterpart system in terms of spatial throughput. Moreover, it is demonstrated that alternative deploying procedures for IRSs and active relays should be utilized to maximize their respective throughput. It is found that when fewer IRSs are deployed, each with more reflecting elements, the system spatial throughput grows, however at the cost of greater spatially varied user rates and this is met with the research article in [61] when the author used one IRS only consisting of 4096 elements to enhance the communication data rate for 50 users distributed randomly in a room of 13 x 14 m^2 and far from the IRS 16.5 m.

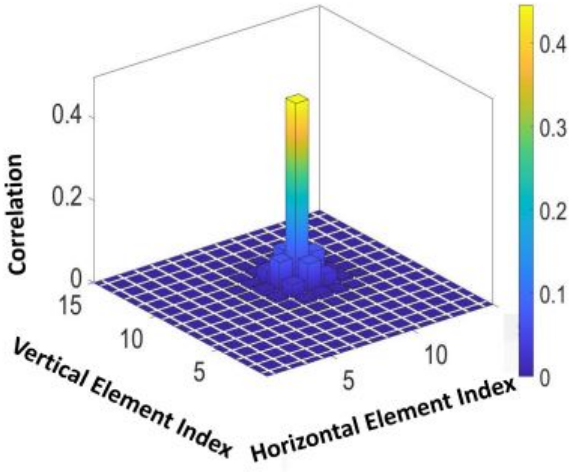

Figure 2.6 – Actual capacitance of the IRS element at column 5 and row 5 is correlated with the intended capacitance of itself and the neighboring elements [61]

In [59], the authors studied the hardware impairments and its impact on the performance data rate while the authors of [61] analyzed in the system model the effect of MC between the adjacent reflecting elements on the achievable data rate per each user as per Figure 2.6 and then the authors represented the MC per IRS elements statistically as follows:

$$C_n = \frac{\sum_{i=1}^{N} \tilde{C}_{i,\theta} 100^{-\left(\frac{d_{n,i}}{\lambda}\right)}}{\sum_{j=1}^{N} 100^{-\left(\frac{d_{n,j}}{\lambda}\right)}} \tag{2.6}$$

Where $d_{n,i}$ is the distance between elements n and i, $\tilde{C}_{i,\theta}$ is the capacitance that they assign to element i and C_n is the actual capacitance of element n. Hence, we might expect that studying parameters like MC, hardware impairments, and discrete phase shifts

in the wireless communication assisted IRS will not only enhance the system performance in general but also establish a new era of communication research based on robust foundations that will end eventually with reliable technology. The implementation of the IRS was near the user equipment's in [61]; however, the authors in [62] studied the centralized and distributed deployments of the IRS in the wireless network. Under symmetric channel topology, it has been demonstrated that centralized deployment exceeds scattered deployment in terms of achievable user rates. Nevertheless, in [63], the authors analyzed and compared two interesting scenarios in a SISO system, namely a finite number of big IRSs and many finite size IRSs, to show which implementation technique is more favorable. The authors calculate the coverage probability in closed form for both instances based on statistical CSI, utilizing the Deterministic Equivalent (DE) approach [19]. Then, the ideal coverage probability is calculated. Numerical findings illustrate, among other things, that adding more surfaces beats the design strategy of adding more elements per surface. Conversely to the early works, [64] reveals a collaborative analytical and empirical investigation to introduce a new spectrum sharing solution for interior situations based on the use of a reconfigurable reflect-array in the wireless channel. The relevant signals for each transmission pair might be enhanced while interferences would be suppressed by managing the phase shift of each element on the reflect array optimally. Accordingly, in the same room, numerous wireless users can simultaneously access the same spectrum band without interfering with one another. As a result, network capacity can be significantly boosted. The smart reflect array panels are suspended on the walls in the indoor setting. Even though the reflected array does not process or buffer any incoming signals, it can change the phase of the reflected wireless signal. In [65], the authors studied the uplink rate in the presence of restrictions such as inaccurate channel estimation, hardware flaws, and interference caused by device specific spatially correlated Rician fading. The authors have proved that, without the use of large simulations, studies can reliably predict the performance of a LIS surface. Also, it is presented that in a LIS based system, a channel hardening occurs, and the authors also found the asymptotic bound for the uplink data rate and proved that as the number of elements increases, hardware impairments, interference, and noise due to channel estimation errors and the NLoS path become insignificant. Compared to conventional massive MIMO, the simulation results show that a

19. a mathematical technique in stochastic optimization where problems involving random variables are reformulated into an equivalent deterministic form—typically by replacing uncertain parameters with their expectations, risk measures, or chance-constraint approximations—so that standard optimization methods can be applied.

large scale IRS can achieve greater reliability in terms of capacity expectation and variation. Noticed that when the number of elements used in the simulations is huge of order of thousands that raises the concern about the MC between the adjacent elements and the practical phase shift model considerations. The authors, in LIS systems, considered at the capacity impacts of HardWare Impairments (HWI) [66]. The authors produced a general model of the HWI based on the distance between a considered point on the LIS and its center, with the latter serving as a reference point in hardware design. To limit the negative impacts of hardware deficiencies, the simulation and analytical results propose dividing a large scale IRS into a succession of smaller IRS units. Similar to [66], the authors in [67] not only did investigate the effects of transceiver HWIs and IRS-HWIs on a general IRS aided MU-MISO system with imperfect CSI and correlated Rayleigh fading, but suggested a novel optimization methodology for Reflecting Beamforming Matrices [20] (RBM) optimization with low computational cost, which is particularly useful in IRS-aided systems with many elements. The authors of [67] had the ability to get the channel's linear Minimum Mean Square error (MMSE) estimate with transceiver HWIs and IRS-HWIs. In addition, utilizing just large scale data, the uplink attainable sum SE with Maximal Ratio Combining (MRC) was calculated in closed form and performed high computationally efficient optimization about the IRS-RBM. In general, the authors showed an approach produced tractable and analytical formulations and superior to prior efforts, as demonstrated by simulation findings. In contrast to other studies that focus on capacity, the paper in [68] looks into the feasibility of employing an IRS with a large number of scattering components for terminal location. The authors discuss in depth about the effects of deployments with a single centralized LIS and numerous smaller distributed LISs constrained to the same total surface area. Dividing the LIS into 16 smaller LISs outcomes in minor benefits, however it also increases the overheads for different small LISs to collaborate with one another. To improve scattering in the surroundings, the authors in [69] used Scatter MIMO for delivering MIMO spatial multiplexing gain that uses a smart surface. Smart surface connects to a wireless transmitter device, like an active AP, and re-radiates the same amount of power as any active AP, producing in virtual passive APs. By using virtual passive APs, Scatter MIMO eliminates the interference, synchronization, and power requirements of traditional dispersed MIMO systems, allowing its smart surface to give spatial multiplexing gain at a cheap cost. In accordance with the

20. Reflecting Beamforming Matrices are mathematical representations used to design the phase shifts applied to the elements of an IRS. These matrices control the reflection pattern of the IRS, allowing for precise beamforming and interference mitigation.

simulation results, Scatter MIMO gives a median throughput gain of 2 over the active AP alone. From the above mentioned references and different illustrations, we would like to mention that the IRS assisted wireless communication systems can be utilized as a receiver, transmitter, and a reflector by modifying the phase shifts of the IRS's scattering units [70]. The IRS's outgoing waves can generate different radiation paradigms that can send data if these patterns can be distinguished and identified at the receiver. This is the basic design concept of spatial modulation, which is commonly introduced using programmable antennas [71]- [72]. This is almost like wireless backscatter communications, that use load modulation to adjust the antenna's reflection coefficients [73].

It's hard to get a high rate Secondary Users (SU) in Cognitive Radio (CR) communication systems when there is a lot of cross link interference with Primary Users (PU). The authors in [74] used the lately developed IRS to solve this problem. Specifically, the authors investigate an IRS aided CR system, where an IRS is used to help with spectrum sharing between a PU and an SU link. By combining an IRS reflect beamforming and SU transmit power to optimise the feasible SU rate for a particular Signal to Interference plus Noise Ratio (SINR) target for the PU connection. The authors used the Alternating Optimization (AO) algorithm to solve the SU rate maximization problem via IRS reflect beamforming and the joint transmit power control. Simulation results demonstrate that the IRS-assisted CR is effective for secondary transmissions, even in the hard scenario when the secondary transmitter is much closer to the PU. The authors in [75] studied in depth the IRS enhanced energy detection for single user spectrum sensing, cooperative spectrum sensing, and diversity reception. For each scenario, a performance analysis is shown, as well as an analysis for the average probabilities of detection and false alarm. Monte Carlo simulations are used to demonstrate the validation of his findings. An IRS is thought to considerably increase detection performance. In [76], the authors investigate IRS concept in the UAV enabled communications to expand network coverage and enhance communication reliability and spectral efficiency of IoT networks. The authors also present that IRS aided UAV communication systems may achieve ten times the capacity of traditional UAV communication systems in terms of achievable ergodic capacity. The impact of imperfect phase knowledge on the BER analysis and system capacity for UAV communications assisted by flying intelligent reflecting surfaces is examined in [77] - [78]. The authors in [77] only addresses a single-hop case, whereas [78] take into account a multi-layer UAV network with several hops. The obtained results proved the need of correct phase estimation for IRS assisted systems, specifically for systems with a limited

number of reflecting elements. The results are also demonstrating the importance of the number of elements in obtaining a reliable performance.

2.2.3 Optimization Techniques and Algorithms

The influence of multipath on the received signal is determined by how big or small the spread of time delays associated with the LoS and other multipath components are concerning the inverted signal bandwidth. The LoS and other multipath components are often non-resolvable in case the channel delay spread is minimal, leading to the narrowband fading model. The LoS and all multipath components are often resolvable into muliple discrete components if the delay spread is large, leading to the wideband fading model [5]. The reflected signals can be merged coherently at the intended receiver to enhance the received signal strength or destructively at the non meant receiver to limit interference by smartly changing the phase shifts of all scattering elements, as shown in Figure 2.4. The experimental demonstration and channel measurements in [24] support this, preparing the way for more theoretical research and system optimization. In the following section, we review the most common optimization formulations and solutions for IRS assisted narrow and wideband wireless systems for single and multi users.

Passive Beamforming Techniques

In this part, we study the passive reflection optimization for IRS aided wireless communications. We assume the knowledge of direct and indirect channels for the purpose of exposition; however, the channel estimation is discussed in section 2.3.
The optimization problem can be stated generally as follows:

$$\max_{s,\Theta} \quad f(S,\Theta) = |\Big(h_{sr}^T \Theta h_s + h_r\Big) S|^2 \tag{2.7}$$

$$\text{s.t.} \quad (\text{C1}) : \|S\|^2 \leq p \tag{2.8}$$

$$(\text{C2}) : \theta_1, \ldots, \theta_N \in [0, 2\pi) \tag{2.9}$$

$$(\text{C3}) : \alpha_1, \ldots, \alpha_N = 1 \tag{2.10}$$

Where S is the transmit beamforming vector, Θ is the IRS matrix with unit modular constraint on each element and $f(S,\Theta)$ denotes the objective function. The joint beamforming optimization problem is a non convex problem due to the fact that both s and Θ are linked to each other. Furthermore, IRS elements require unit magnitude since, not like

relays, they do not decode or amplify, then transmit a received signal. The demand for suboptimal tractable rate optimization solutions is driven by the non convex unit modular constraints in the above mentioned optimization issue. Past works on wideband [79] -[80] and narrowband [81] - [82], IRS assisted wireless communication systems aim to solve the non-convex problem where the main challenge includes the unit modulus constraint. Multiple techniques have been utilized in the literature to address this constraint:

— **Alternating Optimization Technique:** The method style of switching between passive reflection and active transmit beamforming gives it an advantage to deal with active transmit beamforming as a conventional problem when the passive beamforming is fixed; however, under the given active beamforming, the passive beamforming is still a non trivial exercise to handle including the unit modular constraint on each element of the IRS. There are possible ways have been revealed in the literature to deal with this constraint. Such as, the Semi Definite Relaxations [21](SDRs) method is applied to relax the non convex rank one constraint to a standard convex Semi Definite Program [22](SDP). The SDP is utilized then to solve the formulated non convex Quadratically Constrained Quadratic Program [23](QCQP) problem. However, the relaxed problem could not result in a rank one solution in response, requiring obtaining the eigenvalue decomposition by using Circularly Symmetric Complex Gaussian (CSCG) distribution methods. The SDR with large number of Gaussian randomization produce eventually to approximation of $\pi/4$ of the optimal objective value [83]. As a result, the SDR approach can only provide an approximation and solving a SDP program is computationally expensive for great number of antennas and IRS elements.

— **Iterative Techniques:** The concept of these techniques is to detect a locally or near optimal solution for the objective problem at a reasonable computational complexity and acceptable run time. Such as the low complexity successive refinement algorithm [81] - [84] to establish the optimal discrete phase shifts of distinct elements at IRS one by one in an iterative way. In [19] another technique is in-

21. Semi Definite Relaxation is a mathematical optimization technique used to find approximate solutions to non-convex optimization problems. It involves relaxing the original problem into a convex semi definite program, which can be efficiently solved using standard optimization techniques.

22. A Semi Definite Program is an optimization problem where the objective function is linear and the constraints involve symmetric positive semi definite matrices.

23. A non convex Quadratically Constrained Quadratic Program is an optimization problem where the objective function and constraints are quadratic functions. These problems are generally difficult to solve due to their non-convex nature, which often leads to multiple local optima.

vestigated based on fixed point iteration and manifold optimization. The authors in [82] utilized the Projected Gradient Method [24](PGM) to jointly optimize the phases of the IRS elements and the transmitted covariance matrix. The PGM method achieved the same data rate as the AO method, but with lower computational complexity and less number of iterations. The authors in [80] expanded the work of [82] in wideband MIMO communication. The paper in [61] suggested the low complexity power method to compute the dominant eigenvector of the reflection coefficient matrix to configure the IRS phases. Generally, all of these iterative methods have shown good system performance with acceptable computational complexity and reasonable run time.

Active and Passive Beamforming

The authors in [85] investigate an IRS assisted point to point MISO wireless communication system where one IRS is used to aid transmission from a multi antenna AP to a single antenna user. As a result, the user together receives both the signal directly from the AP and the signal reflected by the IRS. By merging the active transmitted beam at the AP with the passive reflected beam at the IRS using phase shifters, the authors aimed to optimize the overall received signal power at the user. Assuming that the IRS contains global CSI, a centralized solution based on the SDR technique was suggested. Due to the centralized approach including excessive channel estimation and signal exchange overhead, a low complexity distributed technique is used where the AP and the IRS modify the transmit beamforming and phase shifts in alternating fashion until convergence is achieved. Compared to benchmark systems, the simulation findings propose that the suggested techniques can obtain high performance gains. In addition, it has been proven that the IRS can significantly enhance link quality and coverage compared to a traditional setup without the IRS.

Figure 2.7 studied four schemes [3] - [85]:

1. AO's joint transmit and passive beamforming design.
2. AP-user Maximum Ratio Transmission (MRT).
3. AP-IRS MRT.
4. MRT without IRS.

24. The Projected Gradient Method is an iterative optimization algorithm used to find the minimum of a convex function subject to linear inequality constraints. It involves projecting the gradient descent step onto the feasible set at each iteration.

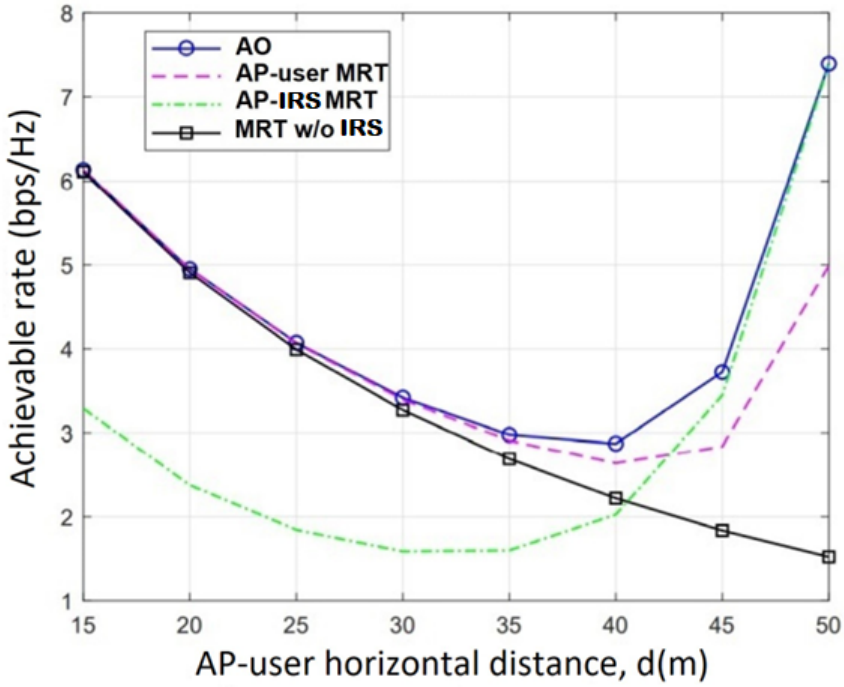

Figure 2.7 – Impact of AP-user horizontal distance on the achievable rate of an IRS assisted MISO system [69] - [85]

.

When the user is near to the AP, the AP-user MRT system works as well to the AO method, however suffers a considerable rate loss when the user is closer to the IRS, as illustrated in Figure 2.7. This is to be predicted, because the AP-user direct link dominates the user-received signal in the former scenario, but the IRS-user link dominates in the latter. In addition, the AP-IRS MRT system operates in the opposite manner compared to the AP-user MRT counterpart. As shown in Figure 2.7, whether the transmit beamforming is not adequately built according to the whole channels, the achievable rate using the IRS might be poorer than the conventional MRT without the IRS, for example, in the application of the AP-IRS MRT scheme for distance $d \leq 40$ m. This highlights the importance of combining passive and active beamforming to achieve the best balance of direct transmission to the user and indirect transmission via IRS reflection in order to maximise the received signal strength at the user. For a desired SNR of 8 dB, the network coverage without the IRS is roughly 33 m, however when the proposed combined beamforming designs with an IRS are used, this value is increased to about 50 m [85]. Another important finding in [85] is that the user's received power increases quadratically as N increases, by a factor of $\mathcal{O}(N^2)$. The power transmitted can be reduced at the AP in the order of

$1/N^2$ without sacrificing the receive SNR. This is owed to the fact that the IRS catches an extra aperture gain of $\mathcal{O}(N)$ in the AP-IRS link additionally to the reflect beamforming gain of $\mathcal{O}(N)$ in the IRS-user link. The power scaling in IRS and its comparison with massive MIMO (m-MIMO), are investigated in [86] in which the authors demonstrated analytically that the gap between an IRS and m-MIMO is enormous; an IRS needs a huge number of reflecting elements to achieve SNRs equivalent to m-MIMO and by concluding such solid fact the authors disapproves of the myths and the wrong understanding of the IRS fundamental concepts. Also in [19], a point to point MISO communication system with the assistance of IRS assistance is investigated. The beamformers at the AP and the IRS phase shifts are tuned at the same time to enhance spectral efficiency. The resultant non convex optimization problem is handled with the aid of two efficient methods that use fixed point iteration and manifold optimization approaches, respectively. The suggested techniques not only enhance spectral efficiency but also reduce computational complexity as compared to the current state-of-the-art approach. The IRS-assisted MISO downlink model described above, in addition to the heuristic AO described in [81] - [19], provide a generic framework for the optimum design of IRS aided systems that may be utilized in a variety of network scenarios. Despite the fact that IRSs with continuously maximum reflection magnitudes and phase shifts were studied, it was discovered that realistic IRS with discrete reflection amplitudes and discrete phase shifts satisfied the hardware criteria [25].

The authors in [84] observe an IRS assisted wireless communication, in which an IRS with a limited figure of phase shifts at each element is used to improve communication between a multi-antenna AP and many individual-antenna users. Specifically, the discrete phase shifts at the IRS and the continuously transmitted precoder at the AP were tuned together to lower power transmitted at the AP while still achieving user SINR requirements. For single user and multiuser cases, both optimum and successive refinement based suboptimal solutions were studied. Also, when the figure of reflecting elements earns asymptotically large, the performance decay of IRS due to discrete phase shifts against the ideal scenario with continuous phase changes was investigated. Unexpectedly, it was found that using an IRS with even 1 bit phase shifters can attain the same asymptotic squared power increase as continuous phase shifts. However, this comes at the cost of a constant power loss in dB. Compared to the situation without IRS, simulation findings revealed that uti-

25. Hardware criteria refers to the specific technical specifications and requirements of hardware components, such as processing power, memory capacity, and input/output capabilities. These criteria are essential for ensuring that a system can meet its performance and functional requirements.

lizing IRS with discrete phase shifts can save significant transmit power. Furthermore, it was presented that immediately quantizing the optimised continuous phase shifts to generate discrete phase shifts offer close optimal performance in the single user scenario, however that performance is significantly reduced in the multi user case due to substantial co-channel interference. Ultimately, owing to the mult iuser channel rank improvement provided by the IRS's extra signal routes, it was demonstrated that the Zero Forcing (ZF) precoder based algorithm performs almost like the MMSE precoder based method.
We reviewed narrow band communication systems with frequency flat fading channels and a single and multiple antennas for the AP and user in the aforementioned works. Hence, the wideband communication is important to delve into in the literature. Passive IRS reflection optimization problems for MIMO systems with multiple antennas at both the AP and the user, in addition to broadband OFDM systems with frequency selective fading channels, must serve to multi antenna channels and multi-path channels with different delays, making them more complicated and challenging to solve. The fundamental capacity limit of IRS based point-to-point MIMO communication systems with multi-antenna transmitter and receiver is quantified in general by concurrently optimising the IRS reflection coefficients and the MIMO transmit covariance matrix, which varies from MISO systems [81]. For frequency flat channels, an AO approach was devised to discover a locally optimum solution by optimising transmitted covariance matrix or one of the reflected coefficients at a time while leaving the others constant, and the best possible solution were found in closed-form. Alternative, less difficult algorithms for asymptotically low and high SNR circumstances, as well as MISO and Single Input Multiple Output (SIMO) channels, were developed. Also, for frequency selective channels, a MIMO-OFDM system was studied, in which a collection of reflection coefficients for all subcarriers must be planned. A novel AO approach utilized the convex relaxation technique to consecutively optimise a group of transmitting covariance matrices across multiple subcarriers or a common reflection coefficient for all subcarriers. Extensive numerical results show that the proposed algorithms outperform several standard methods with and without IRS in terms of rate performance. The performance gain enhances as the number of elements rises.
The authors in [87] studied the wideband beamforming for IRS based mm-wave massive MIMO utilizing a different design. For IRS-aided mm-wave hybrid MIMO systems, the authors attend a geometric mean decomposition-based beamforming method. Simulation results reveal that, with the assistance of IRS, the suggested strategy can achieve

good BER performance in a wideband hybrid MIMO system. In [88], to rise the system sum-rate, the authors updated the source precoders and IRS phase shift matrix in the FD MIMO two-way communication system. To maximise the system sum rate, source precoders, and the IRS phase shift matrix are tuned simultaneously. The Arimoto-Blahut approach [26] is utilized to divide the non convex optimization issue into three sub-problems that are handled alternately. Closed form solutions can be utilized to solve all the sub-problems rapidly. IRS offers a performance raise equal to a relay operating at a transmission power of only 35 dBm to 40 dBm. This is in relation to the IRS's worry with double fading. It's important to remember, however, that IRS does not require any transmission power.

The research studies in [19] - [81] - [88] assume an ideal IRS with infinite phase resolution, i.e., each scattering element's phase shift could be entirely controlled. However, this is hard to accomplish in practice, and devising precise phase control algorithms is similarly strict. Also, for the IRS controller to give precise phase control, a full CSI is usually needed. This implies that data sharing might be incredibly expensive, in particular for IRS that is self-sustaining owing to wireless energy harvesting.

The authors in [79] revealed a novel method to use the IRS to enhance the attainable rate of an OFDM system. The authors produced a workable transmission protocol by assembling the IRS elements and calculating the joint channel for every set, with data transfer based on a shared IRS reflection coefficient. Thereafter, based on the predicted channels under the recommended protocol with any defined grouping, the authors constructed a combined optimization problem of IRS reflection coefficients and transmit power allocation. Based on the first-order Taylor expansion, the non-concave rate function was estimated using its concave lower limit in an efficient Successive Convex Approximation [27](SCA) based technique. The SCA based approach guarantees that IRS's combined reflection and transmission power optimization concern will converge to a stationary point; also it only has polynomial complexity over the number of elements and subcarriers. The simulation results reveal that the enhancements in the data rate are connected with the selection of the set ratio and the coherence time of the channel; however, a performance degradation in the low SNR regime as the design parameters are adjusted based on the

26. The Arimoto-Blahut is an iterative method for calculating the channel capacity of a discrete memoryless channel. It finds the channel capacity by maximizing the mutual information between the channel's input and output.

27. Successive Convex Approximation is an iterative optimization technique used to solve non-convex optimization problems. It involves approximating the original non-convex problem with a sequence of convex sub problems, which are then solved iteratively to obtain a locally optimal solution.

calculated CSI, the CSI obtained at low SNR is inaccurate, resulting in a larger performance decay at both low and high grouping ratios; therefore, to maximize the obtainable rate, the grouping approach as well as the training sequence can be further improved. Furthermore, authors consider continuous phase and maximum amplitude equal one in the optimization schemes instead of suggesting practical discrete phase shift.

To reduce complexity even higher, the authors in [89] proposed a simpler approach called highest Channel Impulse Response [28](CIR) maximization, in which IRS phase alters are only aligned with the time domain channel with the strongest path power. The authors suggest a feasible transmission protocol for an IRS enhanced OFDM system that conducts channel estimation and reflection optimization successively. The IRS proposes a unique reflection pattern to assist channel estimation at the AP based on received pilot signals from the user, for which the channel estimation error is calculated in closed form under the unit modulus constraint. Afterward, the reflection coefficients are optimized using the estimated CSI and a low complexity approach based on the strongest signal route resolved in the temporal domain.

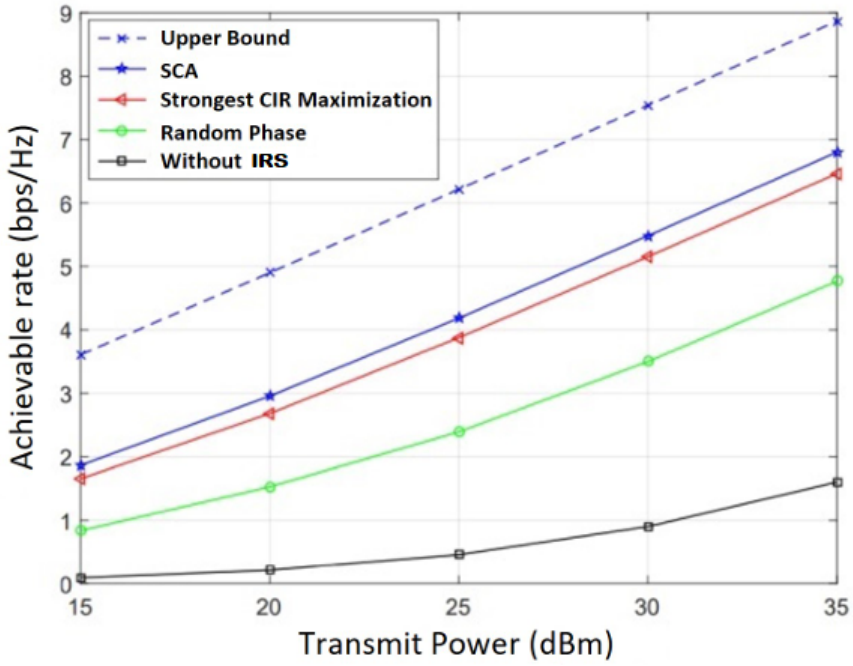

Figure 2.8 – Achievable rate versus transmit power for IRS assisted OFDM system [89].

28. Channel Impulse Response approach is a method used to characterize the time varying nature of wireless channels. It models the channel as a linear time varying system and represents its response to an impulse input as a time varying impulse response function.

It is perceived from Figure 2.8 that in comparison to the OFDM system with random IRS phase shifts and the OFDM system without IRS and the related optimal transmit power allocation, the SCA [29]based algorithm proposed in [79] achieves a much higher rate. Furthermore, the most powerful CIR maximization algorithm provides resembling outcomes to the SCA based method, making it a low-complexity and a cost effective option. Also, the figure sets a possible upper rate limit by suggesting that different IRS reflection coefficients can be produced ideally for different sub-carriers, resulting in a frequency selective IRS reflection system. With the realistic frequency flat IRS reflection, this upper rate limit highly outperforms the SCA based approach, and the rate difference expands as the number of sub-carriers increases. Consequently of its passive functioning, IRS assisted OFDM systems have a basic weakness in the absence of frequency selectivity of the IRS reflection. Owing to the necessity to serve to additional channels in both space and frequency, the IRS reflection design for rate rise is entailed in more general IRS assisted MIMO-OFDM systems where the user and AP are equipped with more antennas. In addition, numerous transmit covariance matrices at distinct sub-carriers should be optimized together with the IRS reflection. As a result, the authors in [81] expanded the narrow band MIMO situation and, utilizing the convex relaxation technique, the authors proposed an effective AO based solution. Despite the absence of frequency selectivity, the outcomes in [81] showed that IRS is still useful to improve the systems rate of MIMO-OFDM with well-planned IRS reflection coefficients when compared to a typical system without considering IRS.

Unlike from the aforementioned researches, the authors in [61] studied a wideband OFDM system supported by a practical IRS configuration with two binary states per each element along with MC between adjacent elements. Utilizing the dataset from [90], new channel estimation and configuration techniques have been suggested and analyzed. Due to the trade-off between multiple subcarriers, finding a good IRS configuration with reasonable complexity is difficult in OFDM systems. In [89] - [91], the Strongest Tap Maximization [30] (STM) approach is investigated, to maximize the magnitude of the channel's biggest entry. This performs well for LoS channels but not for NLoS channels and extending it to the scenario where each IRS element has just two states is difficult [92]. Rather then, the

29. SCA offers several advantages, including its ability to handle complex optimization problems and its convergence to stationary points. However, SCA can suffer from slow convergence and sensitivity to the initial point choice.

30. Strongest Tap Maximization is a beamforming technique that aims to maximize the power of the strongest channel tap to improve the overall system performance. This technique is particularly effective in scenarios with strong line-of-sight components.

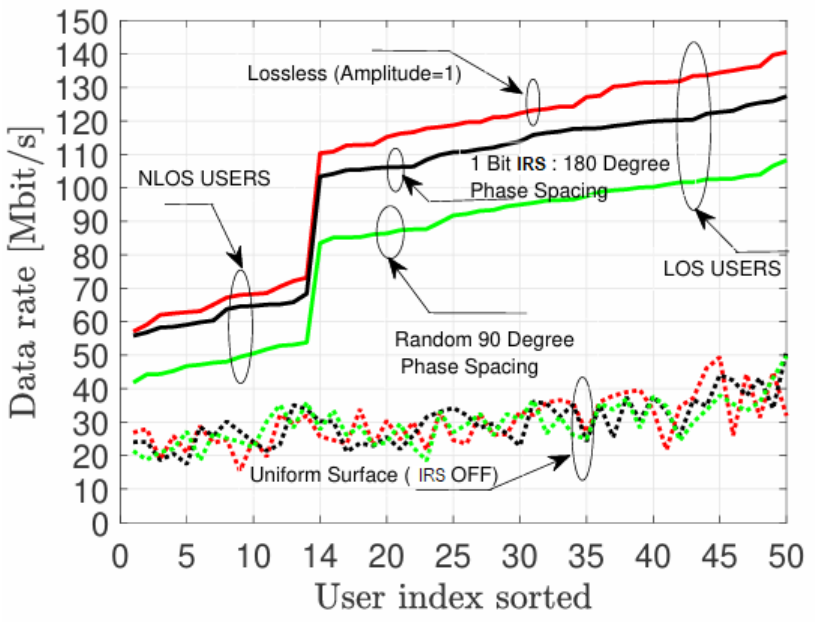

Figure 2.9 – Achieved data rate using dataset in [93]

authors tried to optimize the total signal power received by creating a heuristic algorithm based on the iterative power method, which finds the dominating eigenvalue by iterating the computation until it converges. The simulation results show the achieved data rates by 50 users in the dataset, as depicted in Figure 2.10, organized in rising order based on the data rates using the suggested iterative power technique. Two benchmarks were used:

1. choosing the best configuration from the multiple examined pilot transmission.
2. 2) deactivating all coefficients to model a uniform metal surface.

Over all users, including those in NLoS conditions, the suggested technique consistently yields greater achievable rates. Remarkably, the initial 14 users between the 50 experience NLoS channels from the IRS, while users from 15 to 50 benefit from LoS links from the IRS, resulting in significantly higher data rates. This transition is obvious from user 15 ahead in Figure 2.10. In comparison to a uniform surface, the cumulative rate with an optimized IRS is 3.3 times higher, underscoring the significant advantages of this technology even in complicated setups. The authors in [93] investigated the data rates achieved by 50 users by creating different reflecting phase spacing per element considering the practical phase shift model. Figure 2.10 presents the importance of the IRS technology when compared with the uniform surfaces without considering the IRS configuration. The authors studied the performance of three bits IRS to be compared with 1 bit and random phase. We noticed

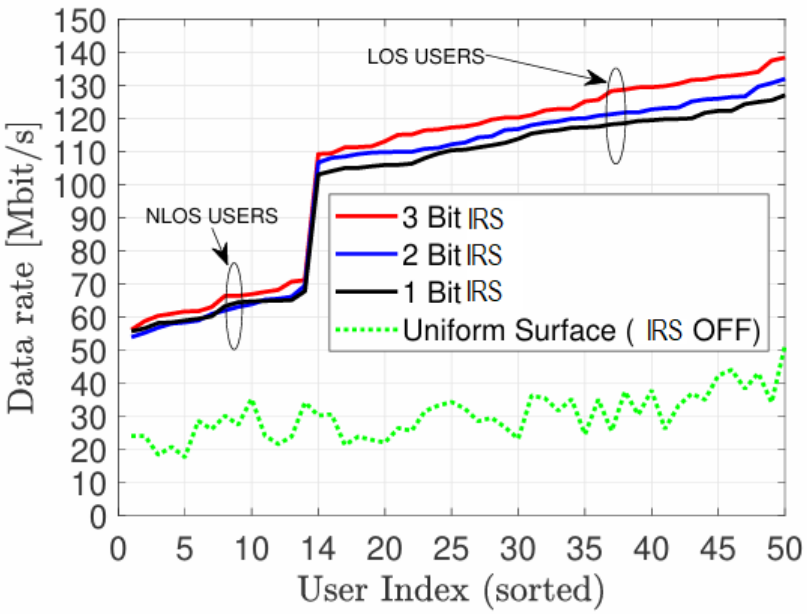

Figure 2.10 – Data rates achieved by 50 users when considering different reflecting phase spacing per element considering the practical phase shift model and compared with the uniform surface (The IRS is OFF) [93]

that the data rate raised when the phase levels designated per each element are raised bearing in mind the equally spaces between the finite number of phases and the purpose of that is the reflective currents are out of phase with the element currents when the phase shift is approximately 180 or -180 degrees and so the electric field and current flow in the element are both reduced, resulting in the least energy loss and maximum reflection amplitude [93]. The effect of the amplitude response has been taken into account and reveal its impact on the gain of the data rate in contrast with many researchers who assumed constant amplitude and ignore the related losses.

Figures 2.11 (a) and 2.11 (b) represent the impact of amplitude variations on the system data rate performance for three and one bits IRS. As a result, considering the assumption of lossless amplitude in the literature gives promising outcomes however, energy loss is inevitable in practical hardware; consequently, a practical phase shift model should be considered taking into account the losses.

Resembling to [61], the authors in [53] studied a wideband OFDM system for MU-MISO system and initial view at the dual phase and amplitude squint effect of reflected signals before presenting a simplified IRS reflection model for wideband signals. Thereafter, a wideband IRS improved MU-MISO-OFDM system is examined. When utilizing both

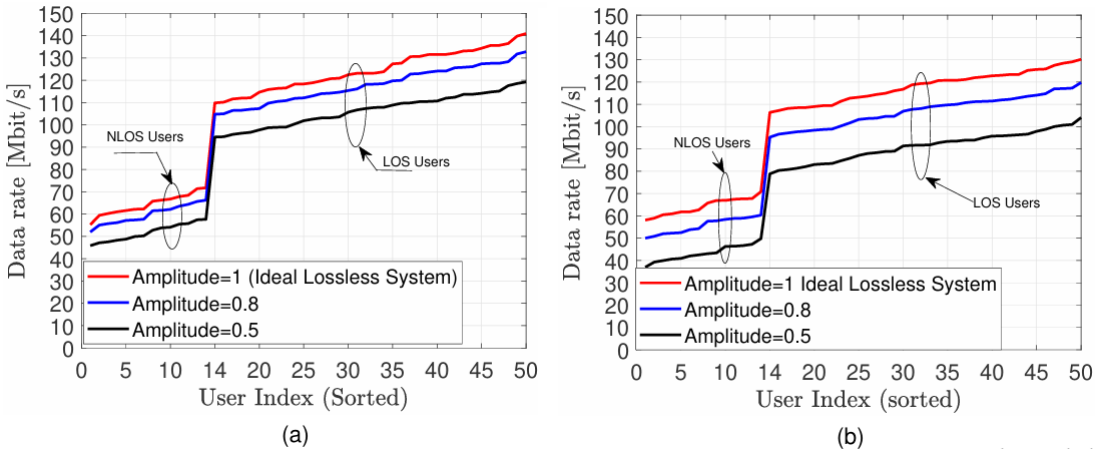

Figure 2.11 – (a) 3-bits and (b) 1-bit IRS for different amplitude variations on the system data rate performance [93]

discrete and continuous phase shifters, the transmit beamformer and IRS reflection are developed jointly to maximize the average sum-rate over all subcarriers. The original problem is turned into a multi-block variable problem that could be solved effectively utilizing the Block Coordinate Descent [31](BCD) approach by leveraging the relationship between sum rate maximization and Mean Square Error (MSE) minimization. In Both scenarios and convergence complexity are discussed. When compared to the ideal IRS reflection model, simulation outcomes demonstrate that the suggested technique could provide considerable average sum-rate augmentation, underscoring the importance of utilizing the realistic model in wideband system design. Nevertheless, the authors impose the assumption that the channels were well known, but in practice, a channel estimating phase is needed. Since the IRS is a passive device, the estimation must be done at the receiver which was not supposed in addition to the proper employment of the IRS.

In summary, performance analysis and optimization techniques, whether focused on maximizing sum rate, minimizing error probability, or mitigating hardware impairments, have conclusively demonstrated the massive potential of IRSs. However, the foundational prerequisite for all these benefits and optimization algorithms is the accurate knowledge of the instantaneous CSI for all cascaded links. Since the passive nature of IRS elements makes traditional sensing impossible, the immediate, critical challenge that arises is that

31. Block Coordinate Descent is an optimization algorithm that iteratively optimizes a subset of variables while keeping the others fixed. This approach can be particularly useful for large-scale optimization problems, as it can reduce the computational complexity of each iteration.

of channel estimation, which is addressed in detail in the following section.

2.3 Channel Estimation

In [94], the authors examine the progression of the reflecting radio idea to IRSs, in addition to the IRS assisted MISO communication model and how it differs from traditional multi-antenna communication models. For the design and investigation of IRS assisted systems, a MMSE based channel estimate technique was suggested. The BS orders the microcontroller to keep all IRS elements turned off throughout the channel estimation phase, also the BS estimates the direct channel for all users. Thereafter, the BS sends a signal to the microcontroller to turn an element of the IRS *ON* whereas leaving the other elements *OFF*, enabling the BS to begin estimating the cascaded channel. Therefore, the microcontroller instructs the IRS's control circuit board in Figure 2.1 to execute the desired sequence, and so forth. The MMSE estimating method is utilized to compute the estimations. Then the BS calculates the optimal beamforming vector employing the channel estimates and transmits it to the IRS microcontroller. Using the estimated channels (direct and cascaded), the phase shifts of the IRS are tuned by using a gradient ascent algorithm.
Similar to [94], the authors in [95] design a unique Passive Intelligent Surface [32](PIS) based energy transfer mechanism from a multi-antenna Power Beacon (PB) to a single-antenna energy harvesting user. A controlled Least Square (LS) channel estimate protocol with binary reflection was suggested. This binary model is utilized since it accounts for the fact that a PIS needs active components, forcing PB to estimate all the channel vectors on its own. The mentioned above works seek at least $N + 1$ pilot symbols for predicting the total $N + 1$ channel coefficients in the system. Owing to only one element is turned on at a time, the ON/OFF based IRS reflection setup suffers from considerable reflection power losses, producing in a weak reflected signal.
Distinct from the preceding study, the authors [89]-[79] developed an effective method of grouping adjacent IRS elements into a sub-surface, referred to as IRS element grouping; as a result, only the effective cascaded user IRS-BS channel connected with each sub-surface requires to be computed, significantly declining the training overhead and simplifying IRS reflection configuration for transmitting data. Nevertheless, it is crucial to mention that,

32. A passive intelligent surface (PIS) is a type of IRS that does not require any external power source. It relies on the incident EM waves to induce currents in its reflective elements, thereby enabling phase shift control.

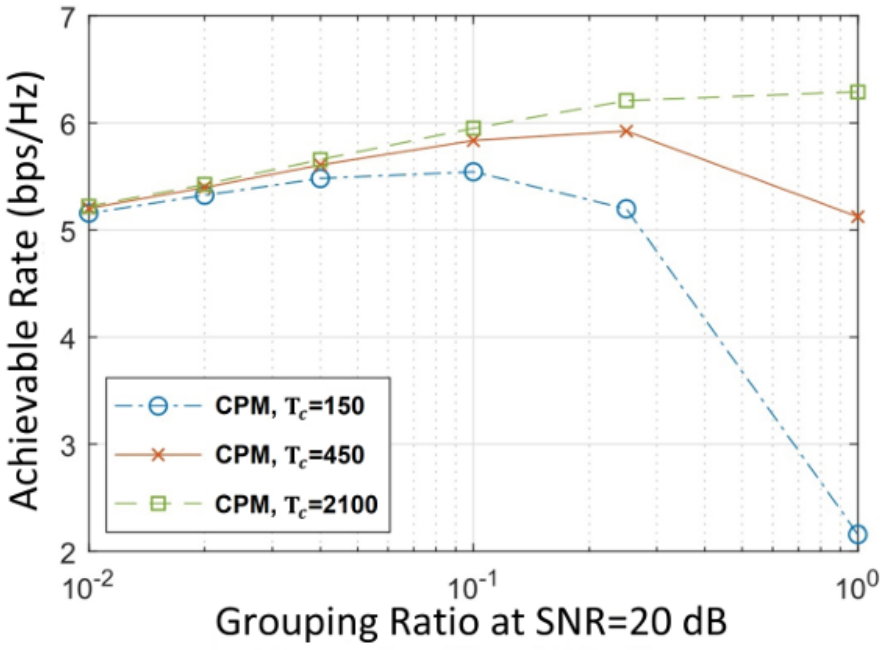

Figure 2.12 – Achievable rate versus IRS Grouping [79]

for practical implementation, the channel coherence time has a significant impact on the appropriate grouping ratio.

The downward and upward trend of the achievable data rate in Figure 2.12 is a clear example of the effect of the grouping ratio on the data rate in a high SNR regime. Similarly to [89]-[79] the authors in [96]-[97] investigated the channel estimation for the broadband system but for MU. The authors in [96] suggested two efficient channel estimate algorithms for various channel configurations in an IRS aided MU broadband communication system using OFDMA. The Sequential User Channel Estimation [33](SeUCE) scheme can support more users for channel estimation than the Simultaneous User Channel Estimation (SiUCE) scheme by exploiting the advantage that all users have the same IRS-AP channel, but at the cost of increased channel estimation complexity and some declining channel estimation performance. In [97], the authors describe a Compressive Sensing (CS) based Channel Estimate (CE) solution for IRS assisted mm-wave massive MIMO systems, by which the angular channel sparsity of large scale array at mm-wave is used for enhanced CE with reduced pilot overhead. Using CS techniques, the authors develop pilot signals based on the preceding knowledge of the LoS dominated transmitter to IRS

33. Sequential User Channel Estimation is a technique used in wireless communication systems to estimate the CSI of multiple users sequentially. This approach can reduce the overhead associated with simultaneous channel estimation and improve the overall system performance.

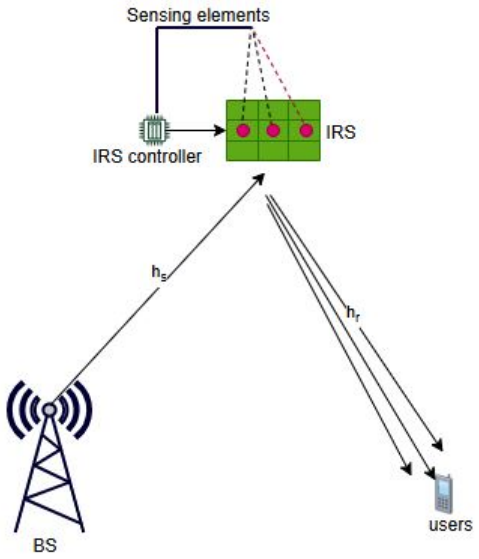

Figure 2.13 – IRS aided wireless communication with sensing elements (nearly passive IRS).

channel and previous experience of the high-dimensional Tx to Rx and IRS to Rx channels. To take advantage of the channel sparsity, a distributed orthogonal matching search method is utilized. Consequently, several writers [98] rise IRS channel features (such as low-rank, sparsity, and spatial correlation) to simplify cascaded channel decomposition and reduce training overhead in IRS aided SU MIMO/MISO systems. Otherwise, the authors in [99]-[100] utilized the same channel properties to study the channel estimation in the MU MISO/MIMO systems.
To accelerate the training process in passive IRS assisted MIMO and MISO systems, hierarchical searching algorithms and Deep Learning (DL) have been developed for channel estimation [101]-[102].

Unlike the previously stated works, the authors in [103]-[104] used some sensing elements interlaced with passive IRS elements to provide the IRS with sensing capabilities for the channel estimation process, as shown in Figure 2.13. Different from the fully passive IRS channel estimation, nearly passive IRS has two modes of operation. All the reflecting elements are held OFF in the first mode or called sensing mode, in addition the sensing elements are powered up to receive pilot signals from the BS or users in the uplink or downlink to estimate their respective channels to IRS, conversely, in the second mode or transmission mode or called reflection , the sensors are deactivated, and the IRS reflecting elements are turned on to reflect the data signals from the BS or users to improve uplink

and downlink communication in both. In [103], the authors revealed a new Deep Reinforcement Learning[34](DRL) framework to estimate IRS reflection matrices by educating the IRS on how to anticipate optimum interaction matrices utilizing the knowledge of the sampling channel itself. This technique does not demand an initial dataset gathering step, unlike supervised learning based methods.

Channel estimation is the critical overhead necessary to realize the gains promised by IRS optimization, with various techniques aimed at balancing accuracy against pilot symbol overhead. Having addressed the fundamental challenges of controlling the reflection and acquiring the necessary CSI, the subsequent step in maximizing system performance moves to the physical domain. Specifically, the ultimate effectiveness of an IRS relies heavily on its physical location, which are the focus of the next section on IRS deployment strategies.

2.4 IRS Deployment

2.4.1 Importance of IRS location

IRS works in FD mode with passive reflection only, avoiding amplification, self-interference, and processing noise. These attractive features of IRS have led to extensive research in using it to greatly enhance the performance of wireless systems in a variety of scenarios, including MU-NOMA, physical layer security, Wireless Power Transfer[35](WPT), multi-carrier communications, multi-antenna, and Mobile Edge Computing [3] - [105] -[70]. In the current literature, the IRS is usually deployed near the distributed users, for the purpose of improvement of coverage that is completely different from that for the active relay, roughly placed in the middle of the transmitter and receiver for balancing the SNRs of the two hop links, that process and amplify the source signal before forwarding it to the receiver.

Otherwise, the alternative deployment method is to position the IRS near the BS taking into account that both methods of deployment minimize the product distance path

34. Deep Reinforcement Learning is a type of machine learning that combines reinforcement learning with deep neural networks. It allows agents to learn optimal policies by interacting with an environment and receiving rewards or penalties for their actions.

35. Wireless power transfer is a technology that enables the transmission of electrical energy without the use of physical wires. This technology relies on EM induction or EM radiation to transfer energy between devices.

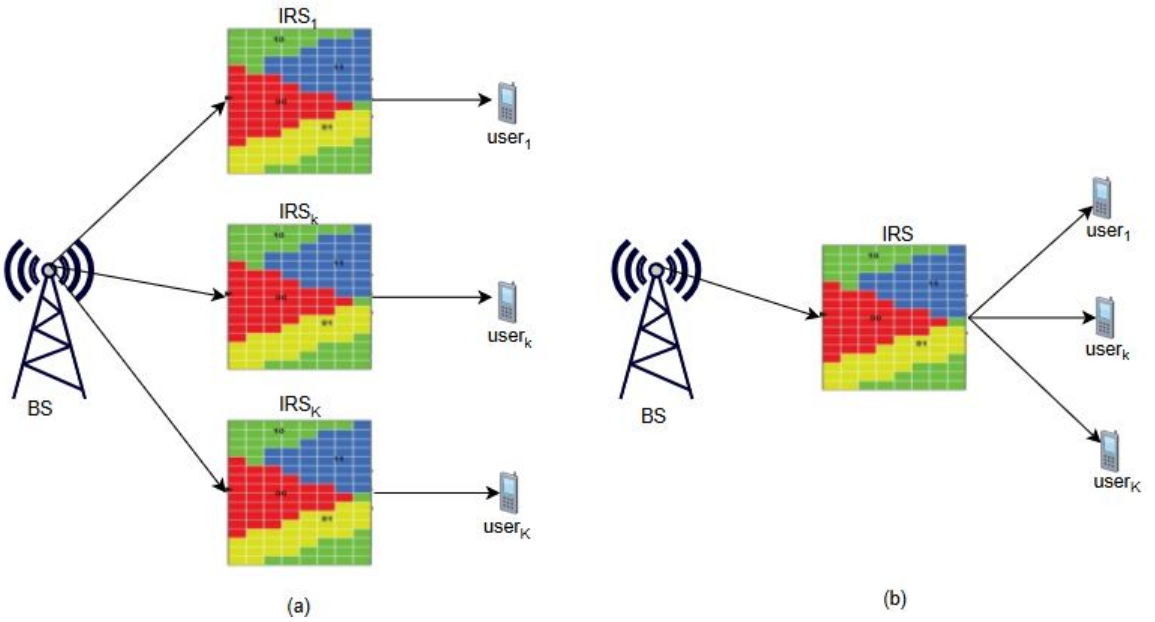

Figure 2.14 – IRS deployment methods, (a) Distributed IRS, (b) Centralized IRS deployment

loss according to Figures 2.14 (a) and 2.14 (b). It is worth noting that IRS could be deployed much more widely across the network, owing to its cheap price, to effectively modify signal propagation. Nevertheless, this causes a considerably larger scale deployment optimization challenge that is far more difficult to address in addition to the fact that because IRS is passive equipment, the strength of their reflected signals decays fast with distance; as a result, if IRSs are placed far enough away, reciprocal interference is essentially non existent, considerably reducing their deployment design so, thanks to the IRS passivity.

2.4.2 State of the Art: IRS deployment

In this section, we study the new IRS deployment problems in a variety of situations to gain significant insight into practical design, coverage, and beamforming performance. For maximum performance, the authors in [106] handle the critical topic of how to place IRSs in a wireless communication network. The two traditional techniques are evaluated, in terms of different communication performance metrics, to install IRS at the BS or at distributed users, and then a novel hybrid IRS deployment approach is proposed that combines their cooperative benefits. Between both each of the user-side IRS and

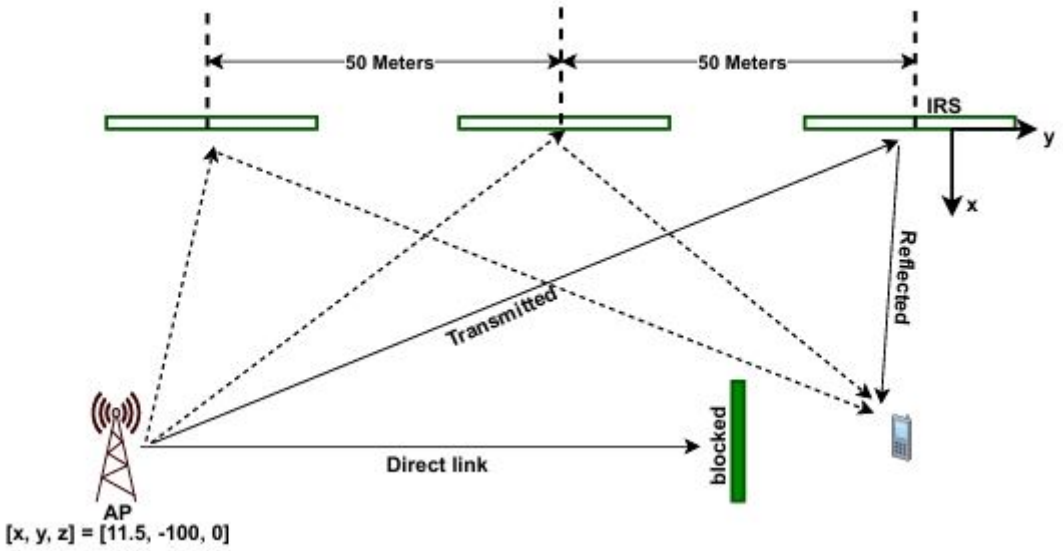

Figure 2.15 – Simulation setup for different IRS deployments.

the BS-side IRS, an inter-IRS reflective link is included in the hybrid IRS installation proposal. Whenever single-reflection and direct links between the BS and its served users are substantially blocked, the double-reflection links can be leveraged to provide alternative accessible LoS pathways between them. The double reflection path may reach a significantly larger asymptotic passive beamforming gain than the single reflection channel given the same total number of reflecting elements N despite the fact that N increased of $\mathcal{O}(N^4)$ versus $\mathcal{O}(N^2)$. The simulation findings present the superior performance of the suggested deployment over conventional ones as per Figure 2.14. Since all users may be assisted by at least one IRS, located whether user or BS side, under the hybrid IRS deployment, it proves its increased efficacy in terms of network coverage.
The authors [107]-[108] used the cooperative IRS method in their work to take advantage of placing more than one IRS near users or BS also to overcome the standalone IRS which suffers a gain loss if it is located far from the base station or user equipment. Concerning standalone IRS, when placing the IRS near the user or near the AP, it provides the highest SNR; however, situating it midway between the user and the AP produces the lowest SNR through the two-cooperative IRS case obtains a significant SNR boost when compared to the highest SNR in the single IRS scenario.

As per Figure 2.15, the authors in [36] showed a communication system from a single antenna source AP to many UEs using an IRS with N intelligent controllable elements. The AP location is [x, y, z] = [11.5, -100, 0] while the users are placed at [x, y, z] =

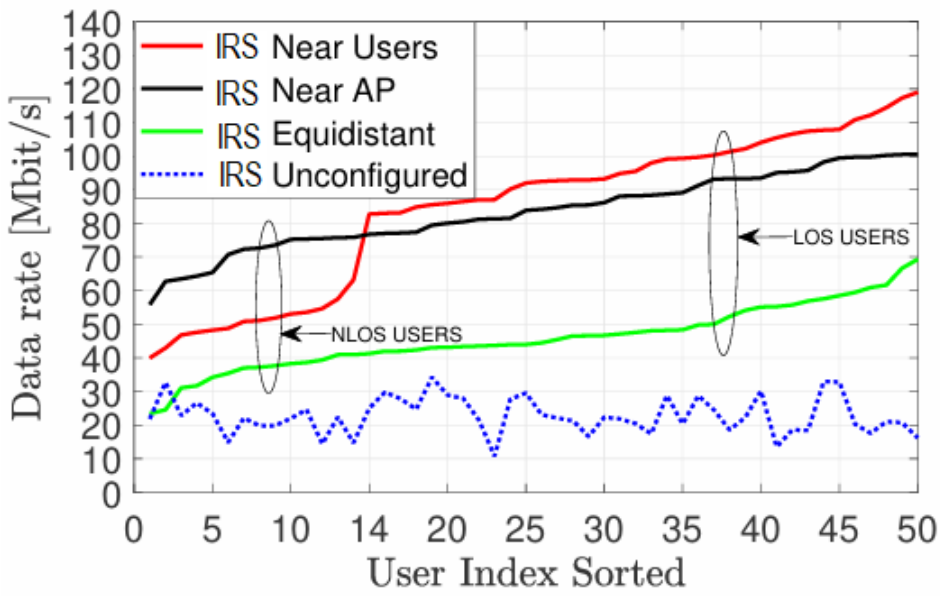

Figure 2.16 – Achievable data rate for different IRS deployments [36].

[16, 1, 0] according to Figure 2.15. The IRS is located in three locations to show the related data rate for all users. It is situated near the AP, near the users, and at the same distance between the AP and the users. To obtain the least pathloss exponent that leads to the minimal pathloss under a given connection distance, it is workable to put the IRS under LoS conditions with AP and users. Even though a single IRS of order $\mathcal{O}(N^2)$ passive beamforming gain, the received signal strength at the users suffers from a twofold pathloss proportionate to the product of the user-IRS and IRS-AP connections' distances.

Simulated findings, as shown in Figure 2.16, proved that the superior data rate was achieved for all users when the IRS is located near the users or AP; however, the data rate is degraded when the IRS is located in the middle [36]. The reason behind that is when the IRS is placed near the user or AP it leads to the largest SNR while placing it around the middle between the user and AP leads to the smallest SNR.
In [107], the authors contribute to current research by suggesting and assessing a wireless communication system with the double-IRS communication system. Considering that the reflection channel from the first IRS to the second IRS is of rank one, a combined passive beamforming design for the two IRSs was produced. An increase in power of order $\mathcal{O}(N^4)$, may be achieved by using two cooperative IRSs with a total of N components, which is preferable than installing one ordinary IRS with a power gain of level $\mathcal{O}(N^2)$. Simulation results demonstrate that implementing two cooperative IRSs perform much better than

deploying one IRS with the same total number of elements. The simulation reveals that when two cooperative IRSs are deployed, their performance is lower than when only one IRS is deployed. Nevertheless, when the total number of elements is large, for example $N = 1600$, deploying two cooperatives' IRSs instead of one can result in substantial performance gains. Another point to note is that increasing the total number of elements by a factor of two, such as, from $N = 800$ to $N = 1600$, rises the received SNR of the benchmark case with one IRS by 6 dB, while increasing the received SNR of the two IRS case with $N_1 = N_2 = N/2$ by 12 dB.

Similar to [107], the authors in [109] study effective channel estimation and passive beamforming solutions for a single and multi user communication system aided by a double-IRSs.

The authors in [110] consider a cooperative passive beamforming design for a double IRS aided MU-MIMO that captures the inter-IRS channel's multiplication beamforming gain. The cooperative passive reflected beamforming at the two distributed IRSs and the constructive received beamforming at the BS, positioned near the users and BS, respectively, are optimized in a general channel structure with both dual and single reflection links to rise the minimum SINR of all users equipment. In the simulation results, the maximum power P = 30 dBm was accepted to study the influence of channel ranking and spatially multiplexing gain on system performance for MU and determined the superiority of the doubled IRS over the single in relation to achievable max-min rate data rate for the users.

In [62], the researchers suggested a wireless network consists of multiple IRSs, which would aid transmission between a multi antenna BS and a big number of single antenna cell edge users. The authors intend to optimize the weighted sum rate of all cell-edge users by adjusting the IRS's phase shifts and the BS's transmit beamforming together. For several schemes, the simulated findings present the transmit power versus the Weighted Sum Rate (WSR). To start, all systems' WSR develops in lockstep with BS power, and when BS has a larger transmit power budget, the suggested multi IRS with continuous phase shifts outperforms the single IRS with continuous phase shifts in terms of WSR. This is due to, in multi IRS systems, having the IRS close to the users minimizes pathloss propagation, allowing the users data rate to increase owing to the IRS passive beamforming gain. This illustrates the value of using several IRSs to increase system performance.

More inter IRS reflections are produced as the number of IRSs in the User-AP connection increases, causing in grows pathloss, backhaul cost, and complexity in the aforementioned activities. Nevertheless, bigger multiplicative beamforming benefits could be obtained by

performing cooperative passive beamforming across a big number of IRSs.
The authors in [62] supposed two workable IRS deployment methods that correspond to various effective channels between users and the AP: scattered deployment, in which the N elements form two IRSs, each located near one user, and centrally managed deployment, in which case all of the N elements are deployed near the AP. The capacity and achievable rate regions for either deployment methods utilizing various multiple access algorithms are calculated supposing the uplink Multiple Access Channel (MAC). It is presented that in symmetric channel settings, the centrally controlled deployment overcomes the scattered deployment in terms of capacity region and achievable user rates.

By exploiting the MAC broadcast duality, the findings were extended to the downlink IRS assisted broadcast channel, where the performance advantage of centralized over distributed IRS deployment was also confirmed to be true. The advantages of centralized vs scattered IRS deployment is particularly apparent when the two users have asymmetric rate demands and channel conditions, according to numerical results. However, the assumption of the downlink and uplink channel duality for both IRS deployments, in practical scenarios, may alter in terms of the LoS and the NLoS which it will by return impact performance gain of the system.
The uplink power control of an IRS assisted IoT network under the QoS limitations at each user is studied in [111]. The objective is to reduce the total user power by concurrently optimizing the receiving beamforming at the BS and the IRS reflecting element phase shifts, while considering each user's unique SINR limitation. The authors utilized the environment diversity by installing many IRSs to produce considerable improvements in energy efficiency through combined optimization of IRS phase shifts and reception beamforming. Particularly, each IRS is made up of N reflecting components that could independently reflect the incident signal with an adjustable phase shift. The simulated findings show that when the number of IRS units increases from 1 to 8, the Riemannian Manifold based Alternating Optimization [36](RM-AO) algorithm saves about 4 dBm transmit power in the single user situation. Also, as the number of users increases, more transmission power can be conserved. Even though the previously stated efforts and advancements in link level performance optimization for different IRS assisted wireless systems, the large-scale deployment of IRSs in large size wireless networks demand methods and tools to optimize the large deployments of the multiple IRS units in the wireless network.

36. Riemannian Manifold based Alternating Optimization is an optimization technique that leverages the geometric structure of manifolds to solve complex optimization problems. It involves iteratively optimizing different variables over their respective manifolds, leading to efficient and accurate solutions.

In [112]-[113]-[60], the researchers offer an analytical framework for the IRS assisted hybrid network relied on stochastic geometry while the authors in [114]-[115] depend on machine learning algorithms in resolving the problems joint IRS deployments, phase shift design, and power allocation in a MISO NOMA network to increase energy efficiency while supposing the data needs of each individual user.

The extensive research into IRS deployment has established that system performance is not only a function of phase shift optimization but also a strong function of the physical placement and cooperative arrangement of the reflective surfaces. Optimal deployment, however, requires jointly considering the location of multiple IRS units, the phase shifts, and power allocation across the entire network, leading to exceptionally complex, high dimensional optimization problems. Given the difficulty of solving these large scale, non convex problems using conventional methods, Machine Learning has emerged as a promising, powerful tool for autonomously and intelligently managing the dynamic, interconnected variables of IRS assisted wireless networks.

2.5 Machine Learning

Beside from all the above, there has been research on implementing ML techniques to optimize the IRS phase shifts [116], also for traffic prediction and action decisions [117]. Authors in [116] insert a new architecture where all of the IRS aided elements are passive except for a select few active elements which are optimizable as well as having imperfect CSI. A DL based solution [37] is executed where the IRS learns to optimally interact with the incident signals at these active elements. The authors present that numerically, the developed solution can approach the achievable rate upper bound of a system that considers perfect CSI while only demanding a small number of active IRS elements. Also, the authors in [118] implement DL but instead it is implemented on the beamforming design in a DL network. The results here show that the proposed design significantly outperforms the conventional iterative optimization algorithms. For IOT applications, [119] develops over the air computation based communication-efficient federated ML framework in which an IRS is used to reduce aggregation error. The findings here present that the suggested approach reaches the benchmark scheme with perfect model aggregation without any dis-

37. A deep learning based solution leverages artificial neural networks with multiple layers to learn complex patterns and make intelligent decisions from large amounts of data.

tortion as training time increases. While in [117], the authors proved the effectiveness with ML with another technique used in order to save energy. By accurately predicting future traffic loads in a two tier HetNet [38]powered by renewable energy and smart grid, binary sleep schemes and energy savings is proposed. ML algorithms, in this case, enable the intelligent application of SM, leading to significant energy savings without compromising QoS. They highlights the importance of considering traffic patterns when implementing energy-saving strategies. While traditional approaches may need manual tuning and a lot of updates, ML based solutions offer a more adaptive and versatile framework that can automatically adjust network operations to altering traffic conditions. The results of this research proposed that ML-driven SM can play a crucial role in enhancing the energy efficiency of Radio Access Networks (RANs), contributing to both environmental sustainability and cost reduction.

Therefore, the application of IRS in wireless systems is envisaged for the future of wireless communications, B5G [120]. As declared in [120], smart systems and energy sustainability are the main objectives for the future of wireless communications. Data rates of up to 10 Gb/s, latencies up to 100 ms, energy efficiency of up to 1 Tb/J, and 1 cm localization accuracy in 3D are some of the key performance targets for B5G [120]. Also, IRS has emerged as a key technology to achieve these performance targets and is the prime motivation for research into IRS aided wireless systems. For example, [24] prove experimentally that their designed IRS was able to achieve a power consumption of $P = 0.33$ mW per active IRS element, which is more power efficient than a relay.

2.6 Sleep Mode Strategies for Energy Reduction in Base Stations

The rapid increase in mobile data traffic, along with the large scale deployment of Small Base Stations (SBSs) in B5G and 6G networks, has brought energy efficiency to the forefront of research priorities. As BSs represent the primary contributors to energy consumption in cellular networks, extensive studies have been devoted to optimizing their power management. One of the most prominent approaches is the implementation of ON/OFF switching strategies, commonly known as Sleep Modes (SM). These mechanisms have progressed from simple binary configurations to more advanced Multi-Level Sleep

38. HetNet is a wireless network that consists of different types of wireless access technologies, such as WiFi, cellular networks, and satellite networks, operating in the same geographical area.

Mode (MLSM) schemes, enabling finer control over energy savings.

2.6.1 Binary Sleep Mode (ON/OFF)

The foundational approach to energy saving is the binary SM scheme, where a BS is completely switched OFF during periods of low or zero traffic demand. This strategy directly addresses the energy consumption exacerbated by network densification:

- **Motivation and Potential**: Densification, while improving capacity, dramatically increases energy needs [121]. The binary ON/OFF scheme directly tackles this by temporarily powering down redundant BSs.
- **Stochastic Geometry and Coverage**: Early works utilized stochastic geometry to analyze the energy-saving potential while maintaining service coverage. For instance, [122] investigated switching off Macro BSs under coverage constraints, demonstrating a substantial energy efficiency gain of around 60% compared to always-active BSs.
- **Small Cell Analysis**: Focusing on Small Cell deployments, [123] detailed the energy consumption profile and discussed various SM strategies, showing energy savings that can range from 10% to 60%.
- **Optimization Techniques**: Following these initial studies, many works focused on optimizing the binary SM decision:
  - **Dynamic Switching**: Studies of [124]-[125]-[126]-[127], and [128] utilized traffic aware policies and dynamic BS switching to determine the optimal ON/OFF state based on real time network load and user distribution. These optimizations ensure that the QoS degradation caused by switching off BSs is minimized.
- **Machine Learning Integration**: To make these switching decisions more intelligent and predictive, researchers began integrating ML:
  - **Traffic Prediction**: [117] highlighted the effectiveness of using ML techniques for accurate traffic prediction, which then informs the optimal binary ON/OFF schedule for the BSs.
  - **Reinforcement Learning (RL)**: RL, particularly Q-learning, has been applied to enable BSs to autonomously learn the best ON/OFF policy by interacting with the dynamic network environment. The studies of [129] and [130] explored Q-learning for cell switching applied a similar tactile RL approach in [131]. Furthermore, [132] proposed a Q-learning algorithm that even adjusts the number of active resource blocks based on traffic load, achieving granular

energy savings.

Despite the effectiveness of binary SM in reducing static power consumption, the abrupt switching between full power and zero power often creates a harsh trade-off between energy savings and service quality (e.g., latency spikes during wake-up).

2.6.2 Multi-Level Sleep Mode (MLSM)

To overcome the limitations of binary switching, the concept of Multi-Level Sleep Mode (MLSM) was introduced. MLSM allows BSs to enter intermediate, lower-power states, offering a more flexible trade-off between energy savings and wake-up delay (service quality):

- GreenTouch Model: A foundational MLSM model was proposed by the GreenTouch consortium [133], which defined four distinct SM levels based on the depth of the power reduction and the corresponding wake-up time. These levels allow for proportional energy savings based on the expected duration of the low-traffic period. RL for Optimal MLSM Depth: The core challenge of MLSM is deciding the optimal time to spend in each level to maximize savings without violating QoS constraints (like latency).
- [134] proposed a Q-learning algorithm to determine the optimal duration a BS should remain in a given SM level, specifically targeting energy minimization while adhering to latency and QoS constraints.
- [135] advanced this with a distributed Q-learning scheme to optimize the energy savings latency trade-off across multiple BSs.
- Location and Mobility-Aware MLSM: The depth of SM can also be adapted to user characteristics. [136] leveraged MLSM to adjust the sleep mode depth based on user location and mobility patterns.
- Distributed Control and Delay Constraints: [137] further applied distributed RL to MLSM systems to maximize energy savings while explicitly considering service delay constraints.

MLSM represents a significant evolution in energy management, offering a fine-grained control that balances operational cost with user experience.

In the most advanced research, the combination of IRSs and SM strategies represents a holistic approach to maximizing system performance and sustainability. Leveraging the adaptability of RL, future networks can move beyond predetermined policies to implement truly autonomous network management. RL allows the system to continuously

learn the optimal joint configuration deciding when and how deep a BS should sleep, while simultaneously determining the precise phase shifts of the IRS to either mitigate service gaps or maximize energy harvesting. This fusion of smart energy management and intelligent wave propagation control, driven by data-centric learning techniques, is the ultimate paradigm for achieving the ambitious performance and energy efficiency targets of B5G and 6G systems.

2.7 Future Research Directions

Multiple techniques, discussed in this research, represent that IRS-based wireless networks can strongly improve the received signal power, boost the capacity and the achievable rate, expand network coverage, minimize transmit power and QoS supply to various users. However, from a communication aspect, the design of IRS assisted wireless communication has novel and unique issues, which are outlined below:

— The passive reflections of all elements at each IRS must be constructed in such a way that they can coordinated signal focusing and interference elimination at the IRS's location. Through, whether or not an associated IRS is positioned near every user, the IRS passive reflections must be built in tandem with the BSs or users' transmissions in order to boost their end to end communications across the IRSs re-designed wireless channels.

— Without RF chains it is difficult to obtain the CSI between IRS and its providing BSs or users, which is necessary for the IRS reflection optimization mentioned earlier. This is particularly true given that IRS typically has a high percentage of reflecting elements and thus related channel coefficients to calculate.

— Owing to their different array structures, operating mechanisms, passive versus active, and reflect versus transmit or receive, the best possible implementation method for IRSs in wireless networks to realize maximum network capacity is observed to be extremely unlike from that for traditional wireless networks with active BSs, APs, and relays, and consequently needs to be thoroughly re-tested. To sum up, adding IRSs into wireless communication networks effectively brings both new possibilities and problems, both of which need further exploration.

2.8 Summary

This chapter presented an overview of the IRS's architecture and uses in wireless communication networks. In the beginning, we have presented the IRS principles to throw novel perspective on the IRS design and different types of control mechanisms that show the applied tuning methods used in various communication models. In addition, different model of channel fading and practical pathloss models which characterize the signal in IRS-assisted communications. Thereafter, the optimization structures and performance analysis methodologies for IRS, are discussed.

The methods have presented promises in rising the rate of wireless networks because of their capacity through intelligent manipulations of the reflections phase shifts under different wireless communication scenarios, including the percentage of saving bandwidth, SNR/data rate/ergodic capacity, transmit power/power consumption/drop of data minimization. The chapter afterwards gives various relevant IRS strategies of deployments and channel estimation to teach the IRS how to recognize the surrounding environments and enhance the system performance despite its passiveness. Lastly, this work opens the door for some research limitations and future directions. This chapter encompasses a wide range of research topics related to IRS and its uses in wireless communication, from its physical tuning, channel modeling to research issues from a wireless communication viewpoint, with a main target on the optimization techniques for IRS-aided wireless systems. The current research methods are still limited to certain assumptions and dropping some practical parameters and limitations. For example, the amplitude reflection coefficient of the IRS, the configuration of the phase shifts of IRSs and the active beamforming of the BS. In addition to the scaling laws in the near/far field regime and the time variant channel mobility which are still required to be explored thoroughly due to their significant effects on the performance of IRS-aided communication. The current solutions mentioned in the literature is depending mainly on some methods and grouping the elements to blocks of resources to reduce the overhead and guarantee the convergence of the algorithms to locally optimal solutions. In the future work, by analyzing more low complex and run time IRS based algorithms using deep Q-learning methods, not only Q-learning, for acceleration the time to decide best policy in SM technique, the IRS-aided wireless systems are predicted to attain not only a higher performance gain but also it will establish for more refined and realistic communication models. Besides, the IRSs provide LoS channels which can be exploited to enhance the coverage in the dead spot zones of the

communication channels. However, the research of IRS enhanced networks is still full of challenges and future directions not only from controlling the wireless channel but also when the IRS is involved in digital coding and information modulations which will drive for revolutionary advances in security communication based IRS systems.

Chapter 3

Resource allocation in Intelligent Reflecting Surfaces assisted Cellular Networks

In this chapter, we focus on how IRSs can be integrated into cellular networks to support the growing demand for users while also limiting energy consumption. Unlike the previous chapter, where we presented the state of the art, here we specifically study how IRSs can be used to efficiently manage more bandwidth. This efficient management will allow more users to be served and significantly reduce the energy footprint of cellular BSs. To this end, we formulate and solve an optimization problem that captures the allocation of IRS resources, and we evaluate the benefits of our proposed approach under different system conditions.

3.1 Introduction

As detailed in the preceding chapter, the IRS has emerged as a compelling solution to address the increasing spectral and energy efficiency requirements of B5G and 6G networks [138]-[105]. While numerous studies have demonstrated the potential of IRS in point to point communications, focusing on goals such as minimizing transmit power [85]-[139] or maximizing achievable rate [79] [20]-[140]-[81], few works consider the application of IRS in practical multi-user cellular networks at the system level [113]-[141]-[142].

This chapter presents our work on users selection and resource allocation in IRS assisted cellular networks, addressing a critical gap in multi-user resource management. Our main contribution is a novel IRS resource model where we consider that the IRS consists of blocks of elements and each block can be controlled independently to assist a specific user. This block based approach provides enhanced flexibility and higher gain in a multi-user environment.

The key contributions of this chapter are summarized as follows:

1. Exploit the IRS to reduce the required bandwidth for users, allowing the BS to serve more users and consequently reduce its energy footprint.
2. Formulate the problem of managing the IRS resources as a Non Linear Integer Problem (NLIP).
3. Propose two low-complexity heuristic algorithms, namely MAX-BS and MIN-IRS, and compare their performance against an exhaustive search approach to manage the IRS block allocation.
4. Evaluate the system's performance under various network configurations, including the variable number of users, IRS position, required bit rate, and cell radius, demonstrating the strong dependency of bandwidth savings on IRS placement.

The findings reveal that significant bandwidth and energy savings are achievable through effective block based IRS resource management. The remainder of this chapter is organized as follows. In Section 3.2, we present the channel models without and with IRS, and then explain the scenarios where the IRS assists several users. The formulation of the problem and the proposed approach are presented in Section 3.3. We present and discuss the results in Section 3.4 before summarizing in Section 3.5.

3.2 System Model and Different Scenarios

We consider a BS equipped with N_{BS} antennas serving a single user with N_{user} antennas in a circular cell of radius Ra. Three scenarios are examined: a reference case without IRS, a case with IRS assistance, and a comparison to the SISO baseline. These scenarios are described as follows:

1. **Reference case (without IRS):** All users equally share an available bandwidth. In this scenario, we calculate the transmit power required for each user to achieve a predefined bit rate.
2. **IRS assisted case:** An IRS module is introduced into the system. Assuming the same transmit powers as in the first case, the IRS improves the spectral efficiency of certain users, hereafter referred to as assisted users. The corresponding gain in spectral efficiency is expressed as a percentage of bandwidth savings. This saving can be translated into either a reduction in the BS transmit power or an increase in the number of users supported by the BS.

3.2.1 First Case: BS–User without IRS

Following [31], the received signal y_k at user k from the BS is expressed as:

$$y_k = h_{s,k}\sqrt{p}s + n_k, \tag{3.1}$$

where $h_{s,k}$ denotes the channel between the BS and user k, p_k is the BS transmit power allocated to user k, s is the unit-power transmitted symbol, and $n_k \sim \mathcal{N}_{\mathcal{C}}(0, \sigma_k^2)$ is noise at the receiver. The SNR for user k is given by [5]:

$$SNR_k = \frac{p \mid h_{s,k} \mid^2}{\sigma_k^2}, \tag{3.2}$$

For a given target bit rate R_k, the required SNR for user k is [5]:

$$SNR_k = 2^{\frac{R_k}{B_k}} - 1, \tag{3.3}$$

where B_k is the bandwidth allocated to user k. Assuming equal bandwidth sharing among K users:

$$B_k = \frac{B_T}{K}, \tag{3.4}$$

where B_T denotes the total available bandwidth at the BS. From Eq. (3.2), the BS transmit power required for user k to obtain SNR_k is:

$$p_k = SNR_k \frac{\sigma_k^2}{\mid h_{s,k} \mid^2}, \tag{3.5}$$

3.2.2 Second Case: IRS Supported Transmission

Next, we consider the presence of an IRS module within the BS coverage area. Let h_{sr} denote the channel between the BS and the IRS with N reflecting elements, and $[h_{sr}]_n$ its nth component. The channel between the BS and user k is denoted $h_{s,k}$, and the channel between the IRS and user k is $h_{r,k}$. Since IRS elements are sub-wavelength in size, they scatter incident signals with approximately constant gain across all relevant directions [26]. The IRS can therefore be represented by a diagonal matrix:

$$\Theta = \boldsymbol{\alpha}\, diag(e^{j\theta_1}, \ldots, e^{j\theta_N}),$$

where $\boldsymbol{\alpha} \in (0, 1]$ is the amplitude reflection coefficient and $\theta_1, \ldots, \theta_N$ are the phase shift variables. According to [26], the received signal at user k is:

$$y_k = (h_{s,k} + h_{sr}^T \Theta h_{r,k})\sqrt{p}s + n_k,$$

where p and n_k represent, respectively, the transmit power and the receiver noise. Note that the transmit powers are the same as in the non-IRS case.

For an IRS assisted user k, the received power relative to the transmit power is:

$$P_{R_k}^I = p \mid h_{s,k} + h_{sr}^T \Theta h_{r,k} \mid^2, \tag{3.6}$$

Since $h_{sr}^T \Theta h_{r,k} = \boldsymbol{\alpha} \sum_{n=1}^{N} e^{j\theta_n} [h_{sr}]_n [h_{r,k}]_n$, the IRS phase shifts can be optimized by setting [31]:

$$\theta_n = \arg(h_{s,k}) - \arg([h_{sr}]_n [h_{r,k}]_n), \tag{3.7}$$

For notational convenience, we define:

$$\mid h_{s,k} \mid = \sqrt{\beta_{s,k}},$$

$$\mid h_{sr} \mid = \sqrt{\beta_{sr}},$$

$$\mid h_{r,k} \mid = \sqrt{\beta_{r,k}},$$

$$\frac{1}{N} \sum_{n=1}^{N} \mid [h_{sr}]_n [h_{r,k}]_n \mid = \sqrt{\beta_{IRS}},$$

From Eq. (3.6) and Eq. (3.7), the received power is:

$$P_{R_k}^I(N) = p\Big(\sqrt{\beta_{s,k}} + N\boldsymbol{\alpha}\sqrt{\beta_{IRS}}\Big)^2, \tag{3.8}$$

The SNR at user k with IRS assistance is then:

$$SNR_k^I = \frac{P_{R_k}^I(N)}{\sigma_k^2}, \tag{3.9}$$

Accordingly, the required bandwidth for user k for a required R_k^I is:

$$\mathcal{B}_k^I = \frac{R_k^I}{\log_2\left(1 + SNR_k^I\right)} = \frac{R_k^I}{\log_2\left(1 + \frac{P_{R_k}^I(N)}{\sigma_k^2}\right)}, \tag{3.10}$$

where R_k^I denotes the target bit rate of user k when assisted by the IRS.

Finally, for one IRS assisted user k, the relative bandwidth saving achieved with N reflecting elements becomes:

$$S_{B_k} = \frac{B_k - \mathcal{B}_k^I}{B_k}, \tag{3.11}$$

3.2.3 IRS assisting Multi Users

An IRS typically consists of a very large number of reflecting elements, which makes it possible to assist multiple users simultaneously. The decision on which users to assist depends on several factors, such as the position of the BS, the placement of the IRS, and the spatial distribution of users. Since the BS is usually fixed, the IRS is preferably positioned close to the users or the BS to maximize its effectiveness [138]. In addition, the number of assisted users depends both on the users' requirements and on the number of available IRS elements.

There are several approaches to enabling IRS to serve MUs. One possibility is to optimize the IRS phase shifts in order to improve the SNR of all assisted users. Another approach is to adjust the IRS configuration so that all assisted users meet a target SNR level [138].

Alternatively, the IRS can be regarded as resources that can be shared among users. For instance, sharing can be achieved in the time domain, thanks to the real time reconfiguration capability of IRS. Another possibility is to divide the IRS elements among users simultaneously, where each user is allocated a specific number of elements. Since the users operate on different frequency bands, interference between their reflected signals can be neglected. However, the number of assigned elements should not be too small, as this would reduce the achievable gain [31].

In this work, we consider that each user must be assigned at least a minimum number of IRS elements, denoted as N_a^{min}. Allocating fewer than this threshold would have little impact on the received power [31]. At the same time, introducing such a lower bound reduces the complexity of the allocation process, since it decreases the number of possible allocation combinations. Furthermore, this will reduce the computation necessary for phase shift optimization.

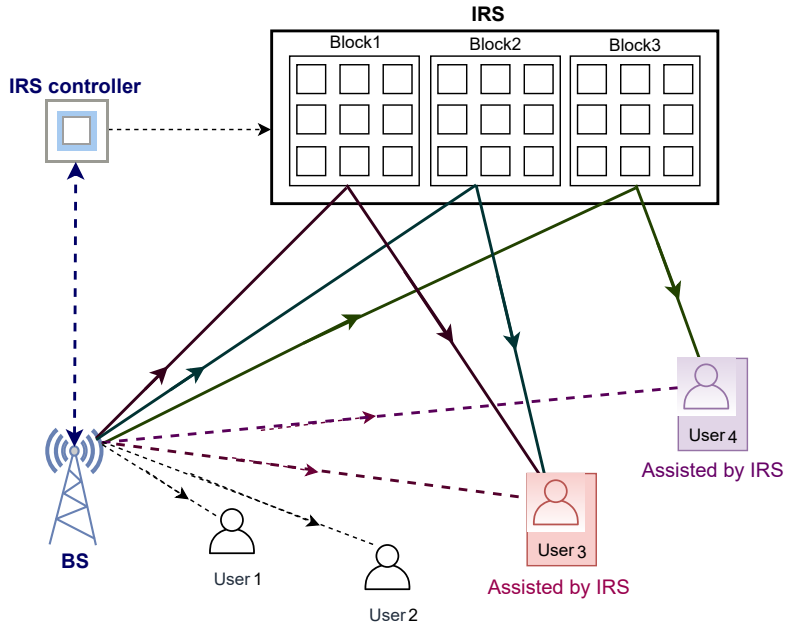

H

Figure 3.1 – An example of IRS containing 3 blocks of IRS elements.

3.3 Problem formulation

Let us consider a BS serving K users, where the IRS assists a subset of these users by allocating block(s) of elements. The size of each block is denoted by N_a^{min}. The total number of available IRS blocks, n_b, can therefore be expressed as:

$$n_b = \left\lfloor \frac{N_{tot}}{N_a^{min}} \right\rfloor, \tag{3.12}$$

where N_{tot} is the total number of elements in the IRS module. Note that n_b also represents the maximum number of users that can be assisted by the IRS.

We consider that the IRS is placed sufficiently far from both the users and the BS, such that all users experience similar IRS assisted effects. If the IRS is deployed very close to the BS (e.g., in the near-field region), the position of the allocated block could influence the assistance provided. However, this aspect is beyond the scope of this work. Figure 3.1 illustrates an example where a BS serves four users, but only two of them are assisted by the IRS. As shown, some users may not be assisted at all, while assisted users can be assigned different numbers of blocks.

Since users equally share the bandwidth when not assisted by the IRS, and the transmit power remains constant whether or not IRS is used, the allocation problem can be

formulated as determining the vector

$$X_K = [x_1, x_2, \ldots, x_K],$$

where x_k represents the number of blocks assigned to user k. The objective function is given by:

$$\max_{X_K} \sum_{k=1}^{K} S_{B_k^{x_k}}, \tag{3.13}$$

where $S_{B_k^{x_k}}$ denotes the bandwidth saving of user k when allocated x_k IRS blocks, calculated using Eq. (3.11). Note that the total number of IRS elements allocated to user k is equal to $x_k \times N_a^{min}$.

The allocation of IRS blocks is subject to the following constraint:

$$\sum_{k=1}^{K} x_k \leqslant n_b, \tag{3.14}$$

This ensures that the number of allocated blocks x_k per user is non negative, and that the total number of allocated blocks does not exceed the available resources. The nonlinear nature of the objective function in Eq. (3.13), combined with the integer constraint on the variables $x_1, x_2, \ldots, x_K$, results in a Non linear Integer Problem (NLIP) [143].

3.3.1 Proposed Algorithms

To evaluate the potential gain from sharing the IRS among multiple users, we analyze the resulting bandwidth savings for a given number of assisted users. Assuming perfect knowledge of users' conditions, an exhaustive search is employed to determine the optimal allocation of IRS blocks. This involves examining all possible combinations of users and their assigned blocks, and selecting the configuration that maximizes the total bandwidth saving. For instance, consider the example in Figure 3.1 with 3 IRS blocks and 4 users. The maximum number of assisted users in this case is 3. If each of 3 users is allocated one block, the optimal configuration is selected from 24 possible combinations. If only 2 users are to be assisted while the remaining 2 rely solely on the BS, the number of possible allocations is 36. Although exhaustive search guarantees the optimal solution, it comes at a high computational cost. To reduce complexity, we propose two heuristic algorithms based on the following strategies:

— **MAX-BS:** Users located farthest from the BS are prioritized and allocated the largest number of IRS blocks. This strategy favors generally users with low SNR.
— **MIN-IRS:** Users closest to the IRS are prioritized and allocated the largest number of IRS blocks. This strategy favors users with the best radio conditions relative to the IRS.

Table 3.1 – Simulation Parameters and Assumptions

Parameter	**Value / Assumption**
Number of users	6 – 30
Cell radius (m)	125 – 1500
Number of elements in IRS	150
Number of antennas	1 at BS, 1 at user
BS antenna gain G_s	15 dBi
User antenna gain G_d	0 dBi
Environment	Urban
Carrier frequency f_c	3 GHz
Total bandwidth B_T	10 MHz
BS power model	Earth [144]
BS-IRS distance d_{sr}	50 m, 200 m
IRS reflection amplitude $\boldsymbol{\alpha}$	1

3.4 Simulation Results

We consider a Macro BS (MBS) serving a circular cell, where users are randomly distributed. The MBS operates at a carrier frequency of 3 GHz with a total bandwidth of 10 MHz. The channel gains are modeled using the 3GPP Urban Micro (UMi) model ([145], Table B.1.2.1-1), considering both the LOS and NLOS versions, which are defined for distances $d \geq 10$ m. The parameters G_s and G_d denote the antenna gains (in dBi) at the BS and at the user side, respectively. Table 3.1 summarizes the system parameters used in this study.

The channel gain β as a function of distance d is given by [31]:

$$\beta(d)\ [\text{dB}] = G_s + G_d + \begin{cases} -37.5 - 22\log_{10}(d/1\text{m}) & \text{if LOS,} \\ -35.1 - 36.7\log_{10}(d/1\text{m}) & \text{if NLOS,} \end{cases} \tag{3.15}$$

The results in this section are obtained through Monte Carlo simulations, with the

environment simulated 10,000 times for different user distributions. Although results are presented in terms of the average percentage of bandwidth savings, this metric can also be interpreted as the increase in the system's SE, which can be further translated into a reduction of the BS energy consumption.

Figure 3.2 illustrates the percentage of bandwidth saved as a function of the number of users served, using an exhaustive search algorithm (required rate $R_b = 1$ Mbps, cell radius $Ra = 250$ m). In this scenario, the IRS is positioned at $d_{sr} = 50$ m from the BS, representing a placement near the BS. It can be observed that up to 47% of bandwidth

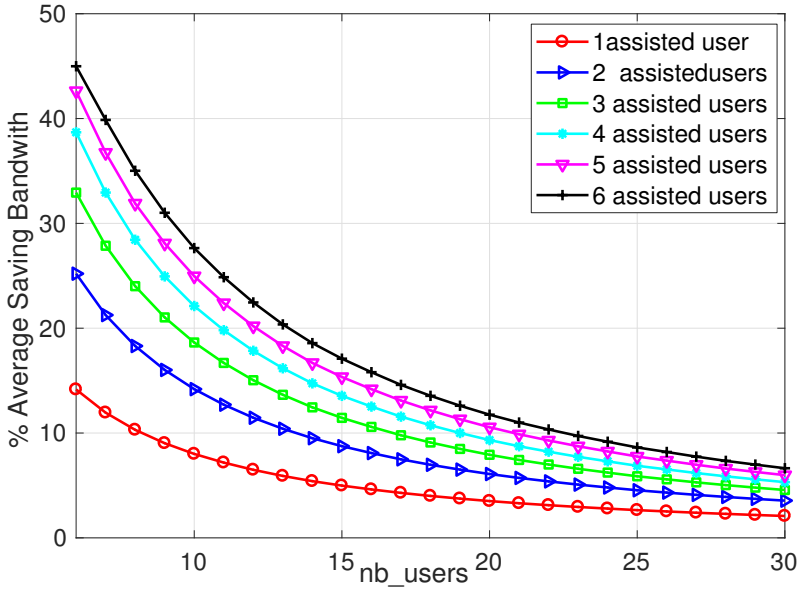

Figure 3.2 – Percentage of bandwidth savings with respect to number of served users for variable number of assisted users by the IRS (d_{sr}=50 m).

can be saved when the number of served users is small and the number of users assisted by the IRS equals n_b. The figure also indicates that increasing the number of assisted users further improves the bandwidth savings, highlighting that distributing IRS blocks among more users enhances the overall spectral efficiency (SE) of the BS. Conversely, the bandwidth saving decreases as the total number of served users grows, due to the smaller proportion of users that can be assisted relative to the total number of users in the cell.

When the IRS is positioned at the edge of the cell ($d_{sr} = 200$ m), the resulting bandwidth savings are shown in Figure 3.3. Similar to the previous scenario, the saved bandwidth decreases as the number of users served by the BS increases. However, compared to the case where the IRS is located near the BS, the overall bandwidth saving is smaller when the IRS is placed at the cell edge. This difference arises from the uniform

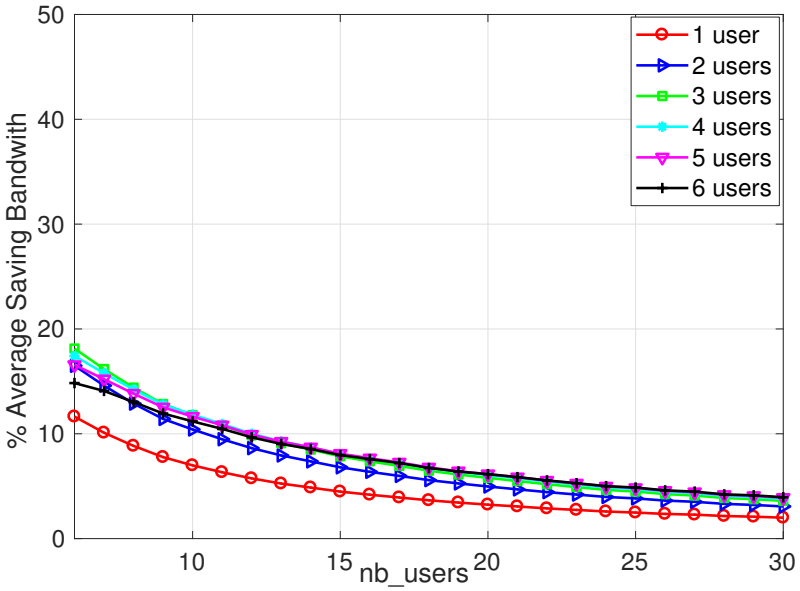

Figure 3.3 – Percentage of bandwidth savings with respect to number of served users for variable number of assisted users by the IRS (d_{sr}=200m, Algorithm: exhaustive search).

distribution of users and the relative position of the IRS. When the IRS is close to the BS, the average distance between the IRS and the users is smaller, resulting in more uniform assistance. In contrast, when the IRS is at the edge, only the users nearby the IRS experience significant enhancements, leading to a lower overall bandwidth saving compared to the IRS near BS scenario.

When the IRS is placed on an edge of the cell (d_{sr}=200m), the saved bandwidth is presented in Figure 3.3. Similarly, the saved bandwidth decreases with the number of users served by the BS. However, in contrast to the case where IRS is positioned near the BS, smaller bandwidth saving is achieved when the IRS is at the edge of the cell. This is due to the uniform distribution of users and the position of IRS. When the IRS is near the BS, the average distance between the IRS and the users is smaller than the case where the IRS is at the edge. In the latter case, edge users that are near the IRS witness more enhancements but the overall bandwidth savings is better when the IRS is near the base station.

Figure 3.4 illustrates the percentage of bandwidth saved for different user bit rates when the IRS is positioned near the BS, using the exhaustive search algorithm. The results indicate that increasing the bit rate reduces the bandwidth savings, as higher rates require more bandwidth to meet users' demands. A similar trend is observed when the IRS is located at the edge of the cell.

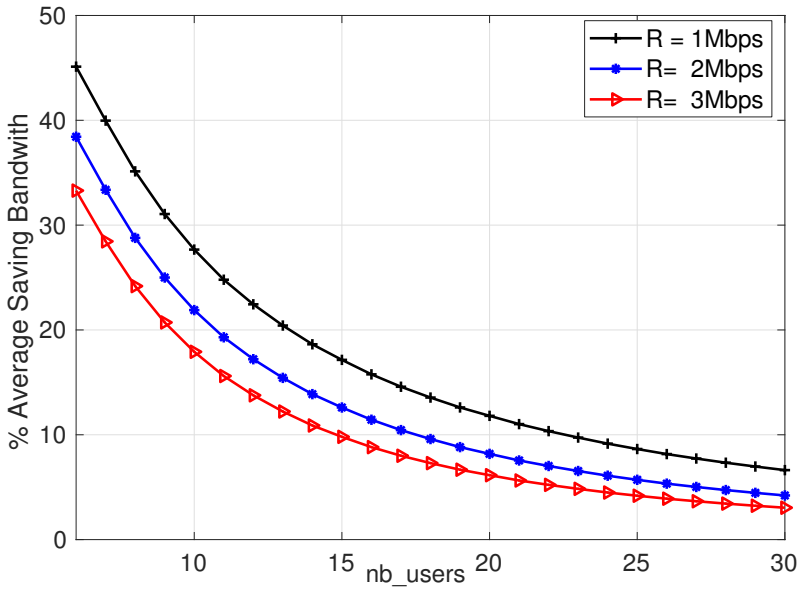

Figure 3.4 – Percentage of bandwidth savings with respect to the number of served users for different bit rates (d_{sr} = 50m, Algorithm: exhaustive search).

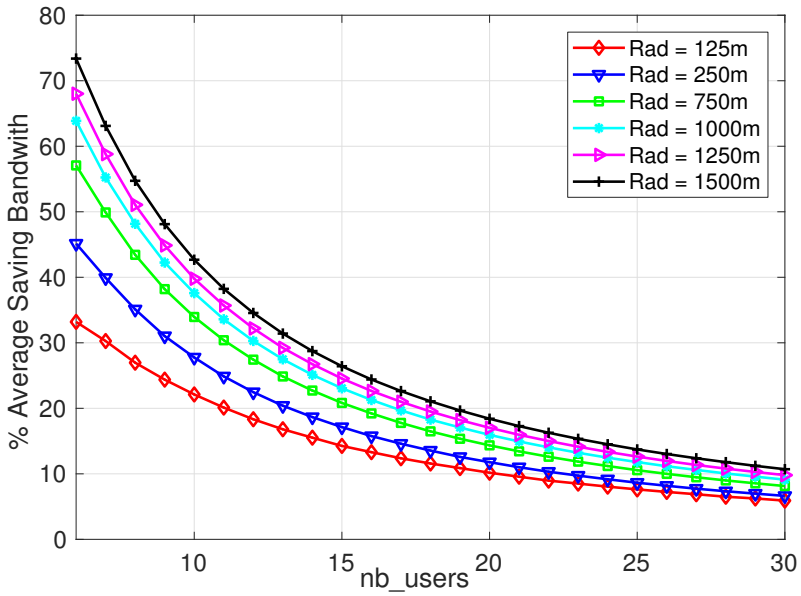

Figure 3.5 – Percentage of bandwidth savings with respect to the number of served users for different cell radii (d_{sr} = 50m, Algorithm: exhaustive search).

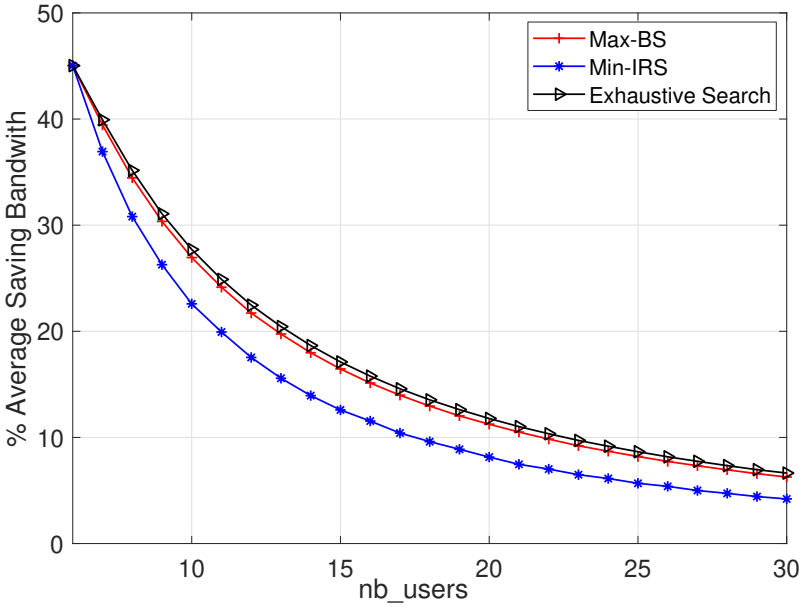

htbp

Figure 3.6 – Percentage of bandwidth savings with respect to the number of served users for the simulated algorithms (d_{sr}=50m, R=1Mbps).

The impact of the cell radius on the bandwidth savings is shown in Figure 3.5. For small cell radii, only a limited bandwidth saving is observed, as the BS transmit power is sufficient to maintain good user conditions. As the cell radius increases, the bandwidth savings improve, since the users are farther from the BS and can benefit more from IRS assistance.

Next, we compare the performance of the proposed heuristic algorithms with the exhaustive search method in terms of both bandwidth and power savings.

Figure 3.6 presents the average bandwidth savings of the simulated algorithms (exhaustive search, MAX-BS, and MIN-IRS) as a function of the number of served users. The results indicate that the performance of MAX-BS closely matches that of the exhaustive search algorithm, whereas MIN-IRS achieves lower savings. This suggests that prioritizing users with low SNR relative to the BS is more effective than assisting users who already have good conditions relative to the IRS, particularly when the IRS is positioned near the BS.

Figure 3.7 illustrates the power savings achieved by the simulated algorithms (exhaustive search, MAX-BS, and MIN-IRS) as a function of the number of served users. The BS power for different scenarios (without IRS and with IRS under the various algorithms) is computed using the power model in [144]. The results indicate that the trend in power

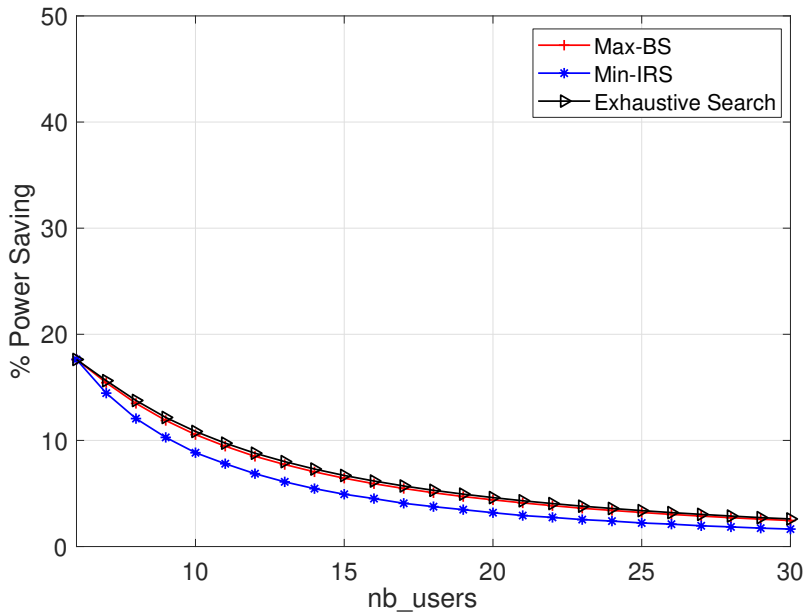

Figure 3.7 – Percentage of power savings with respect to the number of served users for the simulated algorithms (d_{sr}=50m, R=1Mbps).

savings is similar to that of bandwidth savings, with MAX-BS achieving higher savings than MIN-IRS. However, the overall power savings are lower compared to the bandwidth savings, primarily due to the static power consumption of the BS.

3.5 Summary

Reducing the bandwidth required per user and minimizing the energy footprint of cellular networks have become critical objectives for future systems. In this chapter, we investigated the use of IRSs to assist users in a cellular network scenario. We consider that the IRS consists of blocks that can be used to assist several users, and the problem was formulated as a Non Linear Integer Problem. We solved this optimization problem using exhaustive search and proposed two low-complexity heuristic algorithms. Simulation results demonstrated that significant bandwidth and power savings can be achieved when the IRS is optimally positioned near the base station and its resources are properly managed.

These findings provide a foundation for the next chapter, where IRSs are further exploited in combination with statistical CSI to enhance coverage in MISO systems. Specifically, the next chapter extends the concept of IRS assisted resource allocation to improve

network performance, optimize the number of antennas at the BS, and enhance users' SNR, demonstrating how IRS integration can simultaneously improve coverage, efficiency, and system cost effectiveness.

Chapter 4

MISO system with Intelligent Reflecting Surfaces assisted cellular networks

In the previous chapter, we studied the potential of IRSs to reduce the bandwidth requirements and energy consumption in cellular networks by modeling the IRS as a set of blocks that can be allocated to different users. The results confirmed that significant performance gains can be achieved when IRS resources are properly managed and placed near the BS. Building upon this foundation, the present work investigates the integration of IRSs with MISO systems in B5G networks.

4.1 Introduction

While technologies such as massive MIMO and mm-wave communications have been proposed to enhance coverage and capacity [81], they generally lead to higher energy consumption and infrastructure costs due to the deployment of additional active antennas and RF chains. In contrast, IRSs offer a promising low-cost solution [146]-[18], by relying on passive elements that can intelligently reconfigure the wireless propagation environment. In this chapter, we first analyze the benefits of IRSs in Single User MISO (SU-MISO) systems under different channel models, and then extend the study to Multi User MISO (MU-MISO) systems where the IRS is modeled as a block of resources. The problem of selecting assisted users and allocating IRS blocks is formulated as a NLIP, solved using exhaustive search and two proposed heuristic algorithms. The contributions of this work are threefold:

— Evaluate the SNR performance of IRS assisted SU-MISO systems under Rayleigh and Rician fading channels.

— Optimize the number of antennas required at the BS for a given target SNR, thereby reducing the complexity and cost of the infrastructure.
— Extend the analysis to MU-MISO systems, where IRS resources are allocated across users, and propose low complexity algorithms for efficient resource management.

The remainder of this chapter is organized as follows. Section 4.2 presents the system model for SU-MISO and MU-MISO networks. Section 4.3 addresses the planning phase and optimization of antennas at the BS. Section 4.4 formulates the coverage maximization problem, while Section 4.5 introduces the proposed heuristic algorithms. Simulation results are discussed in Section 4.6, and Section 4.7 concludes the chapter.

4.2 System Model

We consider a three-node system in which a BS equipped with M antennas communicates with a single antenna user (destination), assisted by an IRS, as shown in Figure 4.1-b. Both the BS and the IRS employ Uniform Linear Arrays (ULAs). We consider that only statistical CSI is available at the BS, and the user requires a predetermined SNR. The direct channel between the BS and the user is always modeled as Rayleigh fading, which motivates the use of IRS assistance. Our analysis is divided into three main cases:

1. **Reference scenario (SU-MISO without IRS):** A system composed of the BS and a single user, where the channel is modeled as Rician fading. In this case, we estimate the minimum number of BS antennas required to achieve the target SNR. This scenario serves as a benchmark for the subsequent cases.

2. **SU-MISO with IRS assistance:** A three-node system where the BS-IRS and IRS-user channels can follow either Rician or Rayleigh fading, while the BS-user channel remains Rayleigh. We compute the required system parameters to achieve the target SNR under these conditions.

3. **MU-MISO with IRS assistance:** A MU system where the IRS is partitioned into blocks of reflecting elements. The allocation of IRS blocks to users is formulated as a Non Linear Integer Program (NLIP). To reduce complexity, we propose two heuristic algorithms for resource allocation.

4.2.1 First: BS–Destination without IRS

The received signal y at the destination from the BS is given by [146]:

$$y = \sqrt{\frac{p}{d^{\alpha_s}}} h_s^T \mathbf{f} x + n, \tag{4.1}$$

where p denotes the transmitted power, x is the Gaussian input signal such that $E(xx^*) = 1$, $\mathbf{f} \in \mathbb{C}^{M\times 1}$ is the transmit beamforming vector with $||\mathbf{f}||^2 = 1$, and $h_s \in \mathbb{C}^{M\times 1}$ represents the channel between the BS and the user with path loss exponent α_s. The term n denotes the AWGN with zero mean and variance σ^2, while d is the distance between the BS and the destination.

For the case of Rician fading, the channel vector is expressed as

$$h_s = a_s \overline{h}_s + b_s \tilde{h}_s, \tag{4.2}$$

where $a_s = \sqrt{\frac{K_s}{K_s+1}}$ and $b_s = \frac{1}{\sqrt{1+K_s}}$.

K_s is the Rician K factor[1]. The vector $\tilde{h}_s$ represents the NLOS components, whose elements follow zero mean complex Gaussian random distribution with unit variance. The LOS component $\overline{h}s$ is given by $\mathbf{a}_M(\boldsymbol{\theta}_{AoD,s})$, where $\mathbf{a}_M(\boldsymbol{\theta}) \triangleq [1, \exp^{j\boldsymbol{\theta}}, \ldots, \exp^{j(M-1)\boldsymbol{\theta}}]^T$ corresponds to the ULA response, and $\boldsymbol{\theta}_{(AoD,s)}$ is the Angle of Departure (AoD) from the BS.

With CSI at the destination, the instantaneous channel capacity is expressed as [146]

$$C = \log_2 \left(1 + \gamma_0 |h_s^T \mathbf{f}|^2\right), \tag{4.3}$$

where $\gamma_0 = \frac{p}{d^{\alpha_s}\sigma^2}$,

Since the BS has access only to statistical CSI in practice, the goal is to maximize the ergodic capacity rather than the instantaneous capacity. For the optimal transmit beam, the ergodic capacity is upper bounded by [146]:

$$C_{up} = \log_2 \left(1 + \gamma_0 \left(a_s^2 + b_s^2 M\right)\right), \tag{4.4}$$

Correspondingly, the SNR without the assistance of the IRS is given by

1. The Rician K factor measures the strength of the direct (LOS) signal relative to the scattered components. High values indicate strong LOS dominance, whereas $K = 0$ corresponds to Rayleigh fading [147].

$$\mathrm{SNR}_{NIRS} = \gamma_0(a_s^2 + b_s^2 M), \tag{4.5}$$

From this relation, the required number of antennas at the BS to achieve a target SNR can be determined as

$$M = \frac{\frac{\mathrm{SNR}_{NIRS}}{\gamma_0} - a_s^2}{b_s^2}. \tag{4.6}$$

Therefore, in the absence of IRS, the relation between the achievable SNR and the number of antennas at the BS is linear.

4.2.2 Second: IRS Supported Transmission

In all the subcases below with the SU-MISO system, the received signal y from the BS can be expressed as [146]:

$$y = \sqrt{p}\left(\frac{h_r^T \mathbf{\Theta} H_{sr}}{\sqrt{d_{sr}^{\alpha_{sr}} d_r^{\alpha_r}}} + \frac{h_s^T}{\sqrt{d_s^{\alpha_s}}}\right)\mathbf{f}x + n, \tag{4.7}$$

where $\mathbf{\Theta} = \mathrm{diag}\{\theta\}$ represents the phase shift matrix, with $\theta = [e^{j\theta_1}, e^{j\theta_2}, \ldots, e^{j\theta_N}]^T \in \mathbb{C}^{N\times 1}$ and $|\theta_n| = 1$, $n = 1, \ldots, N$. In addition, $H_{sr} \in \mathbb{C}^{N\times M}$ represents the channel between the BS and the IRS with path loss exponent α_{sr}, and $h_r \in \mathbb{C}^{N\times 1}$ represents the channel between the IRS and the destination with path loss exponent α_r. The terms d_{sr} and d_r denote the distances between the nodes of the system.

In the scenario where a Rayleigh fading channel exists between the BS and the user, the IRS becomes effective. The channel vector is expressed as

$$h_s = a_s \tilde{h}_s, \tag{4.8}$$

To avoid repetition, we model the channels between the BS–IRS and IRS–destination as Rician fading channels, which encompass Rayleigh fading as a special case. The channels are expressed as

$$H_{sr} = a_{sr}\bar{H}_{sr} + b_{sr}\tilde{H}_{sr}, \tag{4.9}$$

$$\mathbf{h}_r = a_r \bar{h}_r + b_r \tilde{h}_r, \tag{4.10}$$

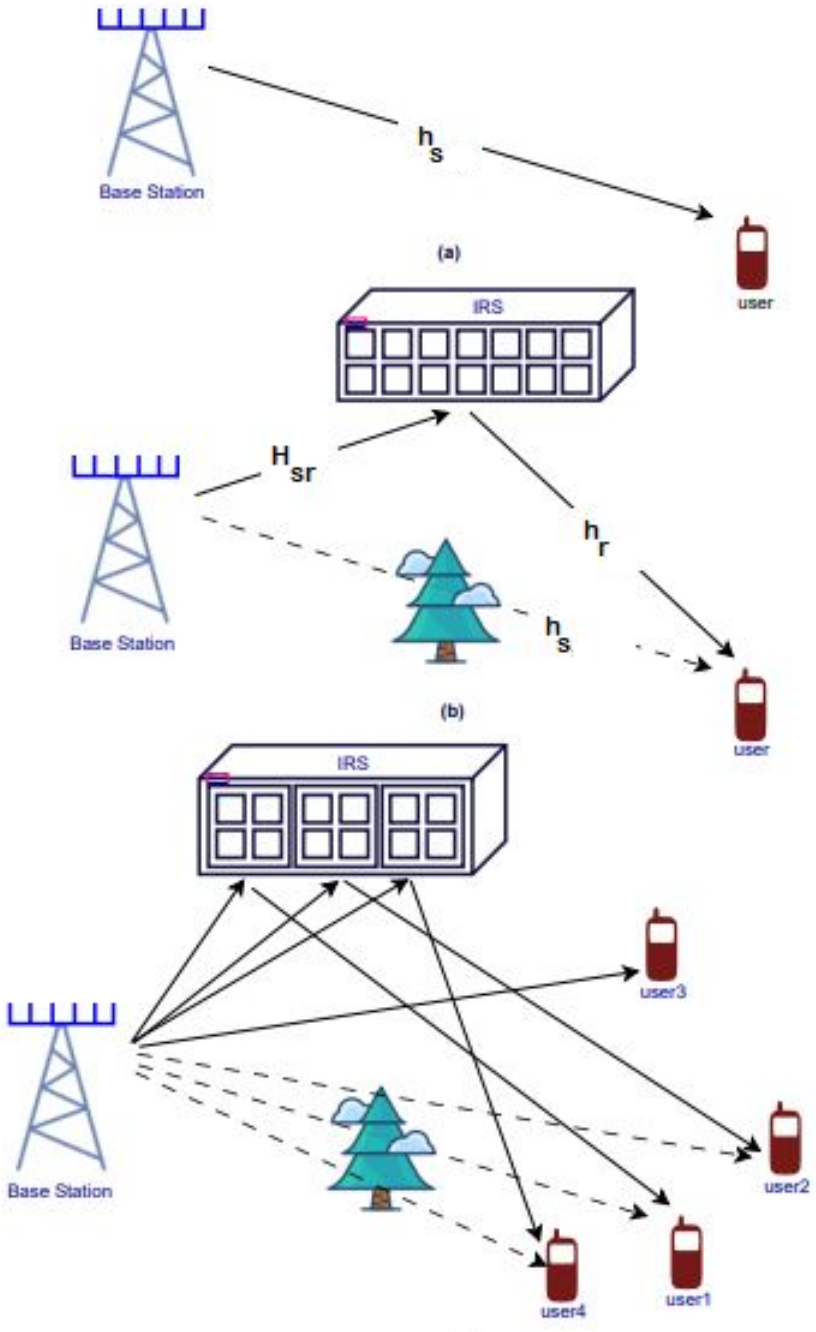

Figure 4.1 – System model: (a) without IRS, (b) with IRS (SU), and (c) with IRS (MU).

with

$$a_{sr} = \sqrt{\frac{K_{sr}}{K_{sr}+1}}, \qquad b_{sr} = \frac{1}{\sqrt{K_{sr}+1}},$$

$$a_r = \sqrt{\frac{K_r}{K_r+1}}, \qquad b_r = \frac{1}{\sqrt{K_r+1}}.$$

Here, $\tilde{H}_{sr}$ and $\tilde{h}_r$ represent the NLOS components, with Independent and Identically Distributed (IID) zero mean complex Gaussian entries of unit variance. K_{sr} and K_r denote the corresponding Rician factors.

The LOS components $\bar{h}_r$ and $\bar{H}_{sr}$ are expressed as

$$\bar{h}_r = \mathbf{a}_N(\boldsymbol{\theta}_{AoD,r}), \tag{4.11}$$

$$\bar{H}_{sr} = \mathbf{a}_N(\boldsymbol{\theta}_{AoA,(sr)})\mathbf{a}_M^T(\boldsymbol{\theta}_{AoD,(sr)}), \tag{4.12}$$

where $\mathbf{a}_N(\boldsymbol{\theta}) \triangleq [1, \exp^{\jmath\boldsymbol{\theta}}, \ldots, \exp^{\jmath(N-1)\boldsymbol{\theta}}]^T$, $\theta_{AoA,(sr)}$ denotes the Angle of Arrival (AoA) at the IRS, and $\boldsymbol{\theta}_{AoD,r}$, $\boldsymbol{\theta}_{AoD,(sr)}$ represent the Angles of Departure from the IRS and the BS, respectively.

With CSI at the destination, the instantaneous channel capacity with IRS assistance is given as [146]:

$$C = \log_2\left(1 + \gamma\left|\left(h_r^T\boldsymbol{\Theta}H_{sr} + \vartheta h_s^T\right)\mathbf{f}\right|^2\right), \tag{4.13}$$

where

$$\gamma = \frac{p}{d_{sr}^{\alpha_{sr}} d_r^{\alpha_r}\sigma^2}, \qquad \vartheta = \sqrt{\frac{d_{sr}^{\alpha_{sr}} d_r^{\alpha_r}}{d_s^{\alpha_s}}}.$$

Thus, instead of maximizing instantaneous channel capacity, the objective is to maximize the ergodic capacity by jointly designing the phase-shift matrix $\boldsymbol{\Theta}$ and the beamforming vector $\mathbf{f}$. Based on [146], the capacity of the system is upper bounded as

$$C_{up} = \log_2\left(1 + \gamma\left(a_r^2 a_{sr}^2 MN^2 + b_r^2 a_{sr}^2 MN + b_{sr}^2 N + \vartheta^2\right)\right). \tag{4.14}$$

Accordingly, the SNR is given by

$$\mathrm{SNR}^{IRS} = \gamma \left(a_r^2 a_{sr}^2 MN^2 + b_r^2 a_{sr}^2 MN + b_{sr}^2 N + \vartheta^2 \right). \tag{4.15}$$

In the preceding, we evaluated the SNR in two main scenarios: with IRS assistance and without it. By considering four distinct channel models, we investigate the effect of fading assumptions on the SNR.

Case 1: BS-IRS and IRS-end user channels are Rayleigh

When H_{sr} and $h_{r,u}$ undergo Rayleigh fading, i.e., $K_{sr} = 0$ and $K_{r,u} = 0$, the SNR becomes:

$$\mathrm{SNR}^{IRS} = \gamma \vartheta^2, \tag{4.16}$$

It can be inferred that the SNR is not impacted by variations in the number of antennas at the BS or the number of elements in the IRS. Instead, the distance between nodes and the transmitted power are the key determinants of the SNR [26].

Case 2: BS-IRS channel is Rayleigh, IRS-end user channel is Rician

In this case, the link between the IRS and the user is subject to Rician fading, whereas the connection between the BS and the IRS experiences Rayleigh fading. Since $K_{sr} = 0$, the number of elements in the IRS has a direct impact on the SNR, which can be expressed as:

$$\mathrm{SNR}^{IRS} = \gamma \left(b_{sr}^2 N + \vartheta^2 \right), \tag{4.17}$$

It can be observed that the SNR increases linearly with the number of IRS elements, highlighting the importance of IRS deployment in enhancing link quality.

Case 3: BS-IRS channel is Rician, IRS-end user channel is Rayleigh

In this case, the channel between the BS and the IRS follows a Rician distribution, while the IRS–user link undergoes Rayleigh fading. The resulting SNR expression is given by [146]:

$$\mathrm{SNR}^{IRS} = \gamma \left(b_r^2 a_{sr}^2 MN + b_{sr}^2 N + \vartheta^2 \right), \tag{4.18}$$

It can be observed that the SNR depends on both the number of IRS elements N and the number of BS antennas M. Specifically, increasing N enhances the IRS reflection gain, while increasing M strengthens the transmit beamforming capability at the BS. Therefore, the combined effect of a larger IRS and a higher antenna count at the BS leads to a significant improvement in the overall system performance.

Case 4: All channels are Rician except BS–destination channel is Rayleigh

This scenario represents the optimal configuration in terms of achievable SNR. Here, the SNR exhibits a linear dependence on the number of antennas at the BS, M, and a quadratic dependence on the number of IRS elements, N, as given by [146]:

$$\mathrm{SNR}^{IRS} = \gamma \left(a_r^2 a_{sr}^2 M N^2 + b_r^2 a_{sr}^2 M N + b_{sr}^2 N + \vartheta^2 \right), \tag{4.19}$$

From the equation, it is evident that increasing both the IRS size significantly enhances the SNR. This highlights the strong benefit of a large IRS when the intermediate channels have a strong LOS component.

4.2.3 Third: MU-MISO System Supported Transmission

The signal received by destination k can be expressed as:

$$y_k = \sqrt{p_k} \left(\frac{h_{r_k}^T \mathbf{\Theta} H_{sr_k}}{\sqrt{d_{sr_k}^{\alpha_{sr_k}} d_{r_k}^{\alpha_{r_k}}}} + \frac{h_{s_k}^T}{\sqrt{d_{s_k}^{\alpha_{s_k}}}} \right) \mathbf{f} x_k + n_k, \tag{4.20}$$

where p_k and n_k denote the transmitted power and noise at destination k, respectively. In this scenario, the channel between the BS and the destination is modeled as Rayleigh fading, whereas the other channels follow Rician fading. Each user k needs to achieve a target SNR, given by:

$$\mathrm{SNR}_k^{IRS} = \gamma_k \Big(a_{r_k}^2 a_{sr_k}^2 M_k N_k^2 + b_{r_k}^2 a_{sr_k}^2 M_k N_k + b_{sr_k}^2 N_k + \vartheta_k^2 \Big), \tag{4.21}$$

with

$$\gamma_k = \frac{p_k}{d_{sr_k}^{\alpha_{sr_k}} d_{r_k}^{\alpha_{r_k}} \sigma_k^2}, \qquad \vartheta_k = \sqrt{\frac{d_{sr_k}^{\alpha_{sr_k}} d^{\alpha_{r_k}}}{d^{\alpha_{s_k}}}},$$

where M_k and N_k denote the number of antennas at the BS and the number of IRS elements assigned to user k, respectively, to achieve the required SNR. This formula-

tion allows us to evaluate the impact of the channel models on the SNR for both SU and MU systems. In the following sections, we will investigate the effect of the number of IRS elements on achieving the desired SNR and optimizing the IRS assisted system performance.

4.3 Planning Phase: SU-MISO System

During the planning of a new BS deployment, the objective is to minimize the number of antennas at the BS while still achieving a predetermined SNR. Unlike other approaches that aim to maximize SNR, our strategy focuses on conserving resources by providing only what is necessary. The goal is to achieve a SNR value equal to or slightly above the required threshold, enabling the BS to serve a larger number of users with the assistance of the IRS. Using Eq. **??**, the required number of antennas can be expressed as a function of N and the target SNR:

$$M = \frac{\frac{SNR^{IRS}}{\gamma} - b_{sr}^2 N - \vartheta^2}{a_r^2 a_{sr}^2 N^2 + b_r^2 a_{sr}^2 N}, \tag{4.22}$$

The task is to determine the minimum number of antennas M at the BS and the number of IRS elements N needed to achieve the desired SNR. It should be noted that not all SNR values are achievable with arbitrary combinations of M and N. According to Eq. **??**, increasing M and N enhances the SNR, but practical limits exist depending on the IRS size for the intended application.
To find the maximum number of IRS elements for a given SNR, we can set $M = 1$ and compute the corresponding N, denoted as $N_{\max}$. More generally, Eq. 4.23 allows us to evaluate the maximum number of IRS elements for any number of antennas at the BS:

$$N = \frac{-(b_r^2 a_{sr}^2 M + b_{sr}^2) + \sqrt{(b_r^2 a_{sr}^2 M + b_{sr}^2)^2 - 4M a_r^2 a_{sr}^2 (\vartheta^2 - \frac{SNR^{IRS}}{\gamma})}}{2 a_r^2 a_{sr}^2 M}, \tag{4.23}$$

In cellular networks, during the planning phase, our goal is to reduce the number of antennas (and thus the cost) with the support of the IRS. Ideally, the IRS is placed close to the BS, and for each number of antennas, a corresponding maximum number of IRS elements is determined depending on the user's location within the cell.

To evaluate coverage, we define the following parameters: Coverage, Percentage of Coverage (P_{cov}), and Percentage of Assistance (P_{ass}). A user is considered covered if the

calculated SNR at their location meets or exceeds the required threshold. For simplicity, we consider a square cell of side S_C, divided into smaller squares of side s_c, where users occupy the center of each smaller square. The total number of possible user positions is:

$$n_p = \lfloor \left(\frac{S_C}{s_c} \right)^2 \rfloor,$$

The percentage of coverage is then:

$$P_{cov} = \frac{100 \cdot n_p^{ser}}{n_p},$$

where n_p^{ser} is the number of positions where the user achieves the target SNR with the assistance of the IRS. The planning phase aims to maximize P_{cov}, ensuring users are served across the cell by optimizing the combination of M and N for a given SNR. Minimization priority is applied first to the number of antennas at the BS and then to the number of IRS elements.

Specifically, for each user position p_k $(k = 1, \ldots, K)$, the optimal combination (M, N) is determined to achieve the desired SNR. Cellular networks operate in two phases:

— **Planning phase:** Defines the number of antennas to install at the BS and configures the network for expected coverage and capacity. Adjustments to M are possible at this stage.

— **Operation phase:** The BS is fully deployed and actively manages traffic. The IRS can assist users to reach the required SNR in a cost-efficient manner, enhancing network performance.

The planning phase offers advantages over the operational phase, such as the flexibility to adjust M. The main goals are to maximize P_{cov}, minimize the number of BS antennas, and then reduce the number of IRS elements required to assist users across the cell.

4.4 Problem formulation

4.4.1 IRS-Assisted MU-MISO System

In the planning phase, the BS can serve multiple single antenna users. In this scenario, the Per_{ass}, is used to evaluate performance. Let IRS have blocks of elements of size N_a^{min},

and a certain number of blocks, n_b, can be allocated to assist multiple users:

$$n_b = \lfloor \frac{N_{tot}}{N_a^{min}} \rfloor, \tag{4.24}$$

where N_{tot} is the total number of elements in the IRS module. Note that n_b also represents the maximum number of users that can be assisted. For a given distribution of users within the cell, Per_{ass} is defined as:

$$Per_{ass} = \frac{100 \cdot n_{ass}}{n_b}, \tag{4.25}$$

where n_{ass} is the number of users actually assisted by the IRS. The primary goal is to maximize Per_{ass} by minimizing the number of BS antennas and the number of IRS blocks assigned to each user, allowing more users to be assisted.

The selection of users to be assisted depends on several factors: their location relative to the IRS and BS, the positioning of the IRS within the cell, and the overall cell size. Without loss of generality, we assume the BS is located at the origin of a Cartesian coordinate system. The number of users assisted depends on both user's condition and the number of IRS elements available.

IRS assistance can be implemented in multiple ways: one approach is to optimize the IRS phase shifts to maximize the SNR for all assisted users; another is to ensure that each assisted user reaches a target SNR [138]. Additionally, the IRS can be shared among users using time division protocols or by allocating different blocks to different users simultaneously. Interference is negligible if users operate on separate frequencies. It is important that each user receives a sufficient number of IRS elements to guarantee a minimum SNR gain [31].

In this study, we simplify the allocation policy by assigning each user a block of IRS elements with size N_a^{min}. The effect of assisting a user with any block is considered identical, considering the IRS is sufficiently far from both the BS and the users. For near field IRS deployments, block positions may need to be considered, which is beyond the scope of this work. The system model is illustrated in Figure 4.1-c, showing a BS serving four users, with three receiving IRS assistance.

The problem can be formulated as finding, for each number of BS antennas M_i, the vector $X_K = [x_1, x_2, \ldots, x_K] \in \mathbb{N}^{1\times K}$ representing the number of blocks allocated to each user, to maximize Per_{ass}:

$$\max_{X_K} \; Per_{ass}, \tag{4.26}$$

where the number of IRS elements allocated to user k is $x_k \times N_a^{min}$.
The optimization problem is subject to the following constraints:

$$0 \leq \sum_{k=1}^{K} x_k \leq n_b,$$

$$SNR_k \geq SNR_{predetermined},$$

$$0 \leq M_i \leq M_{max}.$$

These constraints ensure that each user is allocated a positive number of blocks and that the total number of blocks does not exceed the available resources. The non linear and integer nature of the objective function (Eq. 4.26 and Eq. 4.25) in the MU-MISO scenario results in a NLIP problem [143].

4.5 Proposed Algorithms

The IRS is composed of multiple blocks. Our objective is to optimally allocate these blocks among users for each number of antennas at the BS, in order to maximize the number of assisted users who require a specific SNR. At every position in the cell, for a given number of BS antennas, we aim to determine the allocation of IRS blocks by examining all possible combinations of users to be assisted and the number of blocks assigned to each user, then selecting the configuration that achieves a SNR closest to the predetermined target.
To ensure efficient assistance, the IRS should be placed near the BS [22]. Users are uniformly distributed within the cell. To evaluate the gain of sharing the IRS among multiple users, we compute the percentage of assistance provided by the BS with IRS. An exhaustive search is used to determine, for each user position p_k and BS antenna number, the optimal allocation of IRS blocks. This involves examining all possibilities and selecting users that meet the required SNR with the minimum number of blocks.
For example, consider a scenario with 3 IRS blocks and 4 users, as illustrated in Figure 4.1. The maximum number of assisted users is 3. If each of these 3 users achieves the required SNR using only 1 block, the percentage of assistance reaches 100%. However, if

one user requires 1 block and another requires 2 blocks, only 2 users can be assisted, and the percentage of assistance decreases. In such case, increasing the number of antennas at the BS can help assist more users.

Although exhaustive search provides the optimal solution, it comes with high computational cost. To reduce complexity, we propose two low complexity algorithms:

— **MAX-BS**: Prioritizes users with the largest distance from the BS by allocating them the maximum number of available IRS blocks. This ensures that users with the greatest need for IRS assistance are served first.

— **MIN-IRS**: Prioritizes users based on their proximity to the IRS and assigns them the largest number of IRS blocks. Users with favorable radio conditions relative to the IRS are given highest preference.

4.6 Simulation Results

We consider a MBS serving a square cell of side S_C. In the planning phase, we consider that the user is in the center of a small square with sides of length s_c. The MBS operates with a 3 GHz carrier frequency and 10 MHz bandwidth.

Table 4.1 – Simulation Parameters

Parameter	**Value / Assumption**
Number of users	1 to 30
Cell size	300×300 m^2
Number of elements in the IRS	50 to 500
Number of antennas	BS: 1 to 8, User: 1
Environment	Urban
Carrier frequency f_c	3 GHz
IRS coordinates (x_R, y_R)	Near: $(-5, 50)$, Far: $(-5, 200)$
BS coordinates (x, y)	$(0, 0)$
Path loss exponent with IRS	BS-IRS: 2.2, BS-User: 3.5, IRS-User: 2.2
Path loss exponent without IRS	BS-User: 2.8
Noise power	-94 dBm
Transmitted power	5 dBm for all users
Rician K factor	Normalized to 1

Figure 4.2 illustrates the impact of the number of antennas at BS, M, on the SNR in a system with and without the IRS. This figure is studied according to Eq. 4.5, where

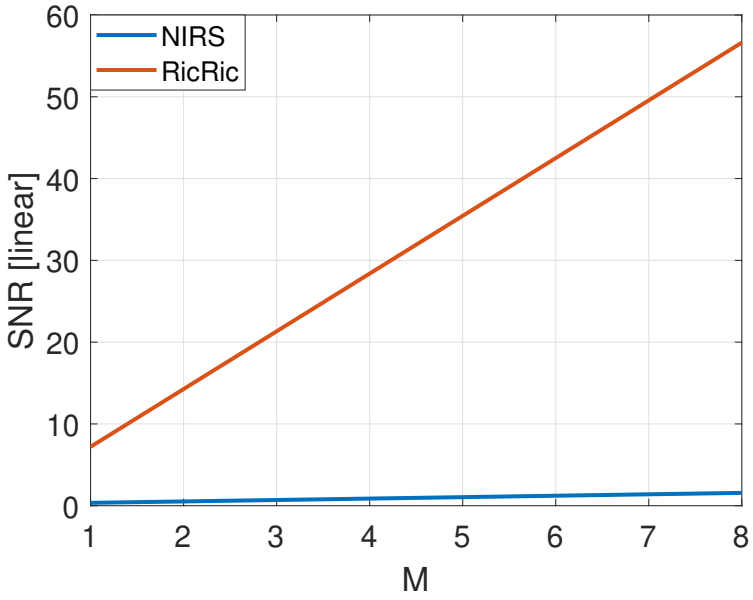

Figure 4.2 – SNR with respect to the number of antennas at the BS for a system model without and with the assistance of the IRS (N=100)

the system is taken without the assistance IRS with a Rician channel model between the BS and the user. The SNRs vary linearly with M, but the slope is very small compared to the other variation in this figure. Whereas, according to Eq. **??**, with 100 elements in the IRS, we obtain a figure with faster slope giving us more effect on the increasing of the number of antennas. Therefore, we can conclude, from this figure that the existence of the IRS can affect the variation of number of antennas at the BS. When using the IRS, different channel models can exist between the nodes of our system. Our objective is to evaluate the effect of these channel models on the required SNR. Figure 4.3 shows us the variation of SNR as a function of the number of elements in the IRS for 2 antennas at the BS. Different channel models that we discussed earlier exist. In Figure 4.3a, we compare the Ric-Ray (where the model of the channel between the BS and IRS is Rician, while the model is Rayleigh between the IRS and the user) with Ray-Ric (where the model of the channel between the BS and IRS is Rayleigh, while Rician is used between the IRS and the user). The effect of the existence of LOS between the BS and the IRS is more significant than between the IRS and the user. Also, when this LOS exists from both sides, the effect is bigger, as we can see in Figure 4.3b. It is worth noting that the primary objective of using the IRS is to overcome obstacles between the BS and the user. Therefore, the existence of the IRS aims to create an indirect LOS first between the BS and the user.

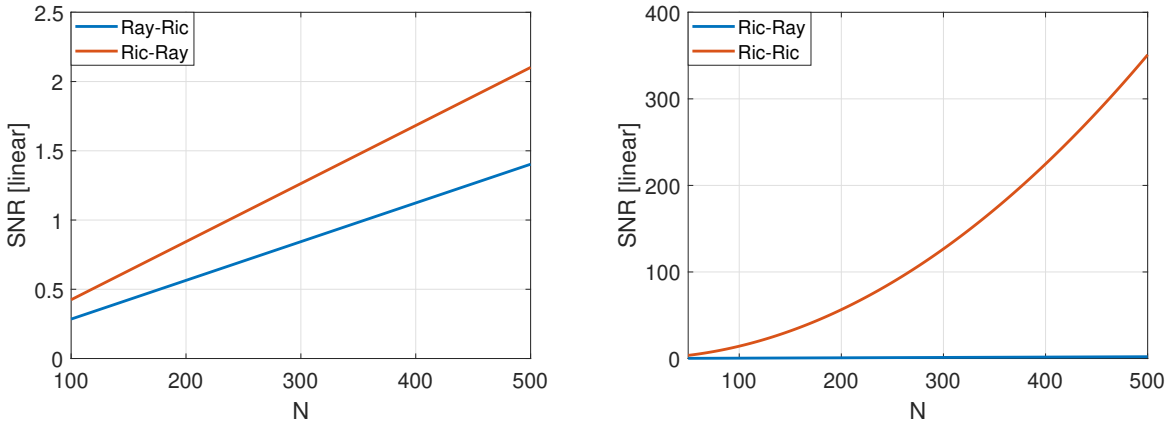

(a) (b)

Figure 4.3 – SNR with respect to the number of elements in the IRS, two types of channel model (M = 2) : (a) Ric-Ray, Ray-Ric (b) Ric-Ray, Ric-Ric.

According to Eq. 4.22, the relation between M and N can be determined for a required SNR. To explore the complete range of variations between these variables, Figure 4.4 is plotted with a wide range of N values to identify any unacceptable regions. This figure shows the curve of M with respect to N for a SNR= 20 dB, for a user placed at the edge of the cell and the IRS placed near the BS. We observe that M decreases significantly at the beginning of increasing N, then this variation gradually decreases, while at the end the impact of increasing N becomes less effective. Note that the variation is confined to the region of the graph where M is a positive integer value. Our objective in analyzing this graph is to determine the specific values of M and N that are required to achieve the desired SNR. It is important to note that this variation depends on the position of the user in the cell and the position of the IRS. This graph can give us an idea about the maximum number of elements (since the user is at the edge) that the user needs to achieve the desired SNR.

Figure 4.5 shows the maximum number of elements required in the IRS to achieve different SNR levels for a user located at the edge of the cell and an IRS placed close to the BS, considering the scenario where the BS has different number of antennas ($M = 1, 2, 4, 8$). For example, for a SNR of 20 dB, a user placed at the edge of the cell requires 374 elements in the IRS. It's worth noting that in our simulations, we consider the user at the farthest distance from both the BS and from the IRS, which represents the worst-case scenario with only one antenna at the BS. Those values of N tell us how much IRS needs

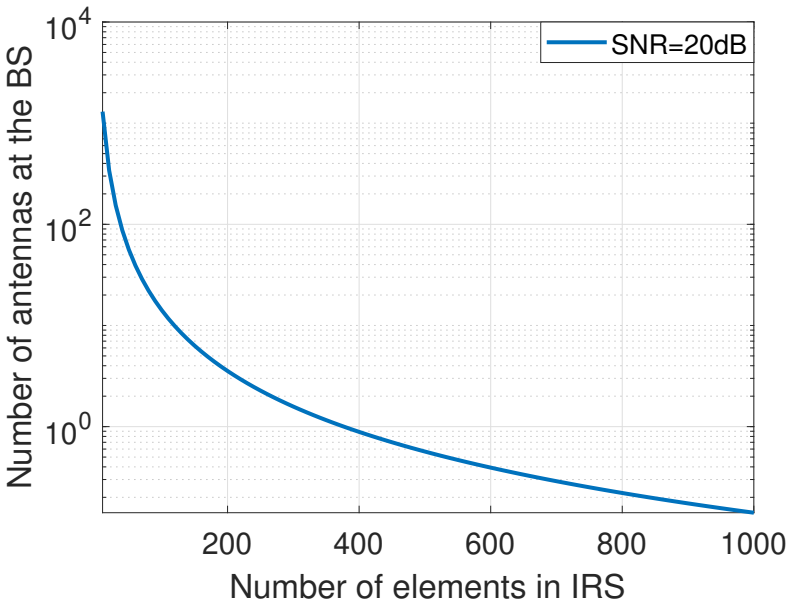

Figure 4.4 – Number of antennas with respect to the number of elements in the IRS for SNR = 20dB

to be to require a desired SNR. Adding more antennas at the BS can decrease the number of elements in the IRS. Our objective is to know how much elements in the IRS are needed to replace a certain number of antennas at the BS. Therefore, to obtain a SNR equal to 20 dB, we have more than one choice: By using 2 antennas, we need almost 265 elements in the IRS, this means that if we add 109 elements, this can replace one antenna in the BS. Also, an addition of 243 elements can satisfy 7 antennas at the BS. Therefore, with an increasing number of 243 low-cost elements in the IRS, almost passive, we can replace a high-cost number of antennas in the BS for a required SNR of 20 dB for a user placing at the edge of the cell.

In Figure 4.6a, we consider an IRS placed near the BS and study the variation of the number of antennas at the BS for three different values of SNR as a function of the number of elements in the IRS. A small change in N (only 23 elements) with a SNR of 0 dB can lead to a decrease in the number of antennas at the BS from 8 to 1. However, when the IRS is far from the BS, as shown in Figure 4.6b, the required variation in N increases, with a change of 88 elements needed for a SNR of 0 dB, and 885 elements needed for a SNR of 20 dB, both measured at the edge of the cell. Therefore, the position of the IRS plays a substantial role in achieving the required SNR. Even a small variation in the number of elements in the IRS and the number of antennas at the BS can lead to

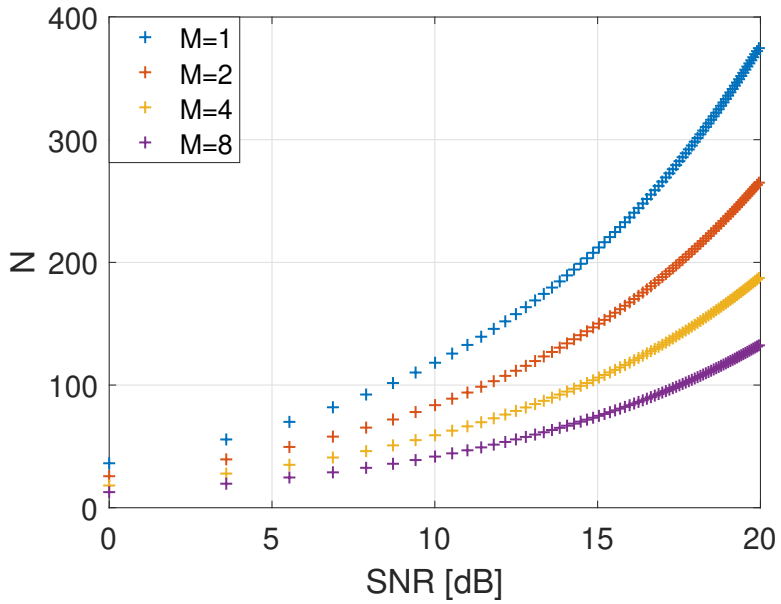

Figure 4.5 – Maximum number of elements in the IRS with respect to SNR (IRS near the BS, user at the edge, M = 1, 2, 4, 8).

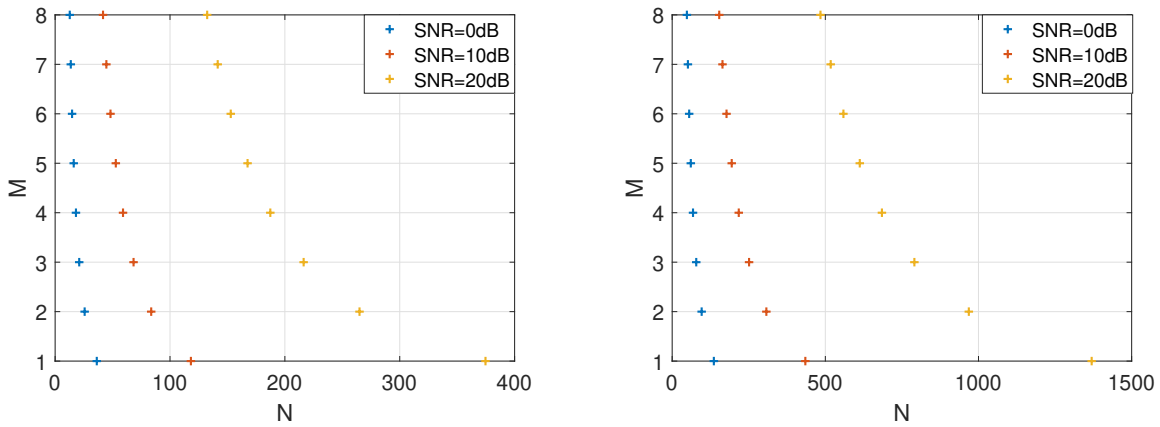

(a) (b)

Figure 4.6 – Number of antennas with respect to the number of elements in the IRS for different SNR (User at the edge) : (a) IRS near the BS, (b) IRS far from the BS.

the desired SNR.

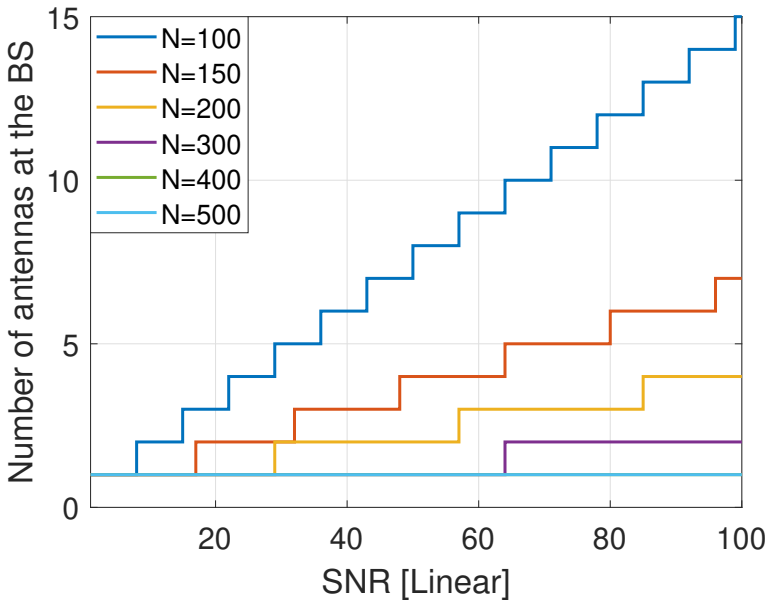

Figure 4.7 – Number of antennas at the BS with respect to the SNR

Figure 4.7 represents only the integer number of antennas at the BS as a function of the SNR for different values of element number in the IRS. The importance of this figure is that it can show that the variation of M is not continuous when N increases.

To study the coverage area of the BS, therefore the percentage of coverage, with the assistance of the IRS, we consider a square cell with a side length of 300 m. In Figure 4.8, the user is located at the center of a smaller square with a side length of 20 m. The BS is represented by a black circle at the origin of a Cartesian coordinate system, while the IRS is shown as a green circle near the BS. The users who can achieve the required SNR are represented by red circles, while the non-covered user is indicated by a black cross. Non-covered users are those who cannot achieve the required SNR even with the assistance of the IRS.

In Figure 4.8, we study the effect of number of antennas at the BS on the percentage of coverage. To know the effect of the position of the IRS on the coverage, we plot Figure 4.9, with only 2 antennas at the BS are and 250 elements in the IRS. One user in this case is not covered when the IRS is near the BS.

Figure 4.8a represents the covered users when only 50 elements are used from the IRS and for 2 antennas at the BS, where in Figure 4.8b, we increase the number of antennas

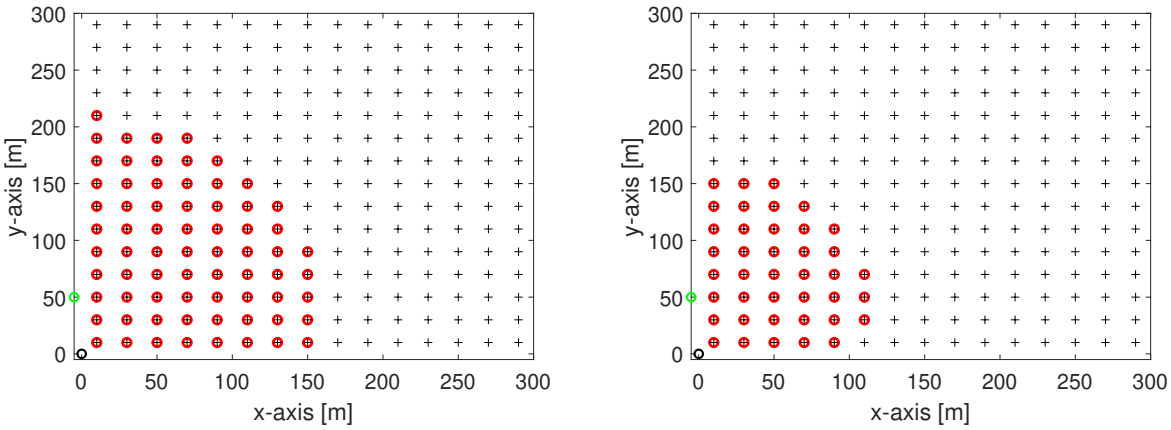

(a) (b)

Figure 4.8 – Covered area, IRS is near the BS (N = 50): (a) M = 2, (b) M = 4.

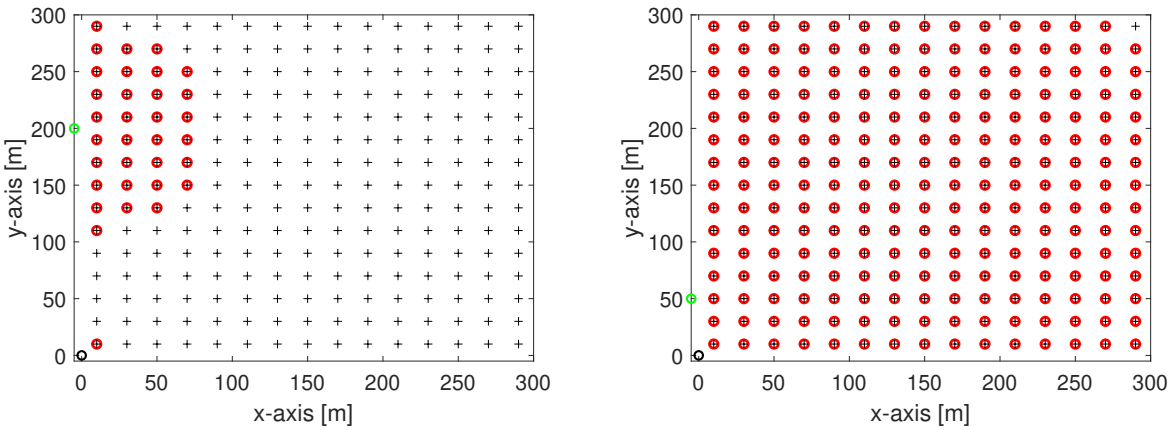

(a) (b)

Figure 4.9 – Covered area, (M = 2, N = 250): (a) IRS far from the BS, (b) IRS near the BS.

at the BS to 4. This variation of M gives us a variation of 8.3%.

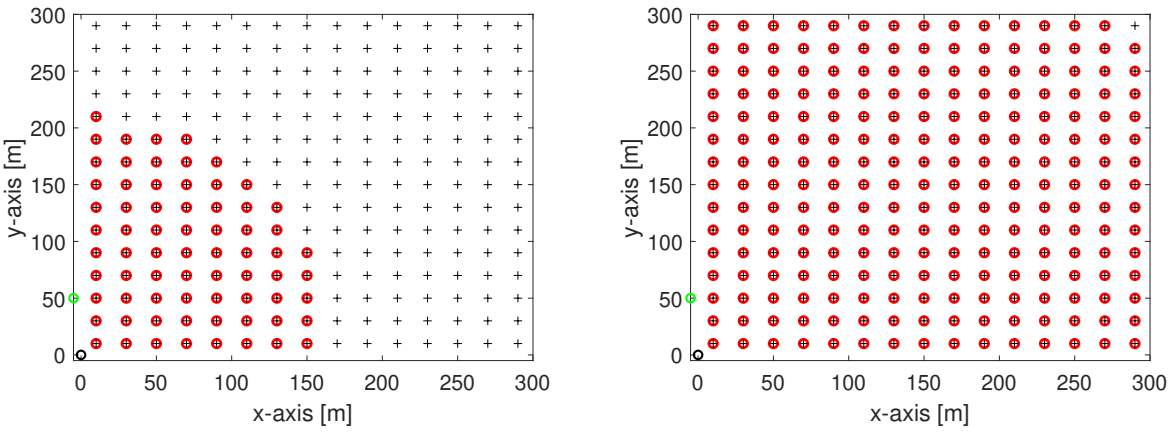

(a) (b)

Figure 4.10 – Covered area when IRS near the BS (M = 2): (a) N = 50, (b) N = 250.

The effect of the number of elements in the IRS on the coverage is considered in Figure 4.10, where we also take 2 antennas at the BS and we consider that the IRS is near the BS. Only 25 users are covered when the number of elements in the IRS is 50, while only 1 user is not covered when N = 250 elements.

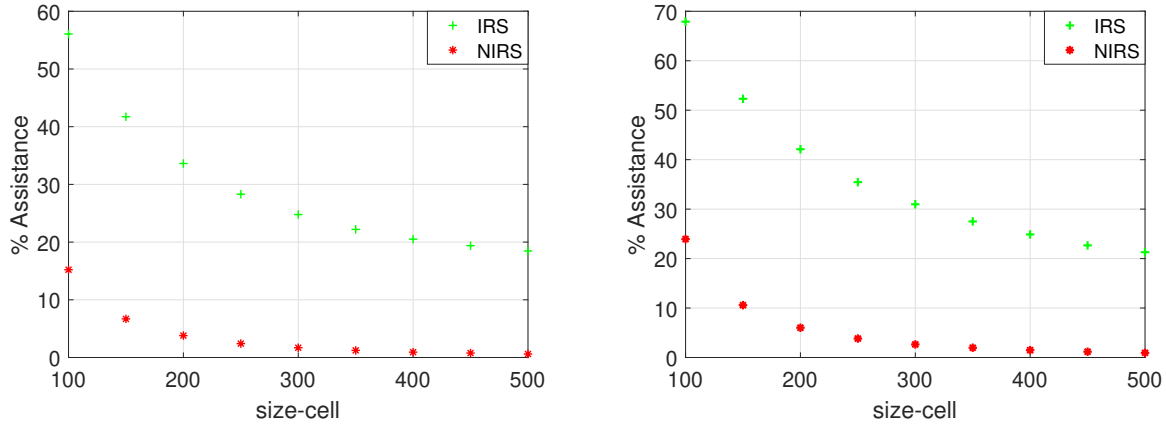

(a) (b)

Figure 4.11 – Percentage of Assistance with respect to the cell size, IRS near BS (N = 50 to 300): (a) M = 2, (b) M = 4.

In all the above work, we studied the case of a SU-MISO system assisted with the IRS. Hereafter, we discuss the case of MU-MISO system assisted with the IRS. We consider the

percentage of assistance P_{ass} and compare the case of a system with and without the IRS. In Figure 4.11, we compare the P_{ass} when we have 2 or 4 antennas at the BS. The IRS is considered formed of blocks of resources of 50 elements each block, is placed near the BS. With or without the assistance of the IRS, we run a Monte Carlo simulation results over 10000 independent trials. We distribute randomly 30 users in the cell then we take different size of the cell; in our case, from 100 m till 500 m.

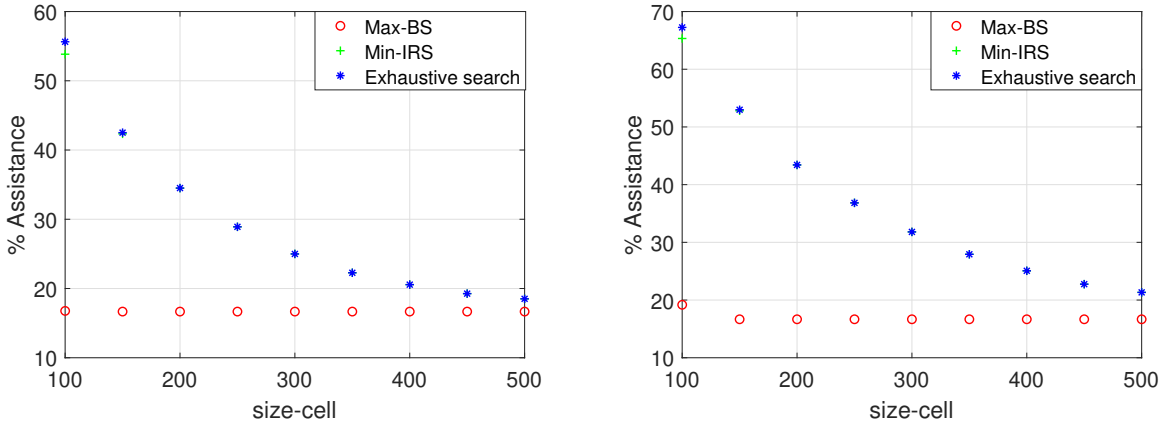

Figure 4.12 – Percentage of Assistance with respect to the cell size, IRS near BS (N=50 to 300). (a) M = 2, (b) M = 4.

Notice that the IRS is formed of 300 elements and it is divided into 6 blocks, therefore if the number of blocks equals to the number of assisted users, then we can say that the percentage of assistance is 100%; since in this case we don't waste any resource on IRS. When using the IRS, Per_{ass} changed from almost 58% till 69%, where the change without the IRS is noted from almost 15% till 22%. Mention that the IRS cannot assist all users, therefore we want to know how we choose the assisted users. First, we begin with choosing users with a SNR smaller the required by using exhaustive search (Figure 4.12). Then, we try to decrease the complexity of search, we propose two low complexity algorithms. The first algorithm, we choose users with minimum distance with the IRS to distribute the blocks. The second algorithm (Max-BS), we choose users with maximum distance with the BS, since those users have less probability to be served by the BS. We take into considerations also two cases, when the number of antennas at the BS is 2 and 4 in function of the cell size. When the cell is of 100 m side size, the percentage of assistance attain almost 55% is the two algorithms, where less than 20% when using the maximum

distance with the BS. When the size of the cell increases to 500 m the 3 algorithms are close to each other, since the users in this case have more probability of being far from the other nodes of the system.

4.7 Summary

This chapter introduces an algorithm to improve the performance of future cellular networks utilizing intelligent reflecting surfaces (IRSs). We investigate the use of IRSs under statistical Channel State Information (CSI) to enhance the coverage of Base Stations (BSs) in Multiple Input Single Output (MISO) systems. Our primary contributions focused on cost and complexity reduction during the network planning phase by studying the effect of the IRS on the required Signal to Noise Ratio (SNR). We proposed using the IRS to reduce the number of active antennas required at the transmitter, thereby decreasing installation costs. For Multi-User (MU) MISO systems, we introduced a novel resource model where the IRS consists of independently manageable blocks. The resulting allocation problem was formulated as a NLIP problem, which we solved using exhaustive search and two proposed low complexity heuristic algorithms. The results demonstrated that leveraging the IRS provides significant system benefits: we achieved a substantial increase in the percentage of coverage (from 11% to 58% with only 2 antennas at the BS and an increase of 100 elements in the IRS), and a meaningful reduction in the number of required antennas, particularly when the IRS is optimally managed and located near the BS.

Building on these insights, the next chapter shifts focus from coverage enhancement to the equally critical aspect of energy efficiency in Beyond 5G (B5G)/6G Small Base Station (SBS) networks. Specifically, the next chapter explores how Reinforcement Learning (RL), supported by IRS, can balance energy consumption with Quality of Service (QoS). By enabling SBSs to adaptively switch between active and multiple sleep modes while maintaining reliable connectivity, the proposed Q-learning scheme extends the role of IRS from improving coverage to facilitating energy savings and network reliability.

Chapter 5

Energy-QoS Trade-off in Intelligent reflecting Surface Assisted Beyond 5G Networks using Reinforcement Learning

In this chapter, we extend our investigation of IRS assisted wireless networks by focusing on the trade-off between energy efficiency and QoS in B5G/6G Small Base Station (SBS) deployments. While the previous chapter emphasized the role of IRS in improving coverage and reducing antenna requirements, here we integrate RL to dynamically manage SBS operational modes. Specifically, we propose an IRS supported Q-learning scheme that enables SBSs to switch between active and multiple SMs in response to real time traffic variations, achieving substantial power savings while maintaining reliable user connectivity.

5.1 Introduction

The relentless increase in traffic demand has necessitated the ultra-dense deployment of SBSs [148]. While this densification is crucial for capacity, it presents a major challenge in energy consumption [121]. Research has therefore focused on Sleep Mode (SM) management [122]-[123]-[124], evolving from simple binary ON/OFF switching to sophisticated Multi Level SM (MLSM) schemes [133]. Further advancements have integrated Machine Learning, particularly RL, to enable autonomous and traffic aware SM adaptation [129]-[134]-[137].

Despite these efforts, SM schemes inherently struggle with service continuity and coverage holes when SBSs are inactive. Our work addresses this critical trade-off by integrating the IRS, a technology proven to enhance coverage and create reconfigurable channels

wu2021intelligent.
This chapter combines a RL based SM management strategy with IRS assisted user support to maximize energy efficiency while sustaining QoS. The core innovations are:

- **Novel RL Framework for Dynamic SBS Management:** We propose a Q-learning based framework that enables SBSs to autonomously switch between four operational modes (Active, LSM, MSM, and DSM) in real time, adapting to daily traffic fluctuations.
- **IRS Enhanced Service Continuity:** The IRS elements dynamically assist active SBSs during deep sleep modes, significantly reducing user drop rates compared to conventional SM approaches.
- **Adaptive Trade-Off Parameter $\Psi(t)$:** The reward function is designed with a dynamic parameter that is proportional to the traffic load, ensuring that the system prioritizes QoS during peak hours and maximizes energy savings during low demand periods.
- **Hierarchical Power Management:** The use of a state discretization scheme (4 power levels per SBS) balances load representation with efficient RL convergence, resulting in optimal learned policies.

The remaining of this chapter is organized as follows. In Section 5.2, we present the system model with the description of the system architecture and the SMs is presented. The problem is formulated in Section 5.4. Section 5.5, details our Q-learning algorithm. In Section 5.6, we present and discuss our results, concluding with a direct comparison between our system's performance *with* and *without* IRS assistance. The paper concludes in Section 5.7.

5.2 System model

This section outlines the cellular network architecture, the operational modes of the SBS under control, the role of the IRS and operation, the traffic model, and the RL framework. We consider that the system comprises three SBSs: SBS1, SBS2, and SBS3, strategically located at predefined positions within a defined geographical area as illustrated in Figure 5.1. Users are randomly distributed within the simulation area following a Poisson process. Users are associated with the SBS providing the strongest received signal, considering a maximum association distance from any SBS.

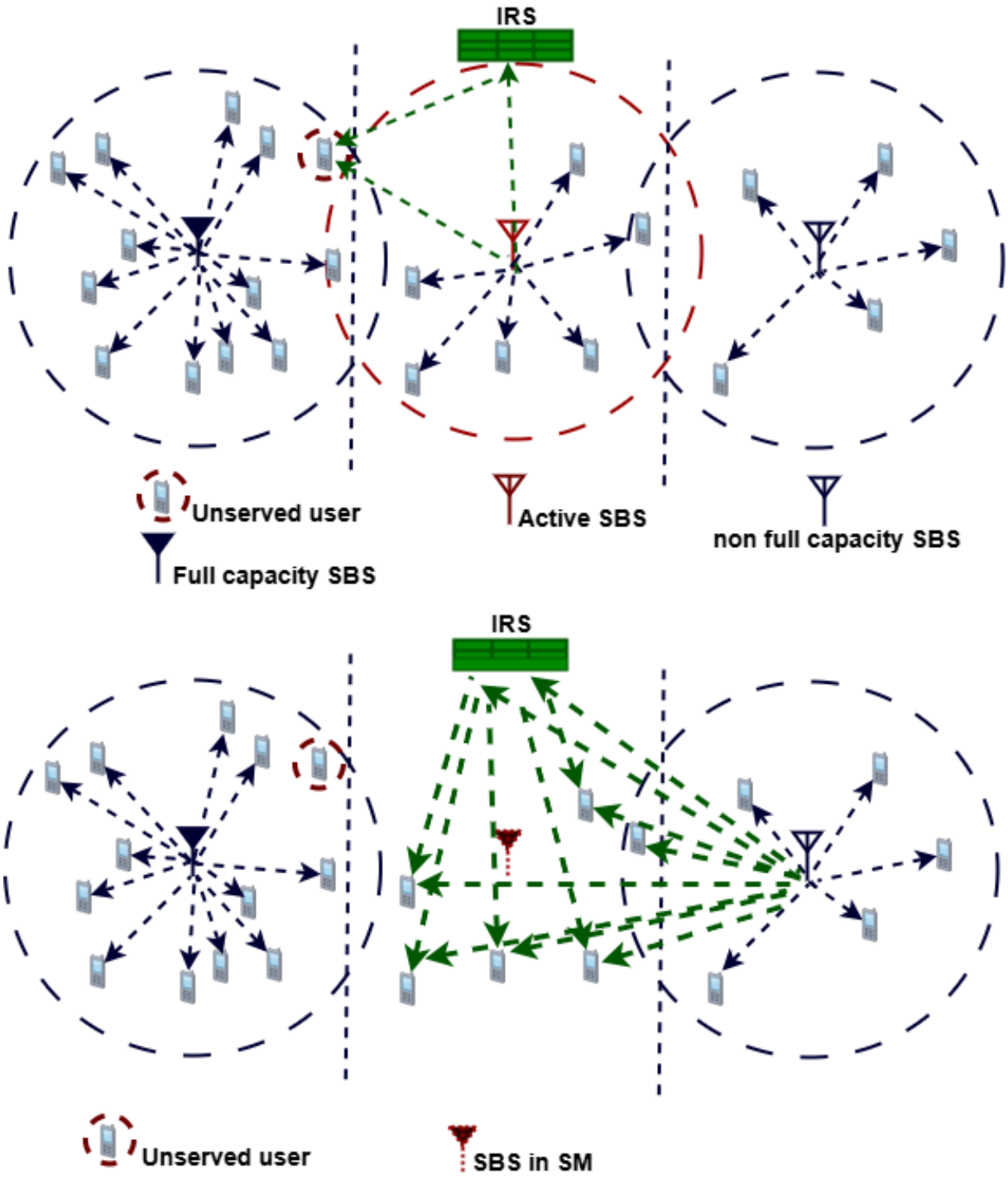

Figure 5.1 – Architecture with 3 SBSs and IRS. (top): Active SBS2 in the middle. (bottom): SBS2 is in SM

5.3 Multi-level SMs and SBS2 Operational Modes

In this system, SBS1 and SBS3 are considered to be continuously active, while our energy efficiency strategy focuses on dynamically controlling the operational mode of SBS2. The RL agent can select from four distinct operational modes, drawing from the Multi Level SM (MLSM) model established by GreenTouch [133]. This model groups sub-components with similar transition latencies when activated or deactivated, allowing for the quantification of power consumption in each mode. The four states available to SBS2 are as follows:

— Active Mode: In this mode, SBS2 is fully operational and able to serve users, consuming the highest power, P_{max}.

— Low Sleep Mode (LSM): This corresponds to the lowest time unit of one OFDM symbol (i.e., 71 μs [133]). Only the power amplifier and some processing components are deactivated, offering some power savings (P_1) with a short transition duration (W_1) to the active mode.

— Medium Sleep Mode (MSM): This level coincides with a sub-frame or Transmission Time Interval (TTI) (i.e., 1 ms [133]). More components enter the sleep state, resulting in greater power savings (P_2) but with a longer transition duration ($W_2 > W_1$).

— Deep Sleep Mode (DSM): This is the deepest SM, corresponding to a frame unit of 10 ms [133]. It offers the most significant power savings (P_3 or P_{min}) as most components are deactivated, but it incurs the longest transition duration ($W_3 > W_2$) to become active again.

— VLSM: This corresponds to the very long sleep level. Its unit corresponds to the entire radio frame of 1 s [133]. It is the standby mode where the base station is out of operation keeps wake up functionality.

Greater energy savings can be achieved by switching the BS to a higher SM level, as more components are deactivated. However, this is associated with a higher risk of user drops, which can negatively impact the system's QoS. The RL agent's choice of an operational mode is dynamic and based on the current state and traffic demand. We do not utilize the Very Long Sleep Mode (VLSM) in our study, as its corresponding wake up periods are not compatible with the periodic signaling bursts required in B5G systems [149], as concurred by the 3GPP. The key characteristics of these SM levels for a 2×2 MIMO SBS are detailed in Table 5.1, although our study for simplicity and convenience

considers a SISO system model. With users' dynamics and SMs, the SBS has to wake up periodically to send signaling bursts. Contrary to Long Term Evolution (LTE) systems where each antenna must transmit every 0.2 ms a unique Cell Reference Signals (CRS) for channel quality estimates and mobility measurements among other Synchronization Signaling (SS), no CRS is required for B5G [149]. Rather than, Physical Broadcast CHannel (PBCH) and SS are transmitted in PBCH/SS block periodically. It was concurred in 3GPP [149], that this periodicity can be set to a value among $[5, 10, 20, 40, 80, 160]$ ms. With these values, VLSM level cannot be employed. Therefore, our work is limited to the first three SM levels.

To simulate a realistic environment, we introduce a real model representing the percentage of maximum traffic at each time, normalized to a 24 h cycle [144]. This traffic profile (Figure 5.2) typically exhibits higher demand during peak hours (e.g., at 10 p.m.) and lower demand during off-peak hours (e.g., at 6 a.m.), as visually confirmed in the traffic level curves in the results. The actual number of users at each time is drawn from a Poisson distribution with a time varying average following these traffic values.

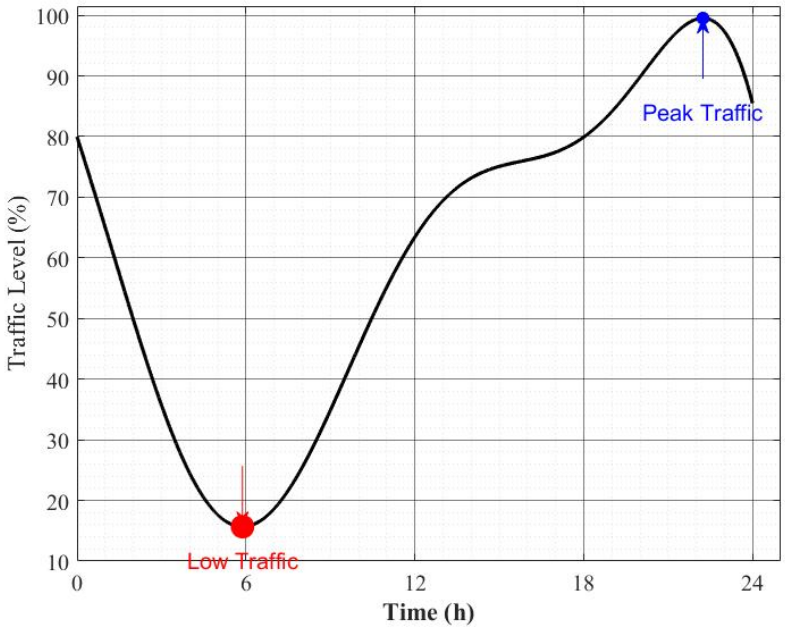

Figure 5.2 – Traffic Model (%) Over Time (h) with Peak and Low traffic annotations.

5.3.1 IRS Operation

The IRS plays a crucial role in maintaining QoS, particularly when SBS2 enters a SM. The IRS can assist users in four primary scenarios:

1. Unserved Users of SBS1 or SBS3 coverage while **SBS2 is Active**: If SBS2 is active and has not saturated and SBS1 or SBS3 cannot serve all users within their coverage areas due to capacity limits, the IRS may assist some of these unserved users.
2. SBS2 reaches its saturation mode: The IRS can assist by enhancing the data rates of nearby users already served by SBS2.
3. **SBS2 is in any of its SMs** (LSM, MSM or DSM), the IRS reconfigures its elements from the continuously active SBS1 and SBS3 to users who would normally be covered by SBS2. This redirection and signal enhancement help to re-associate these users with SBS1 or SBS3, effectively extending their coverage and mitigating potential dropped connections. It is important to note that the ability of the IRS to facilitate connectivity is ultimately constrained by the available capacity of the active SBSs (SBS1 and SBS3).
4. If SBS1 and SBS3 are at full capacity, even with IRS assistance, some users may still be dropped. The IRS in this case, assist fairly users of SBS1 and SBS3 [150].

5.3.2 Reinforcement Learning Framework

We formulate the dynamic SBS2 mode selection as a Markov Decision Process (MDP) problem [151], solved using the Q-learning algorithm [151]. To address this problem, we define the core components of the MDP as follow:

— Agent: The RL agent is the intelligent controller responsible for selecting SBS2's operational mode at each time.

— Environment: The environment encompasses the entire cellular network, including SBS1, SBS2 and SBS3, the dynamically distributed users, and the varying traffic demand.

— States ($\mathcal{S}$): The state of the environment observed by the RL agent is defined by the load levels (or states) of the two continuously active SBSs: SBS1 and SBS3. These levels are discretized to manage the state space complexity and the previous action taken by SBS2.

— Actions ($\mathcal{A}$): The set of possible actions for the agent corresponds to the four operational modes of SBS2: $\mathcal{A} = \{\text{Active, LSM, MSM, DSM}\}$.

— Reward Function $\mathcal{R}$: The agent's learning is guided by a reward function designed to balance energy efficiency and QoS. The reward is calculated based on:

1. Power Consumption Penalty: it is a normalized metric representing the relative savings in power consumption compared to the fully active mode P_{max}. Lower power consumption yields a higher reward.

2. Dropped Users Penalty: A significant negative reward component for the relative number of users dropped compared to the total number of users. More dropped users lead to a lower reward.

3. Adaptive trade-off parameter: A crucial aspect is the adaptive trade-off parameter, which is not constant but dynamically scaled by the normalized instantaneous traffic load. This means that the penalty for relative dropped users is proportionally higher during periods of high traffic demand, compelling the agent to prioritize QoS, while power saving gains a relatively higher weight during low traffic. This parameter Ψ allows for a flexible and intelligent balance between energy efficiency and QoS throughout the day.

4. SM Duration Consideration: When a SM is chosen, the agent does not immediately receive a reward for each instant of that SM. Instead, the reward for a SM is averaged over its duration, implying that the agent considers the long-term impact of its SM decision.

— Q-Learning Algorithm: The Q-learning algorithm is employed to learn the optimal policy. The Q-values, representing the expected cumulative reward for taking an action in a given state, are iteratively updated using Eq. 5.11 [151].

Table 5.1 – BS SMs characteristics [133]

Sleep level	**Deactivation time**	**Minimum sleep duration**	**Activation time**
LSM	$35.5\mu s$	$71\mu s$	$35.5\mu s$
MSM	0.5ms	1ms	0.5ms
DSM	5ms	10ms	5ms
VLSM	0.5s	1s	0.5s

5.3.3 User Offloading Mechanism during SMs

When SBS2 enters a SM (LSM, MSM or DSM), the system executes a coordinated offloading procedure with the following phases:

Primary Association

Let $\mathcal{U}$ denote the set of users originally served by SBS2. These users are reassociated to neighboring base stations (SBS1 and SBS3) according to:

$$\boldsymbol{a}_i^* = \arg\min_{j \in \{1,3\}} \|\mathbf{u}_i - \mathbf{x}_{s_j}\| \cdot \mathbb{I}(N_j < N_{\max}) \tag{5.1}$$

where:

— $\boldsymbol{a}_i^*$ is the best selected SBS for user i

— $\mathbf{u}_i$ is the position of user i

— $\mathbf{x}_{s_j}$ is the position of SBS_j

— N_j is the current connected users at SBS_j

— $N_{\max}$ is the maximum number of users a SBS can serve.

— $\mathbb{I}(\cdot)$ is the indicator function that can take two values 1 if the condition is true and 0 otherwise.

IRS-Assisted Fair Service

Users remaining unserved after primary association ($\mathcal{U}_{\text{uns}}$) are handled through the IRS mediation with fairness distribution of blocks in IRS.

1. Partitioning $\mathcal{U}_{\text{uns}}$ into subsets $\mathcal{U}_1$ and $\mathcal{U}_3$
2. Allocating IRS resources to maximize:

$$\sum_{k \in \mathcal{U}_1} R_{k,1}^{\text{I}}(t) + \sum_{m \in \mathcal{U}_3} R_{m,3}^{\text{I}}(t) \tag{5.2}$$

where $R_{k,i}^{I}(t)$ is the data rate of a user k in a set i (Eq. 3.10).

QoS Preservation

The achievable rate for offloaded user k is given by:

$$R_k(t) = \begin{cases} R^{\text{dir}}_{k,\boldsymbol{a}^*_k}(t) & \text{if } \|\mathbf{u}_k - \mathbf{x}_{s_{\boldsymbol{a}^*_k}}\| \leq d_{\max}, \\ R^{\text{I}}_{k,1}(t) & \text{if } k \in \mathcal{U}_1 \text{ and } \|\mathbf{u}_k - \mathbf{x}_{s_{\boldsymbol{a}^*_k}}\| > d_{\max}, \\ R^{\text{I}}_{k,3}(t) & \text{if } k \in \mathcal{U}_3 \text{ and } \|\mathbf{u}_k - \mathbf{x}_{s_{\boldsymbol{a}^*_k}}\| > d_{\max}. \end{cases} \tag{5.3}$$

where $R_k(t)$ is the achievable rate of user k at time t (3.3), $R^{\text{I}}_{k,j}(t)$ is the IRS-assisted rate for user k via SBS j ($j \in \{1, 3\}$), and $R^{\text{dir}}_{k,\boldsymbol{a}^*_j}(t)$ is direct rate (without IRS) between user k and SBS $\boldsymbol{a}^*_j$, at time t.
Note that $\|\mathbf{V}\|$ represent the Euclidean norm of vector.

5.4 Problem Formulation

The system serves mobile users distributed according to a time-varying Poisson process with mean $\lambda(t)$ that follows a daily traffic pattern. In this work, we consider the problem of minimizing the SBS energy consumption and the service of users (dropped). The problem can be formulated as follows:

$$\min_{a_t \in \mathcal{A}} \underbrace{\sum_{t=0}^{T} (1 - \Psi(t)) P(a_t)}_{\text{Power consumption}} + \underbrace{\sum_{t=0}^{T} \Psi(t) D(a_t)}_{\text{Service degradation}} \tag{5.4}$$

where:
— $P(a_t)$ is the power consumption in mode a_t
— $D(a_t)$ quantifies service degradation when SBS is in SMs.
— $\Psi(t)$ balances the energy-QoS tradeoff.

System States

In order to reduce the energy consumption and the dropped of users, we model the aobve problem as a discrete-state MDP problem, where a SBS in state $\boldsymbol{q}_t$ was taken an action a_{t-1} then moves to another state $\boldsymbol{q_{t+1}}$. The state space $\mathcal{S}$ is defined as:

$$\boldsymbol{q}_t = (\mathcal{L}_1(t), \mathcal{L}_3(t), a_{t-1}) \in \mathcal{S} \tag{5.5}$$

where:
— $\mathcal{L}_i(t)$ represents the discretized user connected level at SBSi (for $i = 1, 3$)
— a_{t-1} is the previous action of SBS2.

Action Space

At each time slot, the agent decides an action. The action space $\mathcal{A}$ consists of four mode configurations:

$$\mathcal{A} = \{a_1, a_2, a_3, a_4\} \tag{5.6}$$

where: a_1: Active mode; a_2: LSM ; a_3: MSM; a_4: DSM

Reward Function

In order to evaluate the cost associated with each action-pair, we use the reward function $re(\boldsymbol{q}_t, a_t)$ that takes into account the energy consumption of the SBS and the users' QoS:

$$r(\boldsymbol{q}_t, a_t) = (1 - \Psi(t))P(a_t) + \Psi(t)D(\boldsymbol{q}_t, a_t) \tag{5.7}$$

where $P(a_t)$ and $D(\boldsymbol{q}_t, a_t)$ represent the SBS power consumption and the amount of users dropped, respectively after an action a_t has been taken. $\Psi(t)$ is the weighting parameter that prioritizes between the power consumption and the drop of users.

User Arrival Process

The mobile users follow a Poisson arrival process with mean arrival rate $\lambda(t)$ that varies according to daily traffic patterns:

$$N_{\text{users}}(t) \sim \text{Poisson}(\lambda(t)) \tag{5.8}$$

where: $\lambda(t) = \mathbb{E}[N_{\text{users}}(t)]$ is the *mean* number of users at time t. The probability mass function [152] is given by:

$$Pr(N_{\text{users}}(t) = k) = \frac{e^{-\lambda(t)}\lambda(t)^k}{k!}, \quad k = 0, 1, 2, ... \tag{5.9}$$

IRS Assistance Mechanism

The IRS with n_b configurable blocks provides:

— Active mode of SBS2: Paths for unserved users or improves data rates for existing SBS2 users.

— SMs: Compensation paths from active SBSs (SBS1 and SBS3)
— Performance improvement quantified by:

$$\Delta_{\text{IRS}}(t) = 100 \times \frac{R_{\text{after}}(t) - R_{\text{before}}(t)}{R_{\text{before}}(t)} \tag{5.10}$$

Trade-off Parameter

The time varying parameter $\Psi(t) \in [0, 1]$ balances energy efficiency and QoS in the reward function (Eq. 5.7).

Operational Modes:
— Low traffic ($\Psi(t) < 0.3$): Favors energy savings (deep sleep).
— Medium traffic ($0.3 \leq \Psi(t) \leq 0.7$): Balanced operation.
— High traffic ($\Psi(t) > 0.7$): Prioritizes QoS (active mode).

5.5 Online Interference-Aware BS Sleeping Algorithm

Preliminaries on Reinforcement Learning

Distributed Q-learning is an online optimization technique to control a system, appropriate SM level without coordination [151]. The SBS has to learn independently a policy through real time interactions with the environment. Q-learning detects the optimal policy that maximizes the expected value of the total reward (Q-value) over all successive episodes. The agent (i.e., SBS) have a partial view of the system, and their actions may differ since the users are randomly distributed over the network. In particular, the decision of a SBS to choose a SM level is affected by the number of actual users, as well as its prior action. In Q-learning, the agent takes an action a_t from an action set $\mathcal{A}$, then moves to a new state $\boldsymbol{q_{t+1}}$ while receiving a reward r_t (in our work, the reward function is the cost function in equation 5.7. This reward is then used to update the Q-value locally, $Q(\boldsymbol{q}_t, a_t)$, indicating the level of convenience of selecting action a_t when in state $\boldsymbol{q}_t$. The Q-value is updated as follows [151]:

$$Q(\boldsymbol{q}_t, a_t) = Q(\boldsymbol{q}_t, a_t) + L_r \left[r_t + dis_f \max_{a_t \in \mathcal{A}} Q(\boldsymbol{q}_{t+1}, a_{t+1}) - Q(\boldsymbol{q}_t, a_t) \right] \tag{5.11}$$

where $\boldsymbol{L_r}$ is the learning rate that represents the speed of convergence, and $dis_f \in [0, 1]$ is the discount factor that determines the current value of future state costs. During the

learning phase, each agent selects the corresponding action based on the ϵ-greedy policy, that is, it selects with probability $(1-\epsilon)$ the action associated with the maximum Q-value, and with probability ϵ selects a random action.

$$a_t = \begin{cases} \arg\max_{a_t \in \mathcal{A}} Q(\boldsymbol{q}_t, a_t) & \text{if } y > \epsilon \\ rand(\mathcal{A}) & \text{otherwise} \end{cases} \tag{5.12}$$

By implementing the ϵ-greedy policy, the SBS would have investigated all possible actions and avoided local minima. For more details on RL and Q-learning, refer to [151]. The Q-learning algorithm is described in Algorithm 1.

Algorithm 1 Q-Learning for Adaptive SBS SM with IRS

Input: Network configuration, Q-Learning parameters, traffic profile
Output: Optimized Q-table for SBS SM policy
Initialization: State space (Eq. (5.5)), Q-table, L_r, dis_f, ϵ
for epoch $e = 1$ to E_{max} **do**
  Update ϵ for exploration-exploitation: $\epsilon = \frac{2}{0.5+\exp\left(\frac{e}{decaying}\right)}$
  for $t = 1$ to I_{max} **do**
    Observe current state $\boldsymbol{q}_t$
    Select action a_t via ϵ-greedy on $Q(\boldsymbol{q}_t, a_t)$
    if a_t = Active Mode **then**
      All SBSs operate; normal user association (IRS assist the nearest users of SBS2)
    else
      SBS2 enters SM; offload users; IRS assists affected users
    end if
    Observe next state $\boldsymbol{q}_{t+1}$, compute reward r_t
    Update Q-table (Eq. 5.11)
  end for
  Monitor Q-table convergence
end for
Policy Deployment: Final Q-table defines optimal SBS, SM control balancing energy and QoS =0

Table 5.2 – Simulation Parameters

Parameters	**Values**
Learning rate ($\boldsymbol{L_r}$)	0.3
Discount factor ($\boldsymbol{dis_f}$)	0.7
Decaying factor ($\boldsymbol{Dec_f}$)	4.8
Total simulation time	24 h
Transition durations	[1, 5, 50, 500] iterations
Power P_{active}, P_{LSM}, P_{MSM}, P_{DSM}	(3, 1.5, 0.75, 0.3) W
Transmit power of SBS1 & SBS3	3 W
Carrier frequency (f_{c1}, f_{c2}, f_3)	(2, 2.5, 3) GHz
Bandwidth	10 MHz
Generation of users	Every 50 iterations
Number of states	64
Number of blocks in IRS	12 blocks

5.6 Simulation Results

In this section, we highlight the performance of our proposed Q-learning algorithm for the SBS controller, comparing the results *with* and *without* IRS assistance. In both cases, the proposed algorithm was evaluated through extensive simulations over 24h periods with $E_{max} = 200$ epochs. The network parameters for simulations were set according to 3GPP specifications [153]. In Table 5.2, we detail the parameters used in our simulation.

RL With IRS

Figure 5.3 provides an insight into the learned policy of our proposed Q-learning algorithm, illustrating how the active state of SBS2 dynamically adapts to the fluctuating traffic demand over time. The red dashed line depicts the percentage of "Traffic Level (%)" which follows a typical daily pattern characterized by low demand during off-peak hours and significant peaks during busy periods. The blue solid line represents the "SBS2 Active %" indicating the average percentage of time SBS2 operates in its fully active mode, while the surrounding green shaded region, labeled "Activity Range" illustrates the standard deviation of this activity percentage across all training epochs, reflecting the consistency of the learned behavior.

The plot demonstrates a positive correlation between the "SBS2 Active (%)" and the "Traffic Level (%)." This direct relationship is a key indicator of the algorithm's effective-

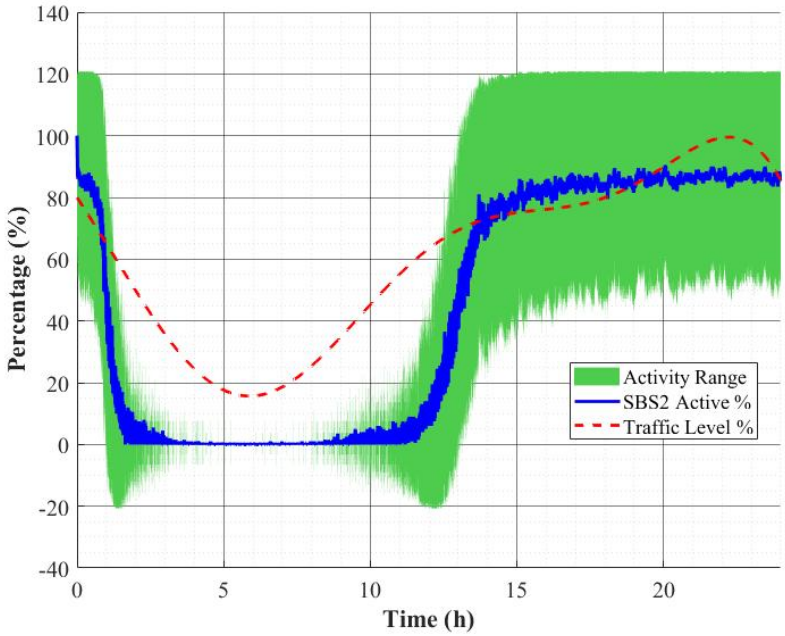

Figure 5.3 – SBS2 Active Mode Percentage vs. Traffic Demand over Time (h) (*with* IRS).

ness in achieving demand aware network operation; Specifically:

— **Optimal Resource during Peak Demand:** During periods of high traffic load, the Q-learning algorithm prompts SBS2 to maintain a high active percentage (approaching 90%). This ensures that the network provides maximum capacity and robust service coverage when it is most needed, thereby minimizing potential user drops and maintaining high QoS.

— **Significant Energy Savings during Off-Peak Hours:** Conversely, when the traffic demand is low, the algorithm intelligently reduces SBS2's active duration, as evidenced by the sharp dips in the blue line. This strategic reduction in active time translates directly into substantial energy savings, as SBS2 consumes considerably less power in its sleep states. This dynamic power management avoids unnecessary energy consumption when network resources are underutilized.

— **Dynamic Adaptation vs. Static Scheduling:** The observed continuous and fluid adaptation of SBS2's active percentage, closely mirroring the granular changes in traffic, highlights the high performance of our RL approach grafting with IRS compared to traditional static scheduling or simple threshold-based SM strategies. Such conventional methods often struggle to capture the complex, real time dynam-

ics of traffic and may lead to either energy wastage (by being active unnecessarily) or service degradation (by being asleep during unexpected demand).

— **Robustness of the Learned Policy:** The relatively narrow band of the "Activity Range" (the shaded area) around the average active percentage line signifies the robustness and consistency of the learned policy. It indicates that the Q-learning agent with the IRS reliably converges to a similar and effective operational strategy across different simulation runs, leading to a stable behavior while taking into consideration varying traffic conditions.

Consequently, Figure 5.3 corroborates the performance of our proposed approach and shows how our proposed Q-learning algorithm feeded with IRS successfully orchestrates SBS2's operational state to dynamically balance energy efficiency with QoS requirements throughout a typical day, adapting intelligently to the inherent fluctuations in user demand.

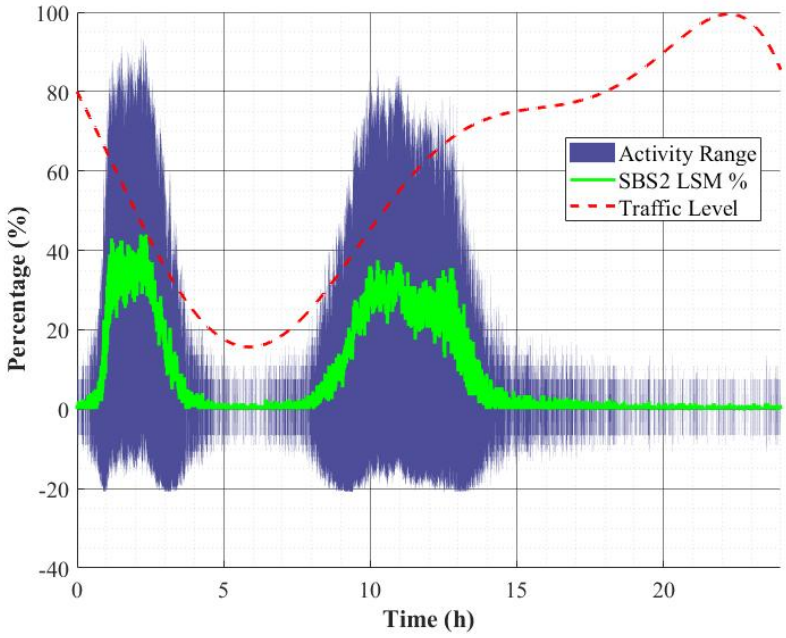

Figure 5.4 – SBS2 LSM Percentage vs. Traffic Demand over Time (h).

Figure 5.4 illustrates the dynamic utilization of LSM by the Q-learning algorithm with the help of IRS for SBS2, in direct relation to the fluctuating traffic demand over time. The plot displays the average percentage of time SBS2 spends in LSM (green line), alongside the traffic level. Also, the shaded "Activity Range" around the green line, signifies the

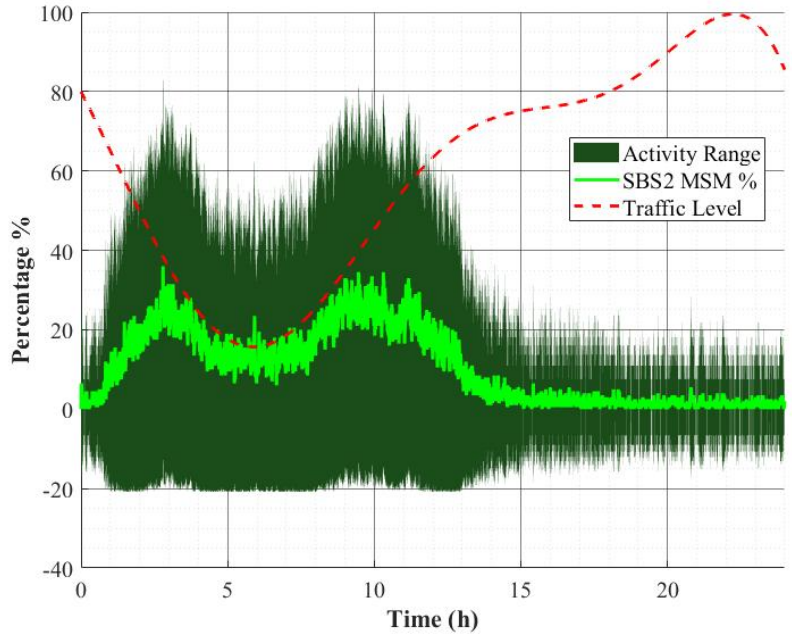

Figure 5.5 – SBS2 MSM Percentage vs. Traffic Demand over Time (h).

standard deviation of LSM usage.

LSM represents the lowest SM, offering the quickest wake-up time at the cost of less power saving compared to MSM and DSM. Its distinct pattern of activation reveals the energy management strategy learned by the Q-learning agent:

— **Strategic Use in Transitional and Moderately High Traffic:** Unlike DSM that are predominantly used during very low traffic, LSM shows notable utilization during periods when traffic is neither at its absolute peak nor its absolute trough. Specifically, we observe increased LSM usage during the rising and falling slopes of the traffic curve. This indicates that the algorithm leverages LSM as a strategic state for scenarios where traffic is moderate or fluctuating, and a rapid return to the active state might be necessary, thus prioritizing lower wake-up latency over maximum energy savings.

— **Optimal Trade-off for Responsiveness:** The algorithm's decision to enter LSM during these intermediate traffic periods demonstrates its learned ability to balance energy efficiency with system responsiveness. By choosing the LSM, some power is saved compared to full activity, while the short wake-up delay ensures that SBS2 can quickly transition back to active mode to handle sudden increases in demand

without significant service interruption.

— **Comprehensive Multi-State Adaptation:** The distinct roles of Active, LSM, MSM, and DSM, as depicted across the series of plots, underscore the proposed Q-learning algorithm's with IRS capability for highly granular power management. It learns to intelligently distribute SBS2's operational time among all available power states, selecting the most appropriate mode based on the real time traffic context to optimize the overarching trade-off between energy consumption and QoS.

— **Consistency of Policy Application:** The relatively narrow "Activity Range" for LSM usage confirms the stability and robustness of the learned policy. This consistency ensures that the algorithm reliably employs LSM in similar traffic conditions across different operational cycles, contributing to predictable and efficient network behavior.

Therefore, Figure 5.4 completes the comprehensive depiction of our Q-learning algorithm's associated with IRS an adaptive power management. It highlights the strategic use of LSM as a flexible, low-latency energy-saving state, enabling the network to achieve optimal performance by finely tuning SBS2's operational mode to the dynamic and diverse demands of wireless traffic.

Figure 5.5 illustrates the dynamic utilization of MSM by the Q-learning algorithm with IRS for SBS2, in direct response to the fluctuating traffic demand. The plot displays the average percentage of time SBS2 spends in MSM (green line) alongside the percentage of traffic level (red dashed line). The shaded "Activity Range" around the green line represents the standard deviation of MSM usage across training epochs.

Compared to DSM, MSM represents an intermediate power-saving state.

— **Utilization in Intermediate Traffic Scenarios:** MSM shows higher utilization during moderately low to intermediate traffic conditions. This indicates that the algorithm allows for significant energy savings when the traffic load does not necessitate full activity, but is not low enough to warrant the DSM.

— **Multi-State Adaptation:** The presence and distinct usage pattern of MSM underscore the IRS with the Q-learning algorithm's ability to discriminate between various power-saving modes. Instead of a simplistic ON/OFF or a binary deep sleep decision, the agent learns to select from a spectrum of sleep states, each offering a different balance between energy consumption and latency/wakeup time. This multi-state adaptation allows for more precise energy optimization tailored to specific traffic conditions.

— **Complementary Role in Overall Policy:** During peak traffic hours, the percentage of SBS2 in MSM drops to near zero, mirroring the behavior of DSM. This confirms that all SMs are largely deactivated when maximum network capacity is required to ensure optimal QoS. Conversely, during the lowest traffic periods, while MSM contributes, the primary deep sleep takes precedence for ultimate energy efficiency.

— **Consistency of Policy:** The relatively narrow band of the "Activity Range" for MSM usage suggests that our algorithm consistently learns to apply this intermediate SM in similar traffic scenarios across different training iterations, demonstrating the robustness and stability of the converged policy.

Overall, Figure 5.5 effectively demonstrates how the Q-learning algorithm, supported with IRS, achieves nuanced control over SBS2's operational states. By strategically employing MSM alongside other power modes, the proposed solution achieves a more granular and efficient energy-QoS trade-off, adapting dynamically to the full range of network traffic variations.

The dynamic behavior of SBS2's operational mode (specifically DSM) in response to varying traffic demands over time is illustrated in Figure 5.6, likely representing a 24h cycle.

— **SBS2 DSM % (Green Solid Line):** During periods of low traffic demand (e.g., 2 a.m.), SBS2 predominantly enters DSM, reaching a high percentage (e.g., up to 90%). This demonstrates the energy-saving strategy where SBS2 is put into deeper SMs when user activity is minimal.

— **Activity Range (Magenta Shaded Area):** Represents the overall variability or range of SBS2's activity across DSM. The wide spread, especially during high traffic periods, suggests that the agent dynamically selects various modes to balance energy efficiency with user QoS.

Effectively, Figure 5.6 visualizes the adaptive policy learned by the RL + IRS agent, showing how SBS2 intelligently switches between operational modes to match the dynamic traffic load, thereby optimizing for energy efficiency during low demand and prioritizing connectivity during high demand.

This pie chart (Figure 5.7) illustrates the aggregated percentage of time SBS2 spends in each of its predefined operational modes averaged over the entire simulated day. This distribution provides an overall view of the RL agent's assisted with the IRS long-term energy management policy.

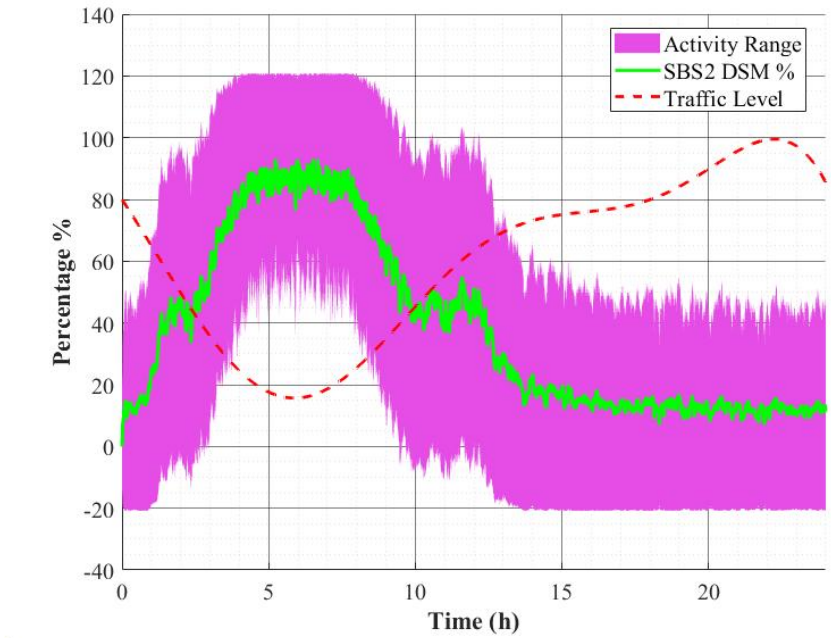

Figure 5.6 – Percentage of SBS2 being DSM vs Traffic Demand over Time (h).

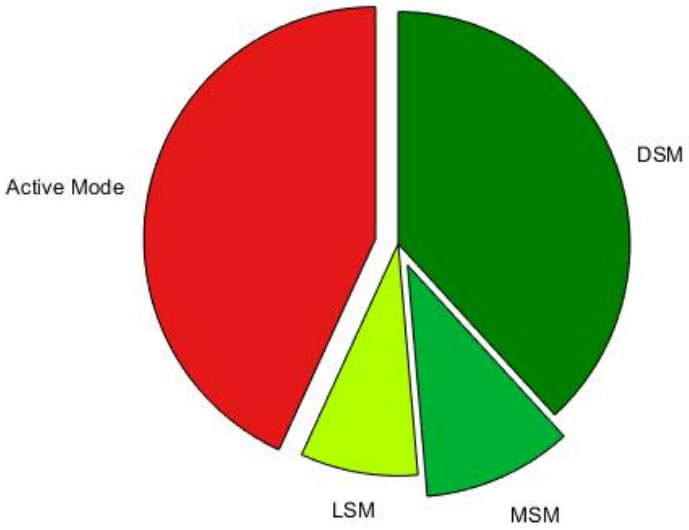

Figure 5.7 – Percentage of time SBS2 spends in each action

— **Active Mode (Red Slice):** Constitutes a significant portion of the day, indicating the necessary time SBS2 spends in its fully operational state to serve user traffic, especially during peak demand periods.
— **DSM (Dark Green Slice):** Highlighting that SBS2 frequently enters its DSM. This demonstrates a strong emphasis on maximizing energy savings during periods of low traffic demand, where DSM offers the most significant power reduction.
— **MSM (Light Green Slice):** Occupies a smaller percentage compared to DSM.
— **LSM (Yellow/Lime Green Slice):** Represents the smallest proportion of time.

The dominance of Active Mode and DSM suggests a binary-like strategy where the SBS2 is either fully engaged to handle traffic or deeply asleep to conserve energy. The minimal usage of intermediate SMs (LSM and MSM) indicates that the learned policy tends to transition directly between active and the deepest sleep state, or that these intermediate states are less frequently optimal under the specific traffic patterns and reward functions used in the simulation. This overall distribution confirms the effectiveness of the RL policy in achieving substantial energy savings by leveraging deep SMs when traffic conditions permit, while remaining active to ensure service continuity during high demand.

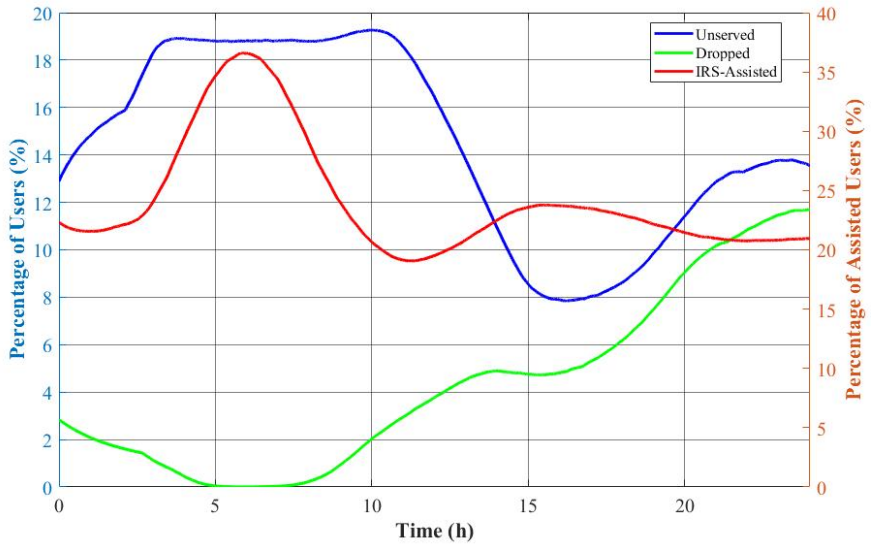

Figure 5.8 – Users Percentage (Unserved, Dropped, IRS-Assisted) for RL + IRS algorithm vs. Traffic Demand over Time (h).

Figure 5.8 provides a view of the system's performance with a RL based SM policy with the assistance of an IRS. This analysis shows the dynamic relationship between unserved, dropped, and IRS-assisted users during the entire day.

— **Unserved Users:** The percentage of unserved users (blue line) peaks at around 19% during the low-traffic period (approximately 3 a.m. to 10 a.m.). This is the period when the RL agent with IRS is most aggressively enforcing SMs to save energy, leading to a higher number of users who are not in direct contact with an active SBS. The percentage of unserved users decreases as the system enters high-traffic periods, where the SBS is more active.

— **Dropped Users:** The percentage of dropped users (green line) is a primary indicator of QoS. Notably, it remains very low, close to 0%, during the extended period of SBS SMs (0 to 10 a.m.). This is a key finding, as it shows that the IRS prevents unserved users from being dropped. The dropped user percentage only begins to increase during the high-traffic hours, rising to a peak of around 12% around 10 p.m., where the system's capacity is most challenged.

— **IRS-Assisted Users:** The percentage of users assisted by the IRS (red line) shows an inverse correlation with the SBS's active time. The IRS-assisted user percentage peaks at over 35% during the low-traffic hours when the SBS is in SM. This demonstrates the IRS's critical role as a coverage extender, providing service for users who would otherwise be unserved during these periods.

In conclusion, the figure demonstrates the success of the RL + IRS system in balancing energy efficiency and QoS. The IRS enables the RL agent to enforce energy-saving SMs, as evidenced by the high percentage of unserved users during off-peak hours. Therefore, the IRS acts as a "safety net," ensuring that these unserved users are not dropped, thus maintaining a high QoS even as the system prioritizes energy conservation. The close relationship between IRS-assisted users and the low dropped user count highlights the indispensable role of the IRS in this dynamic power management scheme.

Figure 5.9 illustrates the dynamic energy consumption of SBS2 under different operational strategies over time, contextualized by the varying traffic load. The left y-axis denotes energy consumption in Watts (W), while the right y-axis indicates the percentage of traffic load.

— **Always Active (Black Dashed Line):** This serves as the upper bound baseline, representing a scenario where the SBS2 remains continuously active, consuming a constant maximum power (e.g., $3W$). This strategy disregards traffic conditions and is maximum energy inefficient, demonstrating the highest energy consumption across all time.

— **Traffic Load (%) (Magenta Dotted Line):** This is the driving factor for adap-

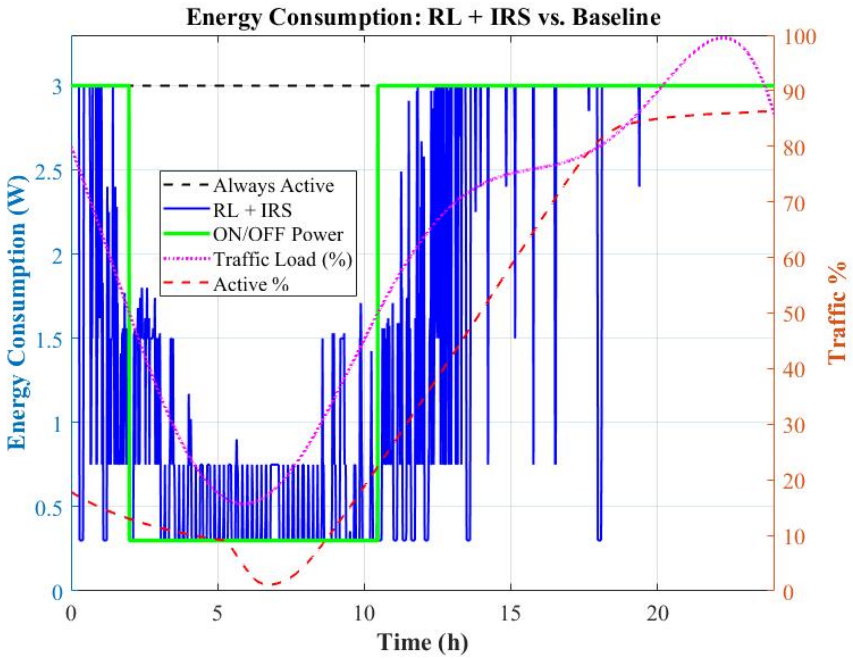

Figure 5.9 – Total Energy Consumption vs. Traffic %: Comparison of Proposed RL + IRS, ON/OFF baseline, and always ON strategies.

tive energy management.

— **ON/OFF Power (Green Solid Line):** This line depicts a simple threshold based ON/OFF strategy, where SBS2 switches between a low-power state and active mode based on a fixed traffic threshold (e.g., 50%). It efficiently conserves energy during low traffic by powering down, but immediately switches to full active power once the threshold is crossed, no matter of the precise traffic level is after that point.

— **Active (Red Dashed Line):** This line represents the active probability curve where SBS2's power consumption adapts to traffic. Peaks align with traffic surges, proving traffic aware adaptation.

— **RL + IRS (Blue Solid Line):** This curve demonstrates the energy consumption of the proposed RL agent integrated with IRS control.

  — During low traffic periods (e.g., from 3 a.m. to 10 a.m.), the RL + IRS strategy significantly reduces energy consumption by leveraging DSM, achieving values close to 0.3 W. This indicates effective energy saving during off-peak hours.

  — As traffic load increases (e.g., from time 10 a.m. onwards), the RL + IRS strategy adaptively increases its energy consumption to meet the demand, reaching

higher power levels during peak hours. Notably, compared to the "Always Active" strategy, the RL + IRS approach achieves approximately 46.3% of power savings without compromising network performance while the ON/OFF strategy, with a threshold of 50% can save 32% only.

Figure 5.9 highlights the high energy efficiency of the RL + IRS approach. By intelligently adapting SBS2's operational mode to real time traffic dynamics, it achieves substantial power savings, particularly during low-traffic periods, while ensuring network performance during high demand, making it a desirable solution for cellular networks.

5.6.1 RL Without IRS

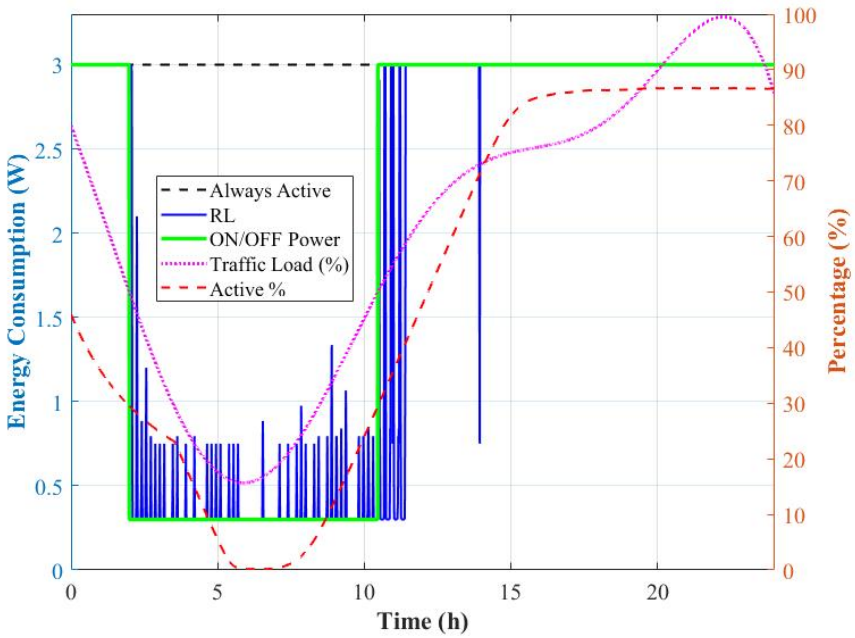

Figure 5.10 – Energy Consumption: RL Only (*Without* IRS) vs. Baseline.

To quantify and evaluate the performance improvements enabled by IRS technology, we study, in terms of energy consumption, and action decision, a comparative analysis between systems incorporating IRS and conventional systems *without* IRS. A comparison of Figures 5.9 and 5.10 reveals the significant impact of the IRS on the system's energy consumption. Both figures show the dynamic energy consumption of a RL policy reacting to a similar daily traffic pattern, but with distinct outcomes.

— ***Without* IRS (Figure 5.10):** In the absence of an IRS, the RL agent's policy is to keep the SBS active for a higher percentage of time to ensure user connectivity. The "Active %" curve (red dashed line) shows that the SBS's active state is also highly correlated with traffic demand, reaching a maximum of over 70% during peak hours. During low-traffic periods (approximately 0 to $10h$), the energy consumption remains low but exhibits frequent, sharp spikes, indicating that the SBS must briefly activate to serve users who would otherwise be dropped.

— ***With* IRS (Figure 5.9):** The introduction of the IRS fundamentally changes the RL agent's behavior and the system's energy profile. The IRS provides an alternative communication path, allowing the SBS to remain in a lower-power SM for longer durations. This is clearly visible in the "Active %" curve, which is consistently lower across the entire 24h period compared to the RL only case. The energy consumption line (blue) in this figure is also less spiky and maintains a lower base level, especially during off-peak hours, as the IRS effectively compensates for the SBS's reduced activity.

In conclusion, the comparison highlights that the IRS enables a stable energy-saving policy. The RL + IRS system's ability to maintain low energy consumption while ensuring user connectivity demonstrates the role of the IRS in enabling high energy efficiency, particularly by reducing the need for the SBS to frequently transition to an active state to cover for service gaps.

Figure 5.11 and Figure 5.12 present a detailed view of the Q-learning agent's learned policy for managing SBS2's operational modes over a 24h period, in the absence of IRS assistance. The agent's behavior is a direct and intelligent response to the varying traffic demand. Several key observations emerge from this baseline configuration:

— The RL controller exhibits an essentially binary behavior pattern for SBS2, with minimal intermediate activity states. This suggests that *without* IRS assistance, the system lacks fine-grained control capabilities.

— Service Modules LSM and MSM show particularly limited activity ranges ($0-5\%$ and $0-10\%$ respectively), indicating these modules play a negligible role in traffic handling without IRS. This limited participation of certain modules leads to suboptimal resource utilization.

— The system demonstrates significant fluctuations in activity levels (ranging from -50% to $+50\%$), reflecting the challenges of maintaining stability without IRS-

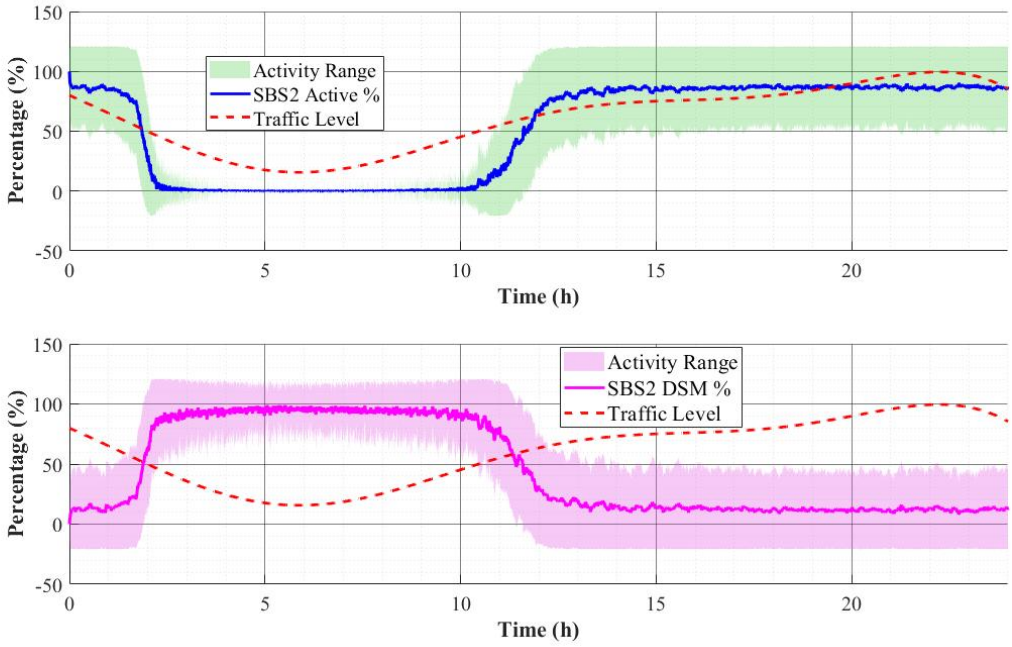

Figure 5.11 – SBS2's Active and DSM operational percentages over a 24h versus the traffic demand *without* IRS assistance.

enhanced channel conditions.

— Notably, in this IRS absent scenario, the unserved users metric exactly equals the dropped users count. This equivalence occurs because without IRS's signal enhancement capabilities, any service interruption immediately results in a complete connection drop.

These baseline results highlight two limitations of IRS less systems that our subsequent IRS implementation addresses:

1. The inability to maintain service continuity for marginal connections (explaining the identical drop/unserved metrics).
2. The restricted participation of certain service modules due to unfavorable propagation conditions.

As we will demonstrate in subsequent results, introducing IRS creates a distinction between unserved and dropped users during moderate traffic conditions. The IRS's beamforming capabilities allow connections to be maintained at reduced rates rather than being completely dropped, while also enabling more balanced utilization across all service modules (including previously underutilized LSM and MSM).

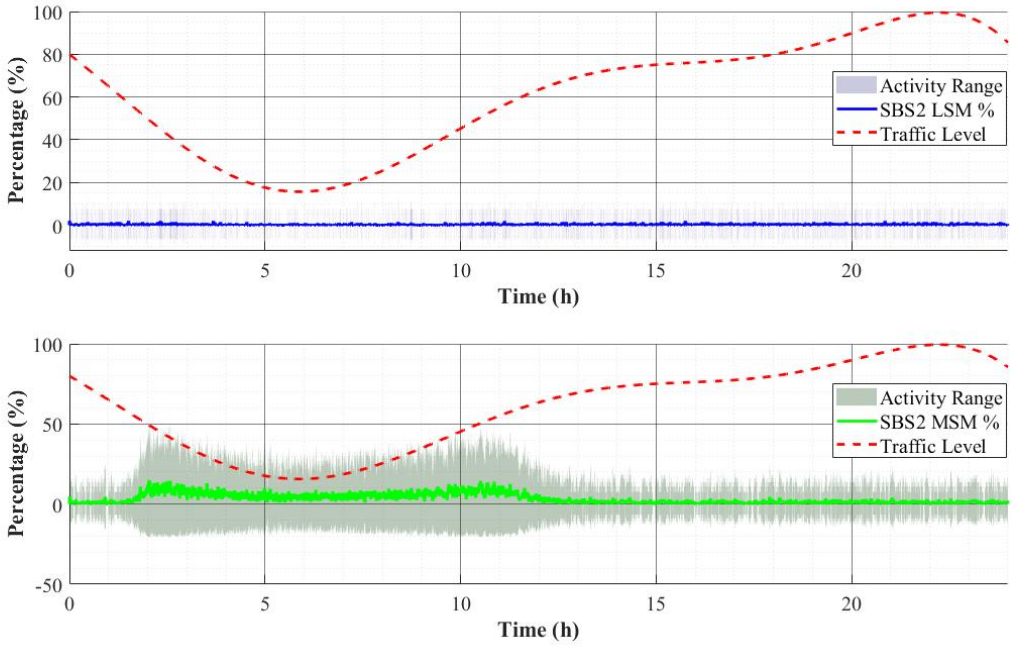

Figure 5.12 – SBS2's LSM and MSM operational percentages over a 24h versus the traffic demand *without* IRS assistance.

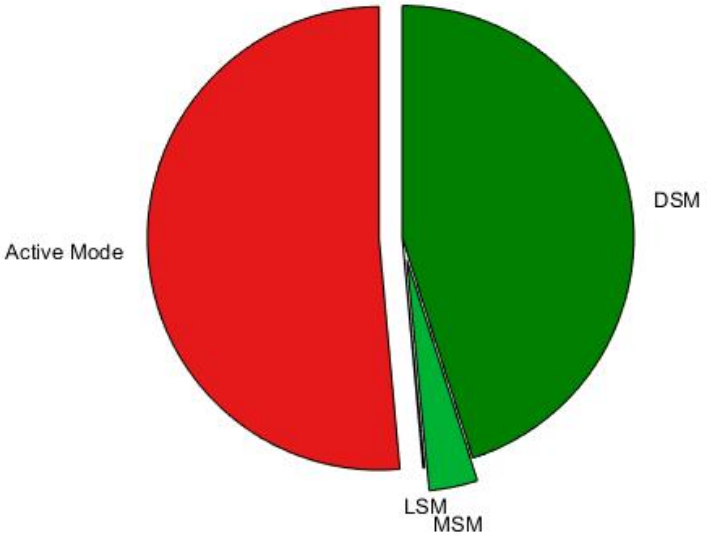

Figure 5.13 – Percentage of time SBS2 spends in each action *without* IRS.

The activation distribution in the IRS absent configuration (Figure 5.13) reveals several characteristics when compared with the IRS enabled case. In the absence of an IRS, the RL agent's policy is to divide its time primarily between Active Mode and DSM. As the pie chart shows, DSM accounts for a large majority of the SM operations. The agent makes very minimal use of the other SMs, LSM and MSM, which together occupy only a tiny fraction of the total time. This indicates that without the support of the IRS, the agent learns a binary like policy: either be fully active to serve users or be in a deep sleep state to maximize energy savings. The introduction of the IRS fundamentally changes the agent's learned policy. The pie chart for the IRS-assisted system shows a more diverse utilization of SMs. While DSM still accounts for a significant portion of the total time, the agent now also makes substantial use of LSM and MSM. The presence of the IRS allows SBS2 to leverage these intermediate SMs more effectively, as the IRS can provide a reliable communication link for users during these periods. The comparison of these two pie charts clarifies a key role of the IRS. Without an IRS (Figure 5.13), the agent's sleep strategy is quite simple and inflexible, favoring DSM for energy savings. With the IRS (Figure 5.7), the agent learns a more nuanced and complex policy, utilizing a wider range of SMs to achieve a better balance between energy conservation and service continuity. The ability to use LSM and MSM more frequently, supported by the IRS, allows for a more adaptive and efficient system overall.

As shown in Figure 5.14, the percentage of unserved users for the RL only system directly reflects the periods when the SBS2 is in a SM. The percentage of unserved users is high during off peak hours, peaking at around 19% between 3 a.m. and 10:00 a.m. Since there is no IRS to provide alternative coverage, these unserved users are essentially dropped from the network. This reveals a fundamental trade-off: the RL agent achieves energy savings by enforcing SMs, but at a direct and significant cost to QoS. The introduction of the IRS changes this dynamic, as seen in Figure 5.8. During the same off peak hours, the percentage of unserved users is similarly high, peaking at around 19%. This indicates that the RL agent's energy saving policy is consistent, keeping the SBS2 in a sleep state. However, the key difference is the dropped user percentage (green line, in Figure 5.8), which remains very low, close to 0%, during this period. The reason for this is the IRS-assisted user percentage, which is at its highest during the same hours. This demonstrates the IRS's role: it steps in to serve the users who are unserved by the sleeping SBS2, preventing them from being dropped and thus preserving a moderate QoS.

The comparison illustrates that the IRS acts as a QoS enabler. It allows the RL agent

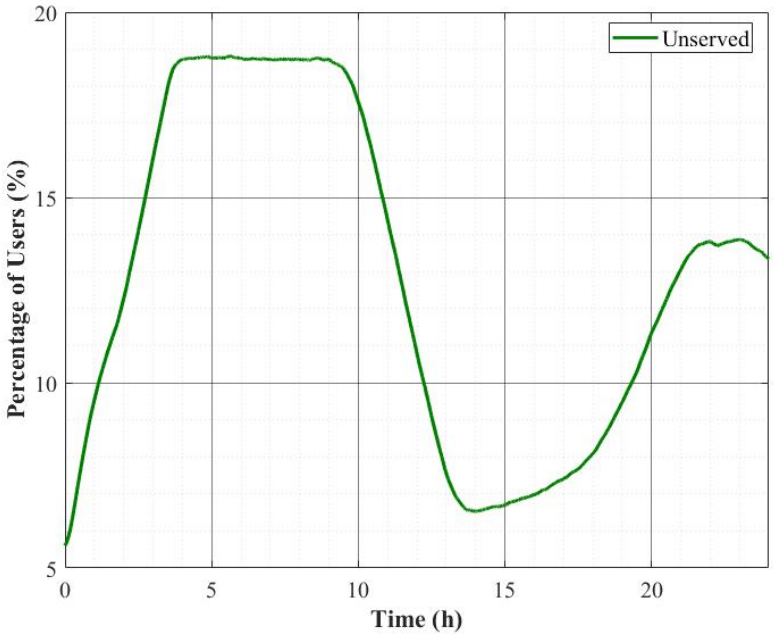

Figure 5.14 – Percentage of unserved users over a 24h period for the RL system *without* IRS assistance (unserved users are equivalent to dropped users).

to pursue an energy saving policy by decoupling the state of the SBS2 from the service provided to the users. The high percentage of IRS-assisted users mitigates what would otherwise be a high percentage of dropped users in the RL only system. This highlights that the IRS is not just a marginal improvement but a component that allows for the co-optimization of energy efficiency and network performance.

The bar charts in Figures 5.15 and 5.16 provides a direct comparison of the system states and corresponding user service metrics for the RL based system operating *with* and *without* IRS assistance. This analysis highlights how the IRS enhances energy efficiency and ameliorates the QoS for the network.

— **Energy Efficiency**: The system with IRS assistance achieves a lower average active mode percentage of 43.2% compared to 51.4% for the system without IRS. This reduction in active time directly corresponds to greater energy savings, as the RL agent can keep SBS2 in a SM for longer periods. Consequently, the total time spent in SMs is higher with the IRS (56.8%) versus without it (48.6%).

— **QoS**: The percentage of dropped users is reduced from 12.8% *without* the IRS to only 4.3% *with* the IRS. This decrease confirms that the IRS provides an alternative communication path, preventing a certain number of users from being disconnected

when the SBS2 enters a SM.

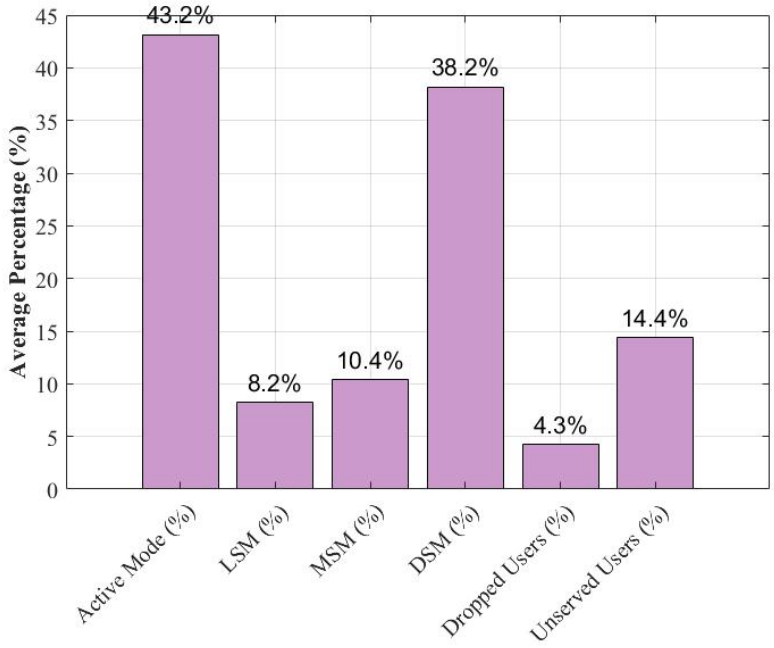

Figure 5.15 – Service Quality and Operational Modes (*with* IRS).

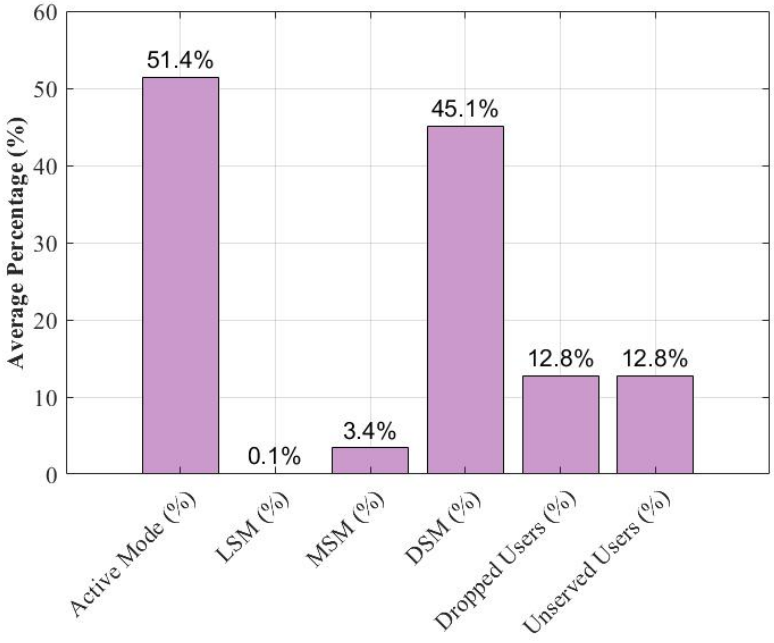

Figure 5.16 – Service Quality and Operational Modes (*without* IRS).

— **SM Strategy**: The RL agent's SM selection also shifts with the presence of the IRS. Without the IRS, the policy favors DSM (45.1%,) with very minimal use of LSM and MSM. With the IRS, while DSM remains dominant (38.2%), the usage of LSM (8.2%) and MSM (10.4%) increases, suggesting that the IRS enables the agent to utilize a wider and more flexible range of SMs.

In conclusion, the IRS enables the RL system to achieve high energy efficiency through reduced active time while simultaneously providing an improvement in QoS by nearly halving the number of dropped users. This makes the RL + IRS system a far more effective solution for balancing energy savings and user experience in dynamic wireless environments. This analysis shows that the RL agent successfully learns to adapt the SBS's state to traffic demand by leveraging a single, deep SM for energy savings. However, without the IRS, the system must either activate the SBS2 more frequently to serve users, or accept a rate of dropped users. The primary role of the IRS is to provide an alternative communication path, allowing SBS2 to remain in a sleep state for longer periods without impacting connectivity.

5.7 SUMMARY

This study demonstrated that an IRS assisted adaptive Sleep Mode (SM) management strategy, empowered by Reinforcement Learning (RL), achieves high energy efficiency while maintaining Quality of Service (QoS) in B5G/6G small cell networks. Our proposed Q-learning algorithm dynamically selects among multiple SM depths (LSM, MSM, DSM) and the active state, based on real time traffic patterns.

Simulation results show that the proposed solution reduced power consumption by 46.3% compared to the conventional Always ON strategy. This energy saving is primarily due to the algorithm's ability to maximize the time SBS2 spends in energy saving SMs under light and moderate traffic conditions, outperforming the baseline.

The control achieved by the Q-learning agent allows for nuanced adaptation: DSM is used for deepest savings during very low traffic, MSM for intermediate traffic, and LSM for quick response power saving during transitional phases, while full activity is maintained during peak demand. Importantly, these energy efficiency gains are achieved without compromising essential QoS metrics, ensuring consistently high user assistance and low drop of users across traffic fluctuations.

In summary, this research demonstrates that the integration of RL with IRS allows for

significant energy savings without service degradation.

Chapter 6

Conclusion and Future Work

This thesis presents theoretical findings from research conducted in the active areas of communication, with particular emphasis on assessing the communication performance in sub 6 GHz with the support of IRSs. In this chapter, we summarize the key outcomes and propose potential avenues for future research.

6.1 Conclusion

This thesis presentes a comprehensive investigation of Intelligent Reflecting Surfaces (IRSs) as a transformative technology for Beyond 5G (B5G) and 6G networks. Motivated by the growing demand for higher data rates, improved coverage, and more energy-efficient communication, we explored the integration of IRSs into different wireless network architectures and analyzed their potential benefits across various scenarios. The results obtained throughout this work underline the significant role that IRSs can play in reshaping the wireless environment and enabling more adaptive, cost-effective, and sustainable communication systems.

Our study began with the analysis of IRS assisted Single Input Single Output (SISO) systems, where IRSs were shown to reduce user bandwidth requirements by intelligently altering the propagation environment. This demonstrated that IRSs can provide tangible performance improvements even in relatively simple system settings. We then extended the analysis to Multiple Input Single Output (MISO) systems under statistical Channel State Information (CSI), where IRSs were found to enhance base station coverage and reduce the number of required transmit antennas. This reduction not only improves spectral efficiency but also decreases the architectural complexity and the overall cost of the system.

A distinctive feature of this work was the consideration of IRSs as a collection of resource blocks that can be allocated to multiple users, rather than treating the surface as a monolithic reflector. This perspective allowed us to formulate new non-linear inte-

ger optimization problems for IRS assisted SISO, MISO, and multi-user MISO systems. The results of these formulations demonstrated how IRSs can be effectively managed to maximize system performance under practical resource-sharing constraints.

In addition, this thesis examines the role of IRSs in improving energy efficiency within small cell networks. By introducing a Reinforcement Learning (RL) framework based on Q-learning, we enabled Small Base Stations (SBSs) to dynamically switch between active operation and multiple sleep modes in response to real-time traffic demands. With the support of IRSs, user connectivity could be preserved during sleep phases, thereby achieving a balance between energy savings and Quality of Service (QoS). This contribution highlighted the dual role of IRSs in both enhancing communication performance and enabling greener, more sustainable network operations.

In summary, the research presented in this thesis has demonstrated the versatility and effectiveness of IRSs in addressing key challenges faced by next-generation wireless networks. By improving bandwidth efficiency, extending coverage, reducing architectural complexity, and enabling adaptive energy management, IRSs emerge as a pivotal enabler for future wireless systems. The findings emphasize that IRSs are not passive reflectors but programmable entities that can fundamentally redefine the way wireless communication environments are designed and optimized.

6.2 Future Work

— **Scalable and robust IRS-aided MISO/MIMO architectures:** While this work showed that IRS can reduce the number of transmit antennas, future studies should address scalability to hundreds or thousands of reflecting elements, incorporating hardware impairments, low-resolution phase shifters, and partial CSI. Research could also explore hybrid active-passive IRS architectures and uplink IRS-assisted transmission.

— **AI-driven IRS optimization and network automation:** The RL framework introduced here can be extended using deep reinforcement learning or multi-agent RL for distributed IRS-SBS coordination. Future models could also integrate traffic prediction, user mobility, and energy price variations to improve real-time decision-making in heterogeneous networks.

— **Integration with emerging technologies and experimental validation:** Future work should explore IRS integration with NOMA, cell-free massive MIMO,

and reconfigurable intelligent surfaces beyond communications (e.g., sensing). Additionally, prototype development and testbed validation are essential to assess real-world performance, calibration requirements, and control overhead.

— **Addressing current modeling limitations:** To improve practical relevance, future studies should incorporate dynamic user mobility, multi-cell interference, phase noise, and other hardware imperfections. Deeper analysis of RL exploration strategies and convergence behavior is also needed, along with comparative studies of different machine learning methods for IRS control.

In summary, the research presented in this thesis has demonstrated the significant potential of IRSs in bandwidth saving, cost reduction, and energy efficiency. Future work should build on these contributions by extending IRSs to multi user and large scale scenarios, developing robust and scalable optimization frameworks, and leveraging advanced machine learning approaches to enable adaptive, intelligent, and energy aware operation of next generation wireless networks. Ultimately, IRSs stand as a key enabler for the vision of programmable, sustainable, and high-performance communication systems in the B5G and 6G eras.

List of Publications

— M. Kassem, H. Haj Hassan, A. Nasser, A. Mansour, K. Yao, "MISO system with Intelligent Reflecting Surfaces Assisted Cellular Networks", Electronics 2023, Volume 12, Issue 11, 2370.

— M. Kassem, H. Haj Hassan, A. Nasser, A. Mansour, K. Yao "Users selection and Resource allocation in intelligent Reflecting Surfaces assisted cellular Network", admitted to the 17th International Conference on Wireless and Mobile Computing, Networking and Communications(WiMob21), Oct. 2021, Bologna, Italy.

BIBLIOGRAPHY

[1] 3GPP, *First 5g nr specs approved*, https://www.3gpp.org/news-events/3gpp-news/1929-nsa, 2021.

[2] W. Saad, M. Bennis, and M. Chen, « A vision of 6g wireless systems: applications, trends, technologies, and open research problems », *IEEE network*, vol. 34, no. 3, pp. 134–142, 2019.

[3] Q. Wu, S. Zhang, B. Zheng, C. You, and R. Zhang, « Intelligent reflecting surface-aided wireless communications: a tutorial », *IEEE Transactions on Communications*, vol. 69, no. 5, pp. 3313–3351, 2021.

[4] S. Research, « The vision of 6g », Samsung Research, Tech. Rep., Jul. 2020.

[5] A. Goldsmith, *Wireless communications*. Cambridge university press, 2005.

[6] S. I. Hassouna, « Investigating the data rate in reconfigurable intelligent surfaces assisted wireless communication », Ph.D. dissertation, University of Glasgow, 2024.

[7] J. G. Proakis and M. Salehi, *Digital communications*. McGraw-hill, 2008.

[8] H.-T. Chen, A. J. Taylor, and N. Yu, « A review of metasurfaces: physics and applications », *Reports on Progress in Physics*, vol. 79, no. 7, 2016.

[9] S. Hassouna, « A survey on intelligent reflecting surfaces: wireless communication perspective », *Authorea Preprints*, 2023.

[10] F. Liu et al., « Programmable metasurfaces: state of the art and prospects », *in 2018 IEEE International Symposium on Circuits and Systems (ISCAS)*, 2018, pp. 1–5.

[11] J. P. Turpin, J. A. Bossard, K. L. Morgan, D. H. Werner, and P. L. Werner, « Reconfigurable and tunable metamaterials: a review of the theory and applications », *International Journal of Antennas and Propagation*, vol. 2014, no. 1, p. 429 837, 2014.

[12] F. Costa, A. Monorchio, S. Talarico, and F. M. Valeri, « An active high-impedance surface for low-profile tunable and steerable antennas », *IEEE Antennas and Wireless Propagation Letters*, vol. 7, pp. 676–680, 2008.

[13] D. Huang, E. Poutrina, and D. Smith, « Analysis of the power dependent tuning of a varactor-loaded metamaterial at microwave frequencies », *Applied Physics Letters*, vol. 96, no. 10, 2010.

[14] A. Katko, A. Hawkes, J. Barrett, and S. Cummer, « Rf limiter metamaterial using pin diodes », *IEEE Antennas and Wireless Propagation Letters*, vol. 10, pp. 1571–1574, 2011.

[15] P. Nayeri, F. Yang, and A. Z. Elsherbeni, *Reflectarray antennas: theory, designs, and applications*. John Wiley & Sons, 2018.

[16] S. Abeywickrama, R. Zhang, Q. Wu, and C. Yuen, « Intelligent reflecting surface: practical phase shift model and beamforming optimization », *IEEE Transactions on Communications*, vol. 68, no. 9, pp. 5849–5863, 2020.

[17] H. Lu, Y. Zeng, S. Jin, and R. Zhang, « Enabling panoramic full-angle reflection via aerial intelligent reflecting surface », *in 2020 IEEE International Conference on Communications Workshops (ICC Workshops)*, IEEE, 2020, pp. 1–6.

[18] Q. Wu and R. Zhang, « Towards smart and reconfigurable environment: intelligent reflecting surface aided wireless network », *IEEE communications magazine*, vol. 58, no. 1, pp. 106–112, 2019.

[19] X. Yu, D. Xu, and R. Schober, « Miso wireless communication systems via intelligent reflecting surfaces », *in 2019 IEEE/CIC International Conference on Communications in China (ICCC)*, IEEE, 2019, pp. 735–740.

[20] C. Huang, A. Zappone, G. C. Alexandropoulos, M. Debbah, and C. Yuen, « Reconfigurable intelligent surfaces for energy efficiency in wireless communication », *IEEE Transactions on Wireless Communications*, vol. 18, no. 8, pp. 4157–4170, 2019.

[21] E. Björnson and L. Sanguinetti, « Rayleigh fading modeling and channel hardening for reconfigurable intelligent surfaces », *IEEE Wireless Communications Letters*, vol. 10, no. 4, pp. 830–834, 2020.

[22] M. Kassem, H. A. H. Hassan, A. Nasser, A. Mansour, and K.-C. Yao, « Users selection and resource allocation in intelligent reflecting surfaces assisted cellular networks », *in 2021 17th International Conference on Wireless and Mobile Computing, Networking and Communications (WiMob)*, IEEE, 2021, pp. 121–126.

[23] E. Basar, M. Di Renzo, J. De Rosny, M. Debbah, M.-S. Alouini, and R. Zhang, « Wireless communications through reconfigurable intelligent surfaces », *IEEE access*, vol. 7, pp. 116 753–116 773, 2019.

[24] W. Tang et al., « Wireless communications with reconfigurable intelligent surface: path loss modeling and experimental measurement », *IEEE transactions on wireless communications*, vol. 20, no. 1, pp. 421–439, 2020.

[25] W. Tang et al., « Path loss modeling and measurements for reconfigurable intelligent surfaces in the millimeter-wave frequency band », *IEEE Transactions on Communications*, vol. 70, no. 9, pp. 6259–6276, 2022.

[26] Ö. Özdogan, E. Björnson, and E. G. Larsson, « Intelligent reflecting surfaces: physics, propagation, and pathloss modeling », *IEEE Wireless Communications Letters*, vol. 9, no. 5, pp. 581–585, 2019.

[27] M. Born and E. Wolf, *Principles of optics: electromagnetic theory of propagation, interference and diffraction of light*. Elsevier, 2013.

[28] M. Di Renzo, F. H. Danufane, X. Xi, J. De Rosny, and S. Tretyakov, « Analytical modeling of the path-loss for reconfigurable intelligent surfaces–anomalous mirror or scatterer? », *in 2020 IEEE 21st International Workshop on Signal Processing Advances in Wireless Communications (SPAWC)*, IEEE, 2020, pp. 1–5.

[29] J. C. B. Garcia, A. Sibille, and M. Kamoun, « Reconfigurable intelligent surfaces: bridging the gap between scattering and reflection », *IEEE Journal on Selected Areas in Communications*, vol. 38, no. 11, pp. 2538–2547, 2020.

[30] S. W. Ellingson, « Path loss in reconfigurable intelligent surface-enabled channels », *in 2021 IEEE 32nd Annual International Symposium on Personal, Indoor and Mobile Radio Communications (PIMRC)*, IEEE, 2021, pp. 829–835.

[31] E. Björnson, Ö. Özdogan, and E. G. Larsson, « Intelligent reflecting surface versus decode-and-forward: how large surfaces are needed to beat relaying? », *IEEE Wireless Communications Letters*, vol. 9, no. 2, pp. 244–248, 2019.

[32] M. Usman et al., « Intelligent wireless walls for contactless in-home monitoring », *Light: Science & Applications*, vol. 11, no. 1, p. 212, 2022.

[33] M. Cui, G. Zhang, and R. Zhang, « Secure wireless communication via intelligent reflecting surface », *IEEE Wireless Communications Letters*, vol. 8, no. 5, pp. 1410–1414, 2019.

[34] X. Yu, D. Xu, Y. Sun, D. W. K. Ng, and R. Schober, « Robust and secure wireless communications via intelligent reflecting surfaces », *IEEE Journal on Selected Areas in Communications*, vol. 38, no. 11, pp. 2637–2652, 2020.

[35] S. Yamamoto, J. Nakazato, and G. K. Tran, « Multi-irs-assisted mmwave uav-bs network for coverage extension », *Sensors*, vol. 24, no. 6, p. 2006, 2024.

[36] S. Hassouna, J. Rains, J. U. R. Kazim, M. U. Rehman, M. Imran, and Q. H. Abbasi, « Investigating the data rate of intelligent reflecting surface under different deployments », *in 2022 IEEE International Symposium on Antennas and Propagation and USNC-URSI Radio Science Meeting (AP-S/URSI)*, IEEE, 2022, pp. 1578–1579.

[37] S. K. Sharma, M. Patwary, S. Chatzinotas, B. Ottersten, and M. Abdel-Maguid, « Repeater for 5g wireless: a complementary contender for spectrum sensing intelligence », *in 2015 IEEE International Conference on Communications (ICC)*, IEEE, 2015, pp. 1416–1421.

[38] R. Liu, Q. Wu, M. Di Renzo, and Y. Yuan, « A path to smart radio environments: an industrial viewpoint on reconfigurable intelligent surfaces », *IEEE Wireless Communications*, vol. 29, no. 1, pp. 202–208, 2022.

[39] C. Xu, L. Yang, and P. Zhang, « Practical backscatter communication systems for battery-free internet of things: a tutorial and survey of recent research », *IEEE Signal Processing Magazine*, vol. 35, no. 5, pp. 16–27, 2018.

[40] H. Zhao, Y. Shuang, M. Wei, T. J. Cui, P. d. Hougne, and L. Li, « Metasurface-assisted massive backscatter wireless communication with commodity wi-fi signals », *Nature communications*, vol. 11, no. 1, p. 3926, 2020.

[41] M. Nemati, J. Ding, and J. Choi, « Short-range ambient backscatter communication using reconfigurable intelligent surfaces », *in 2020 IEEE Wireless Communications and Networking Conference (WCNC)*, IEEE, 2020, pp. 1–6.

[42] M. Di Renzo et al., « Reconfigurable intelligent surfaces vs. relaying: differences, similarities, and performance comparison », *IEEE Open Journal of the Communications Society*, vol. 1, pp. 798–807, 2020.

[43] A. Khaleel and E. Basar, « Reconfigurable intelligent surface-empowered mimo systems », *IEEE Systems Journal*, vol. 15, no. 3, pp. 4358–4366, 2020.

[44] M. Di Renzo and J. Song, « Reflection probability in wireless networks with metasurface-coated environmental objects: an approach based on random spatial processes », *EURASIP Journal on Wireless Communications and Networking*, vol. 2019, no. 1, p. 99, 2019.

[45] X. Tan, Z. Sun, D. Koutsonikolas, and J. M. Jornet, « Enabling indoor mobile millimeter-wave networks based on smart reflect-arrays », *in IEEE INFOCOM 2018-IEEE Conference on Computer Communications*, IEEE, 2018, pp. 270–278.

[46] J. Wang, W. Zhang, X. Bao, T. Song, and C. Pan, « Outage analysis for intelligent reflecting surface assisted vehicular communication networks », *in GLOBECOM 2020-2020 IEEE Global Communications Conference*, IEEE, 2020, pp. 1–6.

[47] A. Narayanan, T. Sreejith, and R. K. Ganti, « Coverage analysis in millimeter wave cellular networks with reflections », *in GLOBECOM 2017-2017 IEEE Global Communications Conference*, IEEE, 2017, pp. 1–6.

[48] B. Lu, R. Wang, and Y. Liu, « Outage probability of intelligent reflecting surface assisted full duplex two-way communications », *IEEE Communications Letters*, vol. 26, no. 2, pp. 286–290, 2021.

[49] R. C. Ferreira, M. S. Facina, F. A. De Figueiredo, G. Fraidenraich, and E. R. De Lima, « Bit error probability for large intelligent surfaces under double-nakagami fading channels », *IEEE Open Journal of the Communications Society*, vol. 1, pp. 750–759, 2020.

[50] E. Basar, « Transmission through large intelligent surfaces: a new frontier in wireless communications », *in 2019 European Conference on Networks and Communications (EuCNC)*, IEEE, 2019, pp. 112–117.

[51] T. Assaf, A. J. Al-Dweik, M. S. El Moursi, H. Zeineldin, and M. Al-Jarrah, « Exact bit error-rate analysis of two-user noma using qam with arbitrary modulation orders », *IEEE Communications Letters*, vol. 24, no. 12, pp. 2705–2709, 2020.

[52] V. C. Thirumavalavan and T. S. Jayaraman, « Ber analysis of reconfigurable intelligent surface assisted downlink power domain noma system », *in 2020 international conference on COMmunication systems & NETworkS (COMSNETS)*, IEEE, 2020, pp. 519–522.

[53] J. Li and Y. Hong, « Intelligent reflecting surface aided communication systems: performance analysis », *in 2021 IEEE 32nd Annual International Symposium on Personal, Indoor and Mobile Radio Communications (PIMRC)*, IEEE, 2021, pp. 519–524.

[54] A. M. Salhab and M. H. Samuh, « Accurate performance analysis of reconfigurable intelligent surfaces over rician fading channels », *IEEE Wireless Communications Letters*, vol. 10, no. 5, pp. 1051–1055, 2021.

[55] M. Jung, W. Saad, M. Debbah, and C. S. Hong, « Asymptotic optimality of reconfigurable intelligent surfaces: passive beamforming and achievable rate », *in ICC 2020-2020 IEEE International Conference on Communications (ICC)*, IEEE, 2020, pp. 1–6.

[56] J. He, H. Wymeersch, T. Sanguanpuak, O. Silvén, and M. Juntti, « Adaptive beamforming design for mmwave ris-aided joint localization and communication », *in 2020 IEEE Wireless Communications and Networking Conference Workshops (WCNCW)*, IEEE, 2020, pp. 1–6.

[57] Ö. Özdogan, E. Björnson, and E. G. Larsson, « Using intelligent reflecting surfaces for rank improvement in mimo communications », *in ICASSP 2020-2020 IEEE International Conference on Acoustics, Speech and Signal Processing (ICASSP)*, IEEE, 2020, pp. 9160–9164.

[58] H. Zhang, B. Di, L. Song, and Z. Han, « Reconfigurable intelligent surfaces assisted communications with limited phase shifts: how many phase shifts are enough? », *IEEE Transactions on Vehicular Technology*, vol. 69, no. 4, pp. 4498–4502, 2020.

[59] J. V. Alegría and F. Rusek, « Achievable rate with correlated hardware impairments in large intelligent surfaces », *in 2019 IEEE 8th International Workshop on Computational Advances in Multi-Sensor Adaptive Processing (CAMSAP)*, IEEE, 2019, pp. 559–563.

[60] J. Lyu and R. Zhang, « Spatial throughput characterization for intelligent reflecting surface aided multiuser system », *IEEE Wireless Communications Letters*, vol. 9, no. 6, pp. 834–838, 2020.

[61] E. Björnson, « Optimizing a binary intelligent reflecting surface for ofdm communications under mutual coupling », *in WSA 2021; 25th International ITG Workshop on Smart Antennas*, VDE, 2021, pp. 1–6.

[62] S. Zhang and R. Zhang, « Intelligent reflecting surface aided multi-user communication: capacity region and deployment strategy », *IEEE Transactions on Communications*, vol. 69, no. 9, pp. 5790–5806, 2021.

[63] A. Papazafeiropoulos, C. Pan, A. Elbir, P. Kourtessis, S. Chatzinotas, and J. M. Senior, « Coverage probability of distributed irs systems under spatially correlated channels », *IEEE Wireless Communications Letters*, vol. 10, no. 8, pp. 1722–1726, 2021.

[64] X. Tan, Z. Sun, J. M. Jornet, and D. Pados, « Increasing indoor spectrum sharing capacity using smart reflect-array », *in 2016 IEEE International Conference on Communications (ICC)*, IEEE, 2016, pp. 1–6.

[65] M. Jung, W. Saad, Y. Jang, G. Kong, and S. Choi, « Performance analysis of large intelligent surfaces (liss): asymptotic data rate and channel hardening effects », *IEEE Transactions on Wireless Communications*, vol. 19, no. 3, pp. 2052–2065, 2020.

[66] S. Hu, F. Rusek, and O. Edfors, « Capacity degradation with modeling hardware impairment in large intelligent surface », *in 2018 IEEE Global Communications Conference (GLOBECOM)*, IEEE, 2018, pp. 1–6.

[67] A. Papazafeiropoulos, C. Pan, P. Kourtessis, S. Chatzinotas, and J. M. Senior, « Intelligent reflecting surface-assisted mu-miso systems with imperfect hardware: channel estimation and beamforming design », *IEEE Transactions on Wireless Communications*, vol. 21, no. 3, pp. 2077–2092, 2021.

[68] S. Hu, F. Rusek, and O. Edfors, « Beyond massive mimo: the potential of data transmission with large intelligent surfaces », *IEEE Transactions on Signal Processing*, vol. 66, no. 10, pp. 2746–2758, 2018.

[69] M. Dunna, C. Zhang, D. Sievenpiper, and D. Bharadia, « Scattermimo: enabling virtual mimo with smart surfaces », *in Proceedings of the 26th Annual International Conference on Mobile Computing and Networking*, 2020, pp. 1–14.

[70] S. Gong et al., « Toward smart wireless communications via intelligent reflecting surfaces: a contemporary survey », *IEEE Communications Surveys & Tutorials*, vol. 22, no. 4, pp. 2283–2314, 2020.

[71] E. Basar, M. Wen, R. Mesleh, M. Di Renzo, Y. Xiao, and H. Haas, « Index modulation techniques for next-generation wireless networks », *IEEE access*, vol. 5, pp. 16 693–16 746, 2017.

[72] D.-T. Phan-Huy et al., « Single-carrier spatial modulation for the internet of things: design and performance evaluation by using real compact and reconfigurable antennas », *IEEE access*, vol. 7, pp. 18 978–18 993, 2019.

[73] N. Van Huynh, D. T. Hoang, X. Lu, D. Niyato, P. Wang, and D. I. Kim, « Ambient backscatter communications: a contemporary survey », *IEEE Communications surveys & tutorials*, vol. 20, no. 4, pp. 2889–2922, 2018.

[74] X. Guan, Q. Wu, and R. Zhang, « Joint power control and passive beamforming in irs-assisted spectrum sharing », *IEEE Communications Letters*, vol. 24, no. 7, pp. 1553–1557, 2020.

[75] W. Wu et al., « Irs-enhanced energy detection for spectrum sensing in cognitive radio networks », *IEEE Wireless Communications Letters*, vol. 10, no. 10, pp. 2254–2258, 2021.

[76] A. Mahmoud, S. Muhaidat, P. C. Sofotasios, I. Abualhaol, O. A. Dobre, and H. Yanikomeroglu, « Intelligent reflecting surfaces assisted uav communications for iot networks: performance analysis », *IEEE Transactions on Green Communications and Networking*, vol. 5, no. 3, pp. 1029–1040, 2021.

[77] M. Al-Jarrah, E. Alsusa, A. Al-Dweik, and D. K. So, « Capacity analysis of irs-based uav communications with imperfect phase compensation », *IEEE Wireless Communications Letters*, vol. 10, no. 7, pp. 1479–1483, 2021.

[78] M. Al-Jarrah, A. Al-Dweik, E. Alsusa, Y. Iraqi, and M.-S. Alouini, « On the performance of irs-assisted multi-layer uav communications with imperfect phase compensation », *IEEE Transactions on Communications*, vol. 69, no. 12, pp. 8551–8568, 2021.

[79] Y. Yang, B. Zheng, S. Zhang, and R. Zhang, « Intelligent reflecting surface meets ofdm: protocol design and rate maximization », *IEEE Transactions on Communications*, vol. 68, no. 7, pp. 4522–4535, 2020.

[80] P. Nuti, E. Balti, and B. L. Evans, « Spectral efficiency optimization for mmwave wideband mimo ris-assisted communication », *in 2022 IEEE 95th Vehicular Technology Conference:(VTC2022-Spring)*, IEEE, 2022, pp. 1–6.

[81] S. Zhang and R. Zhang, « Capacity characterization for intelligent reflecting surface aided mimo communication », *IEEE Journal on Selected Areas in Communications*, vol. 38, no. 8, pp. 1823–1838, 2020.

[82] N. S. Perović, L.-N. Tran, M. Di Renzo, and M. F. Flanagan, « Achievable rate optimization for mimo systems with reconfigurable intelligent surfaces », *IEEE Transactions on Wireless Communications*, vol. 20, no. 6, pp. 3865–3882, 2021.

[83] Q. Wu and R. Zhang, « Intelligent reflecting surface enhanced wireless network: joint active and passive beamforming design », *in 2018 IEEE global communications conference (GLOBECOM)*, IEEE, 2018, pp. 1–6.

[84] Q. Wu and R. Zhang, « Beamforming optimization for wireless network aided by intelligent reflecting surface with discrete phase shifts », *IEEE Transactions on Communications*, vol. 68, no. 3, pp. 1838–1851, 2019.

[85] Q. Wu and R. Zhang, « Intelligent reflecting surface enhanced wireless network via joint active and passive beamforming », *IEEE Transactions on Wireless Communications*, vol. 18, no. 11, pp. 5394–5409, 2019.

[86] E. Björnson and L. Sanguinetti, « Demystifying the power scaling law of intelligent reflecting surfaces and metasurfaces », *in 2019 IEEE 8th International Workshop on Computational Advances in Multi-Sensor Adaptive Processing (CAMSAP)*, IEEE, 2019, pp. 549–553.

[87] K. Ying, Z. Gao, S. Lyu, Y. Wu, H. Wang, and M.-S. Alouini, « Gmd-based hybrid beamforming for large reconfigurable intelligent surface assisted millimeter-wave massive mimo », *IEEE Access*, vol. 8, pp. 19 530–19 539, 2020.

[88] Y. Zhang, C. Zhong, Z. Zhang, and W. Lu, « Sum rate optimization for two way communications with intelligent reflecting surface », *IEEE Communications Letters*, vol. 24, no. 5, pp. 1090–1094, 2020.

[89] B. Zheng and R. Zhang, « Intelligent reflecting surface-enhanced ofdm: channel estimation and reflection optimization », *IEEE Wireless Communications Letters*, vol. 9, no. 4, pp. 518–522, 2019.

[90] E. Björnson and L. Marcenaro, « Configuring an intelligent reflecting surface for wireless communications: highlights from the 2021 ieee signal processing cup student competition [sp competitions] », *IEEE Signal Processing Magazine*, vol. 39, no. 1, pp. 126–131, 2021.

[91] S. Lin, B. Zheng, G. C. Alexandropoulos, M. Wen, F. Chen, et al., « Adaptive transmission for reconfigurable intelligent surface-assisted ofdm wireless communications », *IEEE Journal on Selected Areas in Communications*, vol. 38, no. 11, pp. 2653–2665, 2020.

[92] E. Björnson, H. Wymeersch, B. Matthiesen, P. Popovski, L. Sanguinetti, and E. De Carvalho, « Reconfigurable intelligent surfaces: a signal processing perspective with wireless applications », *IEEE Signal Processing Magazine*, vol. 39, no. 2, pp. 135–158, 2022.

[93] S. Hassouna, J. Rains, J. R. Kazim, M. U. Rehman, M. Imran, and Q. H. Abbasi, « Discrete phase shifts for intelligent reflecting surfaces in ofdm communications », *in 2022 International Workshop on Antenna Technology (iWAT)*, IEEE, 2022, pp. 128–131.

[94] Q.-U.-A. Nadeem, A. Kammoun, A. Chaaban, M. Debbah, and M.-S. Alouini, « Intelligent reflecting surface assisted wireless communication: modeling and channel estimation », *arXiv preprint arXiv:1906.02360*, 2019.

[95] D. Mishra and H. Johansson, « Channel estimation and low-complexity beamforming design for passive intelligent surface assisted miso wireless energy transfer », *in ICASSP 2019-2019 IEEE International Conference on Acoustics, Speech and Signal Processing (ICASSP)*, IEEE, 2019, pp. 4659–4663.

[96] B. Zheng, C. You, and R. Zhang, « Intelligent reflecting surface assisted multi-user ofdma: channel estimation and training design », *IEEE Transactions on Wireless Communications*, vol. 19, no. 12, pp. 8315–8329, 2020.

[97] I.-S. Kim, M. Bennis, J. Oh, J. Chung, and J. Choi, « Bayesian channel estimation for intelligent reflecting surface-aided mmwave massive mimo systems with semi-passive elements », *IEEE Transactions on Wireless Communications*, vol. 22, no. 12, pp. 9732–9745, 2023.

[98] P. Wang, J. Fang, H. Duan, and H. Li, « Compressed channel estimation for intelligent reflecting surface-assisted millimeter wave systems », *IEEE signal processing letters*, vol. 27, pp. 905–909, 2020.

[99] J. Chen, Y.-C. Liang, H. V. Cheng, and W. Yu, « Channel estimation for reconfigurable intelligent surface aided multi-user mmwave mimo systems », *IEEE Transactions on Wireless Communications*, vol. 22, no. 10, pp. 6853–6869, 2023.

[100] L. Wei, C. Huang, G. C. Alexandropoulos, and C. Yuen, « Parallel factor decomposition channel estimation in ris-assisted multi-user miso communication », *in 2020 IEEE 11th sensor array and multichannel signal processing workshop (SAM)*, IEEE, 2020, pp. 1–5.

[101] B. Ning, Z. Chen, W. Chen, and Y. Du, « Channel estimation and transmission for intelligent reflecting surface assisted thz communications », *in ICC 2020-2020 IEEE International Conference on Communications (ICC)*, IEEE, 2020, pp. 1–7.

[102] A. M. Elbir, A. Papazafeiropoulos, P. Kourtessis, and S. Chatzinotas, « Deep channel learning for large intelligent surfaces aided mm-wave massive mimo systems », *IEEE Wireless Communications Letters*, vol. 9, no. 9, pp. 1447–1451, 2020.

[103] A. Taha, Y. Zhang, F. B. Mismar, and A. Alkhateeb, « Deep reinforcement learning for intelligent reflecting surfaces: towards standalone operation », *in 2020 IEEE 21st international workshop on signal processing advances in wireless communications (SPAWC)*, IEEE, 2020, pp. 1–5.

[104] G. C. Alexandropoulos and E. Vlachos, « A hardware architecture for reconfigurable intelligent surfaces with minimal active elements for explicit channel estimation », *in ICASSP 2020-2020 IEEE international conference on acoustics, speech and signal processing (ICASSP)*, IEEE, 2020, pp. 9175–9179.

[105] M. Di Renzo et al., « Smart radio environments empowered by reconfigurable intelligent surfaces: how it works, state of research, and the road ahead », *IEEE Journal on Selected Areas in Communications*, vol. 38, no. 11, pp. 2450–2525, 2020.

[106] C. You, B. Zheng, W. Mei, and R. Zhang, « How to deploy intelligent reflecting surfaces in wireless network: bs-side, user-side, or both sides? », *Journal of Communications and Information Networks*, vol. 7, no. 1, pp. 1–10, 2022.

[107] Y. Han, S. Zhang, L. Duan, and R. Zhang, « Cooperative double-irs aided communication: beamforming design and power scaling », *IEEE Wireless Communications Letters*, vol. 9, no. 8, pp. 1206–1210, 2020.

[108] Z. Li, M. Hua, Q. Wang, and Q. Song, « Weighted sum-rate maximization for multi-irs aided cooperative transmission », *IEEE Wireless Communications Letters*, vol. 9, no. 10, pp. 1620–1624, 2020.

[109] C. You, B. Zheng, and R. Zhang, « Wireless communication via double irs: channel estimation and passive beamforming designs », *IEEE Wireless Communications Letters*, vol. 10, no. 2, pp. 431–435, 2020.

[110] B. Zheng, C. You, and R. Zhang, « Double-irs assisted multi-user mimo: cooperative passive beamforming design », *IEEE Transactions on Wireless Communications*, vol. 20, no. 7, pp. 4513–4526, 2021.

[111] J. Wu and B. Shim, « Power minimization of intelligent reflecting surface-aided uplink iot networks », *in 2021 IEEE Wireless Communications and Networking Conference (WCNC)*, IEEE, 2021, pp. 1–6.

[112] J. Lyu and R. Zhang, « Hybrid active/passive wireless network aided by intelligent reflecting surface: system modeling and performance analysis », *IEEE Transactions on Wireless Communications*, vol. 20, no. 11, pp. 7196–7212, 2021.

[113] M. A. Kishk and M.-S. Alouini, « Exploiting randomly located blockages for large-scale deployment of intelligent surfaces », *IEEE Journal on Selected Areas in Communications*, vol. 39, no. 4, pp. 1043–1056, 2020.

[114] R. E. M. Non-orthogonal, « Multiple access networks: deployment and passive beamforming design », *arXiv preprint arXiv:2001.10363*, 2020.

[115] C. Jia, H. Gao, N. Chen, and Y. He, « Machine learning empowered beam management for intelligent reflecting surface assisted mmwave networks », *China Communications*, vol. 17, no. 10, pp. 100–114, 2020.

[116] A. Taha, M. Alrabeiah, and A. Alkhateeb, « Deep learning for large intelligent surfaces in millimeter wave and massive mimo systems », *in 2019 IEEE Global communications conference (GLOBECOM)*, IEEE, 2019, pp. 1–6.

[117] G. Vallero, D. Renga, M. Meo, and M. A. Marsan, « Greener ran operation through machine learning », *IEEE Transactions on Network and Service Management*, vol. 16, no. 3, pp. 896–908, 2019.

[118] J. Gao, C. Zhong, X. Chen, H. Lin, and Z. Zhang, « Unsupervised learning for passive beamforming », *ieee communications letters*, vol. 24, no. 5, pp. 1052–1056, 2020.

[119] K. Yang, Y. Shi, Y. Zhou, Z. Yang, L. Fu, and W. Chen, « Federated machine learning for intelligent iot via reconfigurable intelligent surface », *IEEE network*, vol. 34, no. 5, pp. 16–22, 2020.

[120] E. C. Strinati et al., « Reconfigurable, intelligent, and sustainable wireless environments for 6g smart connectivity », *IEEE Communications Magazine*, vol. 59, no. 10, pp. 99–105, 2021.

[121] X. Ge, J. Yang, H. Gharavi, and Y. Sun, « Energy efficiency challenges of 5g small cell networks », *IEEE Communications Magazine*, vol. 55, no. 5, pp. 184–191, 2017.

[122] A. Aggarwal, P. Kalita, and D. Selvamuthu, « Stochastic modeling of a base station in 5g wireless networks for energy aspects using advanced sleep mechanism », *Methodology and Computing in Applied Probability*, vol. 27, no. 3, p. 58, 2025.

[123] I. Ashraf, F. Boccardi, and L. Ho, « Sleep mode techniques for small cell deployments », *IEEE Communications Magazine*, vol. 49, no. 8, pp. 72–79, 2011.

[124] M. Feng, S. Mao, and T. Jiang, « Boost: base station on-off switching strategy for green massive mimo hetnets », *IEEE Transactions on Wireless Communications*, vol. 16, no. 11, pp. 7319–7332, 2017.

[125] X. Guo, Z. Niu, S. Zhou, and P. Kumar, « Delay-constrained energy-optimal base station sleeping control », *IEEE Journal on Selected Areas in Communications*, vol. 34, no. 5, pp. 1073–1085, 2016.

[126] Y. L. Che, L. Duan, and R. Zhang, « Dynamic base station operation in large-scale green cellular networks », *Ieee journal on selected areas in communications*, vol. 34, no. 12, pp. 3127–3141, 2016.

[127] H. Jiang et al., « Data-driven cell zooming for large-scale mobile networks », *IEEE Transactions on Network and Service Management*, vol. 15, no. 1, pp. 156–168, 2018.

[128] C. Luo and J. Liu, « Load based dynamic small cell on/off strategy in ultra-dense networks », *in 2018 10th International Conference on Wireless Communications and Signal Processing (WCSP)*, IEEE, 2018, pp. 1–6.

[129] M. Miozzo, L. Giupponi, M. Rossi, and P. Dini, « Switch-on/off policies for energy harvesting small cells through distributed q-learning », *in 2017 IEEE wireless communications and networking conference workshops (WCNCW)*, IEEE, 2017, pp. 1–6.

[130] M. Miozzo, L. Giupponi, M. Rossi, and P. Dini, « Distributed q-learning for energy harvesting heterogeneous networks », *in 2015 IEEE International Conference on Communication Workshop (ICCW)*, IEEE, 2015, pp. 2006–2011.

[131] R. Li, Z. Zhao, X. Chen, J. Palicot, and H. Zhang, « Tact: a transfer actor-critic learning framework for energy saving in cellular radio access networks », *IEEE transactions on wireless communications*, vol. 13, no. 4, pp. 2000–2011, 2014.

[132] H. Sayed, A. El-Amine, H. A. H. Hassan, L. Nuaymi, and R. Achkar, « Reinforcement learning for radio resource management of hybrid-powered cellular networks », *in 2019 International Conference on Wireless and Mobile Computing, Networking and Communications (WiMob)*, IEEE, 2019, pp. 40–46.

[133] B. Debaillie, C. Desset, and F. Louagie, « A flexible and future-proof power model for cellular base stations », *in 2015 IEEE 81st Vehicular Technology Conference (VTC Spring)*, IEEE, 2015, pp. 1–7.

[134] F. E. Salem, Z. Altman, A. Gati, T. Chahed, and E. Altman, « Reinforcement learning approach for advanced sleep modes management in 5g networks », *in 2018 IEEE 88th Vehicular Technology Conference (VTC-Fall)*, IEEE, 2018, pp. 1–5.

[135] A. El-Amine, M. Iturralde, H. A. H. Hassan, and L. Nuaymi, « A distributed q-learning approach for adaptive sleep modes in 5g networks », *in 2019 IEEE wireless communications and networking conference (WCNC)*, IEEE, 2019, pp. 1–6.

[136] A. El-Amine, H. A. H. Hassan, M. Iturralde, and L. Nuaymi, « Location-aware sleep strategy for energy-delay tradeoffs in 5g with reinforcement learning », *in 2019 IEEE 30th Annual International Symposium on Personal, Indoor and Mobile Radio Communications (PIMRC)*, IEEE, 2019, pp. 1–6.

[137] A. El Amine, P. Dini, and L. Nuaymi, « Reinforcement learning for delay-constrained energy-aware small cells with multi-sleeping control », *in 2020 IEEE International Conference on Communications Workshops (ICC Workshops)*, IEEE, 2020, pp. 1–6.

[138] Q. Wu, S. Zhang, B. Zheng, C. You, and R. Zhang, « Intelligent reflecting surface aided wireless communications: a tutorial », *IEEE Transactions on Communications*, 2021.

[139] Q. Wu and R. Zhang, « Joint active and passive beamforming optimization for intelligent reflecting surface assisted swipt under qos constraints », *IEEE Journal on Selected Areas in Communications*, vol. 38, no. 8, pp. 1735–1748, 2020.

[140] H. Guo, Y.-C. Liang, J. Chen, and E. G. Larsson, « Weighted sum-rate optimization for intelligent reflecting surface enhanced wireless networks », *arXiv preprint arXiv:1905.07920*, 2019.

[141] M. Nemati, J. Park, and J. Choi, « Ris-assisted coverage enhancement in millimeter-wave cellular networks », *IEEE Access*, vol. 8, pp. 188 171–188 185, 2020.

[142] Y. Xu, Z. Qin, Y. Zhao, G. Li, G. Gui, and H. Sari, « Resource allocation for intelligent reflecting surface enabled heterogeneous networks », 2020.

[143] D. Li and X. Sun, *Nonlinear integer programming*. Springer Science & Business Media, 2006, vol. 84.

[144] G. Auer et al., « How much energy is needed to run a wireless network? », *IEEE wireless communications*, vol. 18, no. 5, pp. 40–49, 2011.

[145] 3GPP, *Further advancements for e-utra physical layer aspect*, Available at https://portal.3gpp.org/, 3GPP 2015 (accessed April 05, 2021).

[146] X. Hu, J. Wang, and C. Zhong, « Statistical csi based design for intelligent reflecting surface assisted miso systems », *Science China Information Sciences*, vol. 63, pp. 1–10, 2020.

[147] X. Wang et al., *Wireless communication systems: Advanced techniques for signal reception*. Pearson Education India, 2009.

[148] Q. C. Li, H. Niu, A. T. Papathanassiou, and G. Wu, « 5g network capacity: key elements and technologies », *IEEE vehicular technology magazine*, vol. 9, no. 1, pp. 71–78, 2014.

[149] E. U. T. R. Access, « Evolved universal terrestrial radio access (e-utra) and evolved universal terrestrial radio access network (e-utran); physical layer procedures », *Physical Layer Procedures*, 2017.

[150] Y. Ramamoorthi, R. Ohmiya, M. Iwabuchi, T. Ogawa, and Y. Takatori, « Resource allocation and sharing methodologies when reconfigurable intelligent surfaces meet multiple base stations », *Sensors*, vol. 22, no. 15, p. 5619, 2022.

[151] R. S. Sutton, A. G. Barto, et al., *Introduction to reinforcement learning, vol. 135*, 1998.

[152] S. M. Ross, *Introduction to probability models*. Academic press, 2014.

[153] A. Sengupta, A. R. Alvarino, A. Catovic, and L. Casaccia, « Cellular terrestrial broadcast—physical layer evolution from 3gpp release 9 to release 16 », *IEEE Transactions on Broadcasting*, vol. 66, no. 2, pp. 459–470, 2020.

COLLEGE MATHSTIC
DOCTORAL BRETAGNE
BRETAGNE OCEANE

Université de Bretagne Occidentale

Titre : Gestion des ressources radio pour les réseaux cellulaires économes en énergie avec surfaces réfléchissantes intelligentes

Mots-clés : au delà de 5G (B5G), Surfaces Réfléchissantes Intelligentes (IRS), réseaux cellulaires, allocation des ressources, apprentissage par renforcement (RL), consommation d'énergie, qualité de service (QoS), gestion du mode veille (SM).

Résumé : Cette thèse explore l'intégration de surfaces réfléchissantes intelligentes (IRS) dans les futurs réseaux cellulaires (B5G/6G). Les IRS, composées d'éléments passifs et programmables, améliorent les performances en contrôlant l'environnement de propagation. Nos contributions sont les suivantes : Premièrement, nous démontrons que les IRS réduisent la bande passante nécessaire dans les systèmes SISO. Deuxièmement, dans les systèmes SU-MISO, elles étendent la couverture et diminuent le nombre d'antennes requises à l'émission. Notre approche originale considère les IRS comme une ressource partageable entre utilisateurs, menant à des problèmes d'allocation de ressources (mélangeant non-linéarité et nombres entiers) que nous résolvons par des méthodes analytiques et algorithmiques. Enfin, nous proposons un mécanisme d'économie d'énergie pour les petites stations de base (SBS) basé sur l'apprentissage par renforcement (Q-learning). Ce mécanisme permet aux SBS de se mettre en veille dynamiquement, les IRS maintenant alors la connectivité des utilisateurs. Ce travail offre des stratégies d'allocation peu complexes et quantifie les gains permis par les IRS.

Title: Radio Resource Management for Energy Efficient Cellular Networks with Intelligent Reflecting Surfaces

Keywords: Beyond 5G (B5G), Intelligent Reflecting Surfaces (IRSs), Cellular Networks, Resource Allocation, Reinforcement Learning (RL), Energy Consumption, Quality of Service (QoS), Sleep Mode (SM) Management.

Abstract: This thesis investigates the integration of Intelligent Reflecting Surfaces (IRS) into future cellular networks (B5G/6G). Composed of passive and programmable elements, IRS enhance performance by controlling the propagation environment. Our contributions are as follows: First, we demonstrate that IRS reduce the required bandwidth in SISO systems. Second, in SU-MISO systems, they extend coverage and lower the number of required transmit antennas. Our original approach treats IRS as a shareable resource among users, leading to non-linear and integer resource allocation problems that we solve using analytical and algorithmic methods. Finally, we propose an energy-saving mechanism for Small Base Stations (SBS) based on reinforcement learning (Q-learning). This mechanism allows SBS to dynamically enter sleep mode, with IRS maintaining user connectivity. This work provides low-complexity allocation strategies and quantifies the gains offered by IRS.